Leg 192 Preliminary Report

Basement Drilling of the Ontong Java Plateau

Shipboard Scientific Party

Ocean Drilling Program
Texas A&M University
1000 Discovery Drive
College Station TX 77845-9547
USA

January 2001

PUBLISHER'S NOTES

This report was prepared from shipboard files by scientists who participated in the cruise. The report was assembled under time constraints and does not contain all works and findings that will appear in the *Initial Reports* of the ODP *Proceedings.* Reference to the whole or to part of this report should be made as follows:

Shipboard Scientific Party, 2001. Leg 192 Preliminary Report: Basement drilling of the Ontong Java Plateau. *ODP Prelim. Rpt.,* 92 [Online]. Available from World Wide Web: <http://www-odp.tamu.edu/publications/prelim/192_prel/192PREL.PDF>. [Cited YYYY-MM-DD]

Distribution: Electronic copies of this series may be obtained from the Ocean Drilling Program's World Wide Web site at http://www-odp.tamu.edu/publications.

This publication was prepared by the Ocean Drilling Program, Texas A&M University, as an account of work performed under the international Ocean Drilling Program, which is managed by Joint Oceanographic Institutions, Inc., under contract with the National Science Foundation. Funding for the program is provided by the following agencies:

Australia/Canada/Chinese Taipei/Korea Consortium for Ocean Drilling
Deutsche Forschungsgemeinschaft (Federal Republic of Germany)
Institut National des Sciences de l'Univers-Centre National de la Recherche Scientifique (INSU-CNRS; France)
Ocean Research Institute of the University of Tokyo (Japan)
National Science Foundation (United States)
Natural Environment Research Council (United Kingdom)
European Science Foundation Consortium for Ocean Drilling (Belgium, Denmark, Finland, Iceland, Ireland, Italy, The Netherlands, Norway, Spain, Sweden, and Switzerland)
Marine High-Technology Bureau of the State Science and Technology Commission of the People's Republic of China

DISCLAIMER

The following scientists were aboard the *JOIDES Resolution* for Leg 192 of the Ocean Drilling Program:

J. Godfrey Fitton
Co-Chief Scientist
Department of Geology and Geophysics
University of Edinburgh
West Mains Road
Edinburgh, Scotland EH9 3JW
United Kingdom
Phone: (44) 1 31 650 8529
Fax: (44) 1 31 668 3184
E-mail: godfrey.fitton@glg.ed.ac.uk

John J. Mahoney
Co-Chief Scientist
Department of Geology and Geophysics/SOEST
Room 606A/D
University of Hawaii at Manoa
1680 East-West Road
Honolulu HI 96822
USA
Phone: (808) 956-8705
Fax: (808) 956-5512
E-mail: jmahoney@soest.hawaii.edu

Paul J. Wallace
Staff Scientist
Ocean Drilling Program
Texas A&M University
1000 Discovery Drive
College Station TX 77845-3469
USA
Phone: (979) 845-0879
Fax: (979) 845-0876
E-mail: wallace@odpemail.tamu.edu

Maria J. Antretter
Physical Properties Specialist
Institut für Allgemeine und Angewandte Geophysik und Geophysikalisches Observato
Ludwig-Maximilians-Universität München
Theresienstrasse 41/IV
80333 München
Federal Republic of Germany
Phone: (49) 89 2394 4231
Fax: (49) 89 2394 4205
E-mail: maria@geophysik.uni-muenchen.de

Neil R. Banerjee
Metamorphic Petrologist
School of Earth and Ocean Sciences
University of Victoria
Petch 086, 3800 Finnerty Road
Victoria BC V8W 5C2
Canada
Phone: (250) 472-4048
Fax: (250) 721-6200
E-mail: banerjee@uvic.ca

James A. Bergen
Paleontologist (nannofossils)
Department of Geological Sciences
CB 3315, Mitchell Hall
University of North Carolina
Chapel Hill NC 27599
USA
Phone: (919) 962-4379
E-mail: jabergen@flash.net

Graeme Cairns
Logging Staff Scientist
UBO, UMR 6538 Domaines Oceaniques
IUEM, Place Nicolas Copernic
29280 Plouzane
France
Phone: (33) 298-49-87-09
Fax: (33) 298-49-87-60
E-mail: cairns@sdt.univ-brest.fr

Paterno R. Castillo
Igneous Petrologist
Scripps Institution of Oceanography
Geosciences Research Division
University of California, San Diego
La Jolla CA 92093-0212
USA
Phone: (858) 534-0383
Fax: (858) 534-0784
E-mail: pcastillo@ucsd.edu

Lynne M. Chambers
Igneous Petrologist
Department of Geology and Geophysics
University of Edinburgh
Grant Institute, West Mains Road
Edinburgh, Scotland EH9 3JW
United Kingdom
Phone: (44) 1 31 650 8524
Fax: (44) 1 31 668 3184
E-mail: lynne.chambers@glg.ed.ac.uk

William J. Chazey III
Inorganic Chemist
Department of Civil Engineering and Geological Sciences
University of Notre Dame
156 Fitzpatrick Hall
Notre Dame IN 46556
USA
Phone: (219) 631-4308
Fax: (219) 631-9236
E-mail: william.chazey.1@nd.edu

Millard F. Coffin
Geophysicist/JOIDES Logging Scientist
Institute for Geophysics
University of Texas at Austin
Building 600
4412 Spicewood Springs Road
Austin TX 78759-8500
USA
Phone: (512) 471-0429
Fax: (512) 475-6338
E-mail: mikec@ig.utexas.edu

Marguerite M. Godard
Igneous Petrologist
UMR5568 CNRS-UM2
Laboratoire de Tectonophysique cc49
Université de Montpellier 2
Case Courier 49
Place Eugène Bataillon
F-34095 Montpellier
France
Phone: (33) 467-14-39-37
Fax: (33) 467-14-36-03
E-mail: margot@dstu.univ-montp2.fr

Stuart A. Hall
Paleomagnetist
Department of Geosciences
Science and Research I (Room 312)
University of Houston
4800 Calhoun
Houston TX 77204-5503
USA
Phone: (713) 743-3416
Fax: (713) 748-7906
E-mail: sahgeo@uh.edu

José Honnorez
Metamorphic Petrologist
EOST-Géologie
Université Louis Pasteur
1 rue Blessig
F-67084 Strasbourg
France
Phone: (33) 03-88-35-85-38
Fax: (33) 03-88-36-72-35
E-mail: honnorez@illite.u-strasbg.fr

Stephanie P. Ingle
Igneous Petrologist
Département des Sciences de la Terre et de L'Environnement
Université Libre de Bruxelles
C.P. 160/02
Avenue F. D. Roosevelt, 50
B-1050 Brussels
Belgium
Phone: (00) 32-2-650-22-40
Fax: (00) 32-2-650-37-48
E-mail: single@ulb.ac.be

Loren W. Kroenke
Physical Properties Specialist
Hawaii Institute of Geophysics and Planetology/SOEST
University of Hawaii at Manoa
1680 East-West Road, POST 808
Honolulu HI 96822
USA
Phone: (808) 956-7845
Fax: (808) 956-3188
E-mail: kroenke@soest.hawaii.edu

Kenneth G. MacLeod
Stratigrapher
Department of Geological Sciences
101 Geological Sciences Building
University of Missouri
Columbia MO 65211
USA
Phone: (573) 884-3118
Fax: (573) 882-5458
E-mail: macleodk@missouri.edu

Hajime Naruse
Sedimentologist
Department of Geology and Mineralogy
Faculty of Science
Kyoto University
Sakyo-ku Kitashirakawa Oiwakecho
Kyoto 606-8502
Japan
Phone: (81) 75-753-4150
Fax: (81) 75-753-4189
E-mail: naruse@kueps.kyoto-u.ac-jp

Clive R. Neal
Igneous Petrologist
Department of Civil Engineering and Geological Sciences
156 Fitzpatrick Hall
University of Notre Dame
Notre Dame IN 46556
USA
Phone: (219) 631-8328
Fax: (219) 631-9236
E-mail: neal.1@nd.edu

James G. Ogg
Sedimentologist
Department of Earth and Atmospheric Sciences
CIVL Building 1397
Purdue University
West Lafayette IN 47907-1397
USA
Phone: (765) 494-0257
Fax: (765) 496-1210
E-mail: jogg@purdue.edu

Peter Riisager
Paleomagnetist
Danish Lithosphere Centre
Øster Volgrade 10
DK-1350 Copenhagen
Denmark
Phone: (45) 38-14-2638
Fax: (45) 33-11-0878
E-mail: pri@dlc.ku.dk

Takahashi Sano
Igneous Petrologist
College of Environment and Disaster Research
Fuji Tokoha University
Ohbuchi 325
Fuji 417-0801
Japan
Phone: (81) 545-37-2007
Fax: (81) 545-36-2651
E-mail: sano@fuji-tokoha-u.ac.jp

Paul J. Sikora
Paleontologist (foraminifers)
Energy and Geoscience Institute
University of Utah
423 Wakara Way, Suite 300
Salt Lake City UT 84108
USA
Phone: (801) 581-4122
Fax: (801) 585-3540
E-mail: psikora@egi.utah.edu

Rosalind V. White
Petrologist
Department of Geology
University of Leicester
University Road
Leicester LE1 7RH
United Kingdom
Phone: (44) 116-252-3315
Fax: (44) 116-252-3918
E-mail: rvw1@le.ac.uk

Xixi Zhao
Physical Properties Specialist
Center for Study of Imaging and Dynamics
of the Earth
Department of Earth Sciences
University of California, Santa Cruz
1156 High Street
Santa Cruz CA 95064
USA
Phone: (831) 459-4847
Fax: (831) 459-3074
E-mail: xzhao@es.ucsc.edu

Wietze van der Werff
Sedimentologist
Department of Earth Sciences
University of Liverpool
Jane Herdman Building
Brownlow Street
Liverpool L69 3BX
United Kingdom
Phone: (44) 151-749-5141
Fax: (44) 151-749-5141
E-mail: wietzevanderwerff@hotmail.com

SCIENTIFIC REPORT

ABSTRACT

With a surface area of 1.6×10^6 km^2 and a volume of $4–5 \times 10^7$ km^3, the Ontong Java Plateau is the world's largest volcanic oceanic plateau and may represent the largest magmatic event on Earth in the last 200 m.y. During Ocean Drilling Program (ODP) Leg 192 we recovered igneous basement and sediment cores in five widely separated sites in previously unsampled areas across the plateau. Primary objectives of the leg were to determine (1) the age and duration of emplacement of the plateau, (2) the compositional range of magmatism, and (3) the environment and style of eruption.

Acoustic basement at the four sites on the main or high plateau consists of pillow and/or massive basalt flows with rare, thin sedimentary interbeds. Biostratigraphic evidence indicates that basement ages at Sites 1183, 1186, and 1187 are Aptian. At Site 1185, two groups of basalt are present; the lower group is Aptian, whereas the age of the upper group is estimated only loosely as latest Cenomanian to Albian. These results, together with data from Deep Sea Drilling Project (DSDP) Site 289 and ODP Site 807, demonstrate that the great bulk of the high plateau formed in a single episode in the early Aptian. Later volcanic events, including the ~90-Ma event recorded at Site 803 and in the eastern Solomon Islands, appear to have been volumetrically minor on the high plateau and mainly confined to its margins. One of these late-stage events is recorded in our fifth site, Site 1184, on the plateau's eastern lobe or salient, where we cored 338 m of a middle Eocene basaltic volcaniclastic sequence.

The basalt at Sites 1183 and 1186 and that making up the lower group of lava flows at Site 1185 are closely similar in composition and belong to the remarkably homogeneous Kwaimbaita magma type found at Site 807 and in the eastern Solomons. Thus, much of the high plateau's upper crust seems to consist of Kwaimbaita-type basalt. The Eocene volcaniclastic rocks of Site 1184 also have a Kwaimbaita-like bulk composition. No flows of Singgalo-type basalt, which overlies Kwaimbaita-type lavas at Site 807 and on the island of Malaita, were encountered. An exciting discovery of Leg 192 was that basement at Site 1187 and the upper group of flows at Site 1185 are composed of a high-MgO (8–10 wt%), incompatible element–poor (e.g., TiO_2 = 0.72–0.77 wt%; Zr = 36–43 ppm) type of basalt not found previously on the plateau. These rocks appear to represent very high total fractions of partial melting of their mantle source, and their presence in >100-m-thick lava piles at two sites 146 km apart suggests that such basalt is voluminous on the eastern edge of the high plateau.

Emplacement of lavas at all four high-plateau sites was entirely submarine. The shallowest estimated Aptian water depth for basement is several hundred meters, at Site 1183 on the broad dome of the plateau. Together with previous evidence, our results indicate that most of the Ontong Java Plateau formed well below sea level. The only evidence that a portion of the high plateau was ever at shallow depth is two thin intervals of Aptian vitric tuff above basement at Site 1183 and possibly a vitric tuff just above basement at DSDP Site 289. The mainly submarine emplacement of the plateau probably accounts for its apparently limited

paleoenvironmental effects. However, ferruginous claystone layers above basement at Sites 1183 and 1187 provide evidence for at least local Aptian "dead zones."

INTRODUCTION

Volcanic oceanic plateaus are formed by immense volumes of magma emplaced in pre-existing oceanic lithosphere or at spreading centers. Nearly all of the plateaus in the oceans today were formed in the Cretaceous period and may reflect a major mode of mass and energy transfer from the Earth's interior to its surface that was different from the ocean ridge–dominated mode of the Cenozoic (e.g., Stein and Hofmann, 1994; McNutt et al., 1996). Since the mid-1980s, oceanic plateaus have been recognized as the counterparts of continental flood basalt provinces and associated thick volcanic sequences at many passive continental margins, collectively termed large igneous provinces (LIPs) by Coffin and Eldholm (1994). In the last decade, these features have been ascribed by many workers to the initial plume-head stage of hot-spot development (e.g., Richards et al., 1991; Saunders et al., 1992). Alternative, nonplume models have been proposed (e.g., Smith, 1993; Anderson, 1996) but have thus far not received widespread support. The plume-head model predicts that LIPs are formed from ocean-island-like mantle in massive eruptive outpourings lasting only a few million years or less (e.g., Campbell, 1998). For many continental LIPs and at least some volcanic passive margins, eruption indeed probably occurred rapidly, but continental lithospheric contamination usually has overprinted the sublithospheric mantle-source signature. Most oceanic LIPs formed in locations remote from any continental lithosphere, but comparable data on eruption ages and source composition are lacking because very few basement sites have yet been sampled. Because of the thick sediments that blanket oceanic plateaus, drilling is generally the only way to sample basement crust effectively.

The climatic, oceanographic, and associated biospheric effects of plateau emplacement are poorly known but appear to have been very significant in some cases (e.g., Jones et al., 1995; Kerr, 1998; Tarduno et al., 1998). After emplacement, plateaus appear to have important effects on subduction patterns, plate motions, continental growth, and crustal evolution. Large oceanic plateaus, in particular, tend to resist subduction and thus may form an important early stage in the growth of continents (e.g., Kroenke, 1974; Cloos, 1993; Tejada et al., 1996; Albarède, 1998; Wessel and Kroenke, 1999; Polat et al., 1999).

The Ontong Java Plateau in the western Pacific (Figs. 1, 2) is the largest volcanic oceanic plateau in the world, with a crustal volume of ~5×10^7 km^3 (Mahoney, 1987; Coffin and Eldholm, 1993). If the great bulk of this plateau formed in a single, geologically brief magmatic episode, then the rate at which it was emplaced would have rivaled the entire magma production rate of the global midocean-ridge system at the time. The plateau would then represent the largest igneous event of the last 200 m.y. (Tarduno et al., 1991; Mahoney et al., 1993).

The goal of Leg 192 was to sample the acoustic basement of the Ontong Java Plateau at four widely spaced sites, one of which was to be drilled at least 150 m and three at least 100 m into

basement. Shipboard and shore-based studies of the rocks recovered would provide insights into the age and duration of magmatism, the compositional range of the mantle sources, and the processes of magmatic evolution. We also hoped to evaluate the environment and style of eruption and the association of plateau emplacement with changes in paleoceanographic and paleoclimatic conditions.

BACKGROUND

Previous Basement Sampling

Although sampled in only a few locations, the basement of the Ontong Java Plateau was already the best sampled of any Pacific plateau before Leg 192, with drill holes (see Fig. 1) at Deep Sea Drilling Project (DSDP) Site 289 (9-m basement penetration) and Ocean Drilling Program (ODP) Sites 803 (26 m) and 807 (149 m). In contrast to other Pacific plateaus, slivers of the southern edge of the Ontong Java Plateau are exposed above sea level in the eastern Solomon Islands. The principal outcrops are on the islands of Malaita and Santa Isabel where, respectively, 3.5- and ~2-km-thick basement crustal sections have been sampled recently (Tejada et al., 1996, 2000; Parkinson et al., 1996; Petterson et al., 1997; R. Arculus, pers. comm., 2000). A thick pile of lava flows also is exposed on the island of San Cristobal (also called Makira) (e.g., Birkhold-VanDyke et al., 1996), and smaller basement sections are present on Ramos, Ulawa, and possibly Choiseul (e.g., Coleman, 1965; Petterson et al., 1999).

Physical Features and Gross Structure of the Plateau

The Ontong Java Plateau covers an area $>1.5 \times 10^6$ km^2 (roughly the size of Alaska or six times that of the United Kingdom) and consists of two parts: the main or high plateau in the west and north and the eastern lobe or salient in the east and south (Fig. 1; Kroenke, 1972). The plateau surface rises to depths of about 1700 m below sea level (mbsl) in the central region of the high plateau but generally lies at water depths of between 2 and 3 km. The plateau is bounded by the Lyra Basin to the northwest, the East Mariana Basin to the north, the Nauru Basin to the northeast, and the Ellice Basin to the southeast. Along its southern and southwestern boundaries, the plateau has collided with the Solomon Islands arc and now sits at the junction of the Pacific and Australian plates. Much of the high plateau's surface is relatively smooth, although several large seamounts have been built on it. In many areas, the basement crust is covered with pelagic sediments >1 km thick. The eastern lobe consists of a large but unnamed northern ridge and the Stewart Arch, which are separated by the ~300-km-wide Stewart Basin; at its southeastern end, the Stewart Basin merges with the Ellice Basin (Kroenke and Mahoney, 1996). Physiography around the margins of the plateau is complicated. In the north and northeast, numerous horst-and-graben structures appear to predate much of the sediment cover (e.g., Kroenke, 1972; Berger et al., 1992). Faulting and deformation along the Ontong Java Plateau's southern and southwestern margins are associated with the plateau's collision with the

Solomon arc (e.g., Petterson et al., 1997). An extensive fold belt, the Malaita Anticlinorium, embraces the island of Malaita and the northern half of Santa Isabel.

Crustal thickness on much of the high plateau is considerable, even in comparison to other plateaus. Seismic and combined seismic and gravity evidence indicates that crustal thickness is generally in the 25- to 37-km range (e.g., Furumoto et al., 1976; Hussong et al., 1979; Miura et al., 1996; Gladczenko et al., 1997; Richardson et al., 2000). Over much of the high plateau, the depth to the top of Layer 3A (i.e., to the base of the seismically defined upper crust) is 10–16 km (see review of Neal et al., 1997). Lower crustal seismic-wave velocities suggest a granulite-grade gabbroic lower crust, whereas sub-Moho *P*-wave velocities of 8.4–8.6 km/s detected in the northwest and southwest portions of the plateau may indicate the presence of eclogite at depth (Saunders et al., 1996; Neal et al., 1997). The maximum extent of Ontong Java–related volcanism may go well beyond the plateau proper, as the Early Cretaceous lava flows filling the Nauru Basin and similar flows in the East Mariana and Pigafetta basins to the north appear likely to be related closely to the plateau (e.g., Castillo et al., 1994; Neal et al., 1997; Gladczenko et al., 1997).

Tectonic Setting and Age of Emplacement

The original plate-tectonic setting of the Ontong Java Plateau is open to some question because well-defined magnetic lineations have not been found on the plateau. However, block-faulting structures along the eastern margin of the high plateau, interpreted as roughly north-northeast–trending fracture zones, led to proposals that the plateau formed at a west-northwest–trending ridge (Hussong et al., 1979) and possibly at a triple junction (Winterer, 1976; Hilde et al., 1977). Preliminary isotopic study of Ontong Java basement lava flows suggested a hot-spot connection and that the plateau may have formed at a ridge-centered or near-ridge hot spot (Mahoney, 1987). Subsequent geochemical work indicated that plateau basement lavas were formed from a hot-spot–type mantle source by large percentages of partial melting (estimated at 15%–30%), consistent with the plateau having formed on relatively thin and young lithosphere (Mahoney et al., 1993; Tejada et al., 1996; Neal et al., 1997). From bathymetry and satellite-derived gravity fabric, Winterer and Nakanishi (1995) inferred that a north-northeast–trending spreading axis ran through the plateau, whereas Neal et al. (1997) argued that the north-northeast–trending fabric represents fracture-zone orientation. M-series magnetic lineations adjacent to the plateau in the Nauru and Lyra basins run east-northeast to west-southwest. Coffin and Gahagan (1995) reviewed the available geophysical evidence and concluded that it weakly favors emplacement of most of the plateau in an off-ridge location.

Richards et al. (1991), Tarduno et al. (1991), and Mahoney and Spencer (1991) all favored the starting-plume head of the Louisville hot spot (now at ~50°S) as the source of the Ontong Java Plateau. However, 0- to 70-Ma lava flows dredged from sites along the Louisville Ridge, the plume-tail seamount chain formed by the hot spot, are isotopically distinct from Ontong Java basalt (Mahoney et al., 1993). Moreover, a recent plate reconstruction suggests that the plateau formed 10°–15° north of this hot spot's current location (Neal et al., 1997).

As noted above, the plume-head model predicts that plateaus are emplaced in massive eruptive events lasting only a few million years or less. Surprisingly, however, ^{40}Ar-^{39}Ar ages of Ontong Java Plateau lava flows in the Solomon Islands and the pre–Leg 192 drill sites revealed a sharply bimodal distribution (Fig. 3), with ages of 122 ± 3 Ma and 90 ± 4 Ma (total ranges). Thus, most of the plateau may have formed in two relatively brief episodes (Mahoney et al., 1993; Tejada et al., 1996; 2000; Parkinson et al., 1996). Because sampling over the plateau's huge area was very limited, the relative importance of these two episodes remained unclear. However, Tejada et al. (1996) argued that the 122-Ma event was significantly larger than the 90-Ma event. On the basis of abundant 90-Ma lavas (and some dikes) in Santa Isabel and Cenomanian–Coniacian ash layers at DSDP Site 288, they suggested that the 90-Ma episode may have been focused on the eastern salient; shortly thereafter, 90-Ma basalts were also found to be abundant on San Cristobal (Birkhold-VanDyke et al., 1996). An alternative possibility, however, was that further sampling (and dating) could show that eruptions on the plateau actually occurred over a span of 30 m.y. or more (e.g., Tejada et al., 1996; Birkhold-VanDyke et al., 1996; Ito and Clift, 1998).

Between 124 and 100 Ma, the plateau appears to have been positioned close to the Pacific-plate Euler pole, so that it would have moved little relative to the inferred hot-spot source (see Neal et al., 1997). At ~100 Ma, plate motion changed from a northwestward to a more northward trajectory, which continued until ~85 Ma. At ~90 Ma the southeastern corner of the plateau may have been situated rather close to the 122-Ma position of the central high plateau. Following the 90-Ma eruptive episode, rifting and seafloor spreading may have occurred for several million years within the plateau's eastern salient, forming the Stewart Basin in conjunction with spreading in the Ellice Basin to the east (Kroenke and Mahoney, 1996; Neal et al., 1997). An ^{40}Ar-^{39}Ar age of 83 Ma was measured by Duncan (1985) for an ocean ridge–type basalt from the eastern Ellice Basin.

Relatively localized Tertiary volcanism is recorded in Malaita in the 44-Ma alkalic lavas of the Maramasike Formation (Tejada et al., 1996; Petterson et al., 1997). Malaita is also peppered with small intrusions of 34-Ma alnöites (e.g., Davis, 1977; Nixon and Neal, 1987). In San Cristobal, a sequence of tholeiitic basalts with ages of ~61 and ~36 Ma overlie the ~90-Ma basalt and are compositionally similar to it (Birkhold-VanDyke et al., 1996). The causes of these later magmatic events are uncertain.

After a long period of northward and northwestward motion, the Ontong Java Plateau collided with the old Solomon arc during the early Neogene, initially in a diachronous "soft docking" without significant deformation. Following a reversal of subduction direction, the intense deformation of the Malaita Anticlinorium occurred in the late Miocene through Pliocene (see Petterson et al., 1997). The bulk of the plateau appears to be more or less unsubductible (Cloos, 1993; Abbott and Mooney, 1995), but the post-Miocene removal of a portion of the lower Ontong Java Plateau between Santa Isabel and San Cristobal is evident from recent seismic surveys (Mann et al., 1996).

Results from Previous Sampling of Cretaceous Igneous Basement

Ontong Java Plateau basement at all previously drilled sites and in the Solomon islands of Malaita, Santa Isabel, Ulawa, Ramos, and San Cristobal consists of pillowed or massive flows of basalt averaging ~10 m in thickness. Dikes are rare in the island exposures, and, hence, the eruptive vents for most of the lava flows may be rather distant. All of the basalt flows appear to have been emplaced well below sea level and are overlain by bathyal or abyssal pelagic marine sediments (see Neal et al., 1997, and references therein). However, all of the locations studied prior to Leg 192, except Site 289, were at the margins of the plateau; thus it remained possible that the central regions of the high plateau and eastern lobe were formed under shallow-marine or even subaerial conditions. Basement of the 122-Ma age group comprises lava flows from Sites 289 and 807, Malaita, Ramos, and part of Santa Isabel, whereas the 90-Ma flows are found at Site 803, in Santa Isabel, and in San Cristobal (Fig. 3) (Mahoney et al., 1993; Tejada et al., 1996, 2000; Parkinson et al., 1996; Birkhold-VanDyke et al., 1996). Also, volcanic ash layers of late Cenomanian to Coniacian age (i.e., in roughly the ~95- to 87-Ma range) are present at DSDP Site 288 (which did not reach basement) on the southern edge of the high plateau (Andrews, Packham, et al., 1975). A glass-shard-rich interval in Aptian limestone at Site 288 and several late Aptian ash layers above basement at Site 289 (Andrews, Packham, et al., 1975) may indicate fairly prolonged shallow or subaerial volcanism in some areas on the crest of the plateau following eruptions at 122 Ma (early Aptian).

Lava flows drilled at all pre–Leg 192 sites are composed of unmetamorphosed, moderately evolved, low-K tholeiite (Fig. 4). They have relatively flat primitive mantle–normalized incompatible element patterns (intermediate between those of normal ocean-ridge basalt and most oceanic island or continental tholeiites) (Fig. 5) and a narrow range of ocean-island-like Nd-Sr-Pb isotopic ratios (Fig. 6). Major and trace element modeling indicates that the basalt represents high-degree partial melts (Mahoney et al., 1993; Tejada et al., 1996; Neal et al., 1997). Two geochemically and stratigraphically distinct groups of 122-Ma lava flows are apparent in the thick basement section on Malaita (Tejada et al., 1996, 2000) and in the much thinner one at Site 807 (Mahoney et al., 1993). The upper 46 m of lava flows at Site 807 (Unit A) (1) is isotopically and chemically closely similar to those of the Singgalo Formation, which comprises the upper 750 m of flows in central Malaita, and (2) tentatively has been correlated with them by Tejada et al. (2000). The lower basalt units at Site 807 (Units C–G) and the single flow encountered at Site 289 resemble the flows forming the lower 2.7 km of the volcanic pile on Malaita, termed the Kwaimbaita Formation, with which they have been correlated. The 90-Ma lava flows of Site 803, Santa Isabel, and most of those of San Cristobal are isotopically similar to the 122-Ma Kwaimbaita Formation basalt. Thus, an isotopically ocean-island-type mantle source containing (at least) two distinct components was involved in magma generation at the northern and southern margins of the plateau at 122 Ma. Further, the mantle source of most 90-Ma lava flows was similar to that of the Kwaimbaita Formation, the stratigraphically lower of the two 122-Ma basalt groups.

SCIENTIFIC OBJECTIVES

Age and Duration of Emplacement

Hypotheses that involve mantle plumes in the formation of large igneous provinces include rapid-eruption, age-progressive, and episodic growth models.

1. Rapid-emplacement models are of two main types. The plume-head or plume-impact model (e.g., Richards et al., 1991; Saunders et al., 1992; Campbell, 1998) predicts that large oceanic plateaus are formed by widespread basaltic flood eruptions as the inflated head of a rising new mantle plume approaches the base of the lithosphere. An alternative model devised specifically for continental and continental-margin flood basalt provinces (White and McKenzie, 1989), sometimes called the plume-incubation model (e.g., Saunders et al., 1992), considers flood volcanism to result from cataclysmic pressure-release melting when a rift propagates above the enlarged top of a more or less steady-state mantle plume that has accumulated gradually (perhaps over several tens of millions of years) beneath thick, slow-moving continental lithosphere. Both types of model predict that the great bulk of magmatism occurs in only a few (probably <5) million years.
2. In contrast, an age-progressive, Icelandic style of construction in which plateaus are formed over much longer intervals (tens of millions of years) remains a distinct possibility for many plateaus (e.g., Mahoney and Spencer, 1991; Coffin and Gahagan, 1995; Ito and Clift, 1998).
3. Alternatively, plateau growth may occur in two or more discrete pulses of activity, dependent on mantle plume dynamics or the interplay between episodes of lithospheric extension and mantle melting (Bercovici and Mahoney, 1994; Larson and Kincaid, 1996; Neal et al., 2000; Ito and Taira, 2000).

As the world's largest oceanic plateau, the Ontong Java Plateau provides an important test case. Its great crustal volume implies partial melting of at least $1.5–4.0 \times 10^8$ km^3 of mantle, which virtually necessitates involvement of the lower mantle if the bulk of the plateau was formed in the 122-Ma event (e.g., Coffin and Eldholm, 1994). Melting on such a scale is not happening in the Earth's mantle today, and this consideration has helped fuel suggestions of fundamental differences between Cretaceous and Cenozoic mantle convection. However, if the plateau accreted more slowly over several tens of millions of years (like the much smaller Iceland Plateau) or in two or more discrete pulses, then this partial melting requirement is eased considerably, but simple plume-head models either would need to be modified significantly or would not apply. The few basement locations sampled prior to Leg 192 demonstrated that both 122- and 90-Ma lava flows are present in widely separated areas, but the importance of the 90-Ma episode remained unclear. In many places, 90-Ma lava flows may simply form a relatively thin carapace over a thick 122-Ma pile.

Range and Diversity of Magmatism

Laboratory and numerical modeling suggests that starting-plume heads should be strongly zoned because of entrainment of large amounts of ambient, nonplume mantle during their rise to the base of the lithosphere (e.g., Campbell, 1998). Thus, even if a plume's source region (usually assumed to be at the base of, or deep within, the mantle) is compositionally homogeneous, significant isotopic and trace element variability is nevertheless predicted in magmas erupted from different parts of the plume head or at different times. Major element compositions are predicted to vary as well, with magmas erupted above the hottest (axial) parts of the plume head having picritic (e.g., Campbell, 1998) or possibly even komatiitic (Storey et al., 1991) affinities, and more ordinary basaltic magma predicted above cooler, more distal regions. In this regard, the two most remarkable features of the Ontong Java Plateau basement samples available before Leg 192 were (1) the limited overall range of chemical and isotopic variation in the 122-Ma lava flows and (2) that the 90- and 122-Ma flows are so chemically and isotopically similar to each other. The isotopic and incompatible element results could indicate that the world's largest plateau had a much more homogeneous source (both relative to the scale of melting and in time) than predicted by plume-head models. Furthermore, the combined major and trace element data imply that storage and homogenization in large reservoirs was a dominant process in the evolution of the magmas.

Eruptive Environment and Style

Plume-head models predict as much as 1–3 km of dynamic uplift associated with the arrival of a large starting-plume head at the base of the lithosphere (e.g., Hill, 1991; Neal et al., 1997). The associated constructional volcanism also creates a much thicker crust than normal oceanic crust. The combination of these effects is predicted to elevate parts of a plateau's surface to shallow water depths or even cause portions to emerge above sea level. Indeed, significant portions of several plateaus are known to have been initially shallow or subaerial (e.g., Richards et al., 1991; Coffin, Frey, Wallace et al., 2000). However, although most of the Ontong Java Plateau stands 2–3 km above the surrounding seafloor today, basement lava flows from all locations studied before Leg 192 were emplaced beneath fairly deep water, probably below the calcite compensation depth (CCD) in some cases (Neal et al., 1997; Ito and Clift, 1998; Michael, 1999). The reasons for this behavior and whether it is typical of the plateau as a whole were unknown, but critical for understanding how plateaus are constructed and for testing the plume-head model. Moreover, whether or not parts of the Ontong Java Plateau were shallow at the time of volcanism has important implications for how its emplacement affected large-scale climatic, oceanographic, and biospheric conditions. If significant amounts of magma were erupted in shallow water or subaerially, the flux of climate-modifying volatile species (particularly SO_2, Cl, and F) to the atmosphere would have been much greater than if the bulk of plateau volcanism occurred at greater water depths.

The physical volcanology of large-scale submarine lava flows is poorly known, as are the nature and scale of hydrothermal fluid fluxes associated with plateau magmatism. Knowledge of the physical volcanology of lava flows is important for understanding eruption mechanisms and

how the volcanic pile accumulated, whereas data on hydrothermal activity are critical for understanding the oceanographic and climatic effects of plateau formation. Flows making up continental flood basalt provinces are typically 10–30 m thick and, in some cases, have been traced for distances of several hundred kilometers (e.g., Hooper, 1997). Areas distant from eruptive sources tend to be made up of simple flows, whereas compound flows are more indicative of relative proximity to eruptive vents. Previous sampling of the Ontong Java Plateau basement revealed that flow thickness varies from <1 m to 60 m, although most of the flows are in the 4–12-m range (e.g., Neal et al., 1997). The flows are dominantly simple, consistent with the locations of most pre–Leg 192 basement sites at the margins of the plateau and presumably far from their eruptive vents. Very little interlava ash has been found. With regard to hydrothermal activity, pre–Leg 192 Ontong Java basement sites show almost no evidence of anything but low-temperature seawater-mediated alteration in either the lava flows or overlying sediments (e.g., Babbs, 1997). This lack of higher-temperature hydrothermal alteration again is consistent with the inferred distance from eruptive vent systems. Major hydrothermal systems would be expected to be centered around major eruptive loci, postulated by Tejada et al. (1996) to be the comparatively shallow regions of the high plateau and eastern lobe.

DRILLING STRATEGY

Despite the considerable geodynamic significance of LIPs, relatively little is known about the composition and origin of large oceanic plateaus. The Ontong Java Plateau's enormous size and thick blanket of marine sediments constitute particularly formidable obstacles to systematic sampling of basement crust. A widely agreed-upon strategy for plateau basement sampling involves a reconnaissance phase of drilling several holes ~100 m into basement in key areas, followed by a small number of much deeper holes selected on the basis of results from reconnaissance drilling (e.g., Dick et al., 1996). On the two largest plateaus, Ontong Java and Kerguelen–Broken Ridge, the deeper drill holes would consist of one or two holes penetrating ~1 km of basement and one hole with >2 km of basement penetration. Leg 192 was designed to complete the reconnaissance phase of Ontong Java drilling that began with Sites 289, 803, and 807 and was complemented by recent field-based work in the Solomon Islands. We selected four sites that would cover as much as possible (in a 2-month cruise) of the history of major, but previously unsampled, parts of the plateau. Because basement penetration was the main objective, we planned to drill through (i.e., not core) the upper parts of the sedimentary section at all sites.

Site 1183 lies near the crest of the high plateau; Site 1184 is on the northern ridge of the eastern salient; and Site 1185 sits at the edge of the eastern flank of the high plateau, near where it adjoins the Nauru Basin (see Fig. 1). The fourth site (proposed Site OJ-7) was an eastern-salient site located atop the Stewart Arch to the north-northeast of Malaita, in waters claimed by the Solomon Islands. However, because of civil and political turmoil in the Solomons throughout much of 2000, ODP was unable to obtain approval for drilling this site before or during the cruise. At sea, guided by our results from Sites 1183 and 1185, we chose an alternative site, Site

1186. This site is roughly midway between Sites 1183 and 1185, thereby forming a four-site basement transect (including DSDP Site 289) from the crest to the eastern edge of the main plateau. After penetrating ~65.4 m of Kwaimbaita-type basalt flows at Site 1186 (i.e., the same magma type we found at Site 1183 and in the lower 92 m of basement at Site 1185; see below), we decided that the time remaining in the cruise would best be used by drilling a fifth site rather than attempting to deepen Site 1186. On the basis of our results at Site 1185, in particular, we selected Site 1187, on the extreme eastern edge of the plateau north of Site 1185 and southeast of Leg 130 Site 803. Details of each of the five sites drilled during Leg 192 are given in Table 1.

Objectives at all sites were similar. Basement penetration was the priority in order to address the primary questions of the age of the plateau and the range of composition and temperature of the mantle source. We also hoped for good recovery because it would permit assessment of the character and mode of emplacement of basement rocks and allow us to address the question of whether volcanism was submarine or subaerial. Ideally, we also would obtain some information on how far from their eruptive vents the basement rocks were emplaced. Wireline logging of basement was planned at two sites (one of which was the proposed OJ-7 site) in order to obtain additional information on lava flow morphology and volcanic stratigraphy. We planned to core much of the lower portion of the sedimentary cover at each site because the age of the sedimentary rocks immediately overlying basement, their environment of deposition, and the early crustal subsidence history are all important for understanding the origin and environmental impact of the plateau. Moreover, coring of the lower sedimentary section would allow us to ascertain the ages of some of the sequence boundaries observed in the seismic reflection record.

PRINCIPAL RESULTS

Site 1183

Site 1183 is located near the crest of the main edifice of the Ontong Java Plateau (Figs. 1, 2). We chose this site because it is in the shallowest region of the high plateau, where the seismically defined upper-crustal layer is thickest but the sediment cover is relatively thin (see Neal et al., 1997, and references therein). The original basement depth of the high plateau may have been at its shallowest in this region, and eruptive activity may have been at its most vigorous. Because of this, we thought it possible that the compositional range of basement lava flows here may have been greater than in previously studied areas located much closer to the margins of the plateau (Malaita, Santa Isabel, and ODP Sites 803 and 807). Also, a distinctive sediment package appears above basement on the multichannel seismic-reflection line across this area (Fig. 7), and we thought that this package might correspond to much shallower-water deposits than those found elsewhere on the high plateau.

The sedimentary succession (cored from 328.0 to 452.7 meters below seafloor [mbsf] and from 752.0 mbsf to basement at 1130.4 mbsf; Table 1) is dominated by nannofossil foraminifer chalk and limestone. We divided the sequence into three lithologic units and seven subunits (Fig. 8). Unit I consists of ooze and chalk, with the transition between the two (at 337.6 mbsf)

defining the boundary between Subunits IA and IB. However, because we did not core the upper part of the succession, only a single core of ooze (Subunit IA) was recovered. *P*-wave velocities in the ooze and chalk sections of Unit I increase downward from a mean of 1700 m/s to a mean of 2240 m/s. Oligocene chalk cored from 752.0 to 838.6 mbsf contains abundant volcanic ash layers and is designated Subunit IC.

Unit II is Paleocene to middle Eocene limestone. Conspicuous bands of chert between 838.6 and 958.3 mbsf characterize Subunit IIA, and the presence of zeolite-rich bands (probably altered ash layers) and less pronounced chert bands below 958.3 mbsf define Subunit IIB. The base of Unit II is placed at the lowest significant zeolite-rich horizon (986.6 mbsf), which coincides approximately with the base of the Cenozoic. Bulk density increases sharply in the lowest part of Subunit IIB, and both the water content and porosity decrease. A marked *P*-wave velocity increase occurs at the boundary between the chert-rich limestone of Subunit IIA (generally <2500 m/s) and the zeolite-rich limestone of Subunit IIB (generally >3000 m/s); the highest velocities of 3500–4400 m/s are at the bottom of the unit. Cretaceous limestone Unit III is subdivided on the basis of color, with the change from a white Subunit IIIA to a mottled gray and pinkish white Subunit IIIB at 1088.8 mbsf, corresponding approximately to a hiatus and condensation of the Cenomanian through upper Coniacian portion of the sequence. Subunit IIIB, directly above basement, contains microfossils (*Eprolithis floralis* and *Leupoldina cabri*) restricted to a short interval straddling the boundary between the early and middle Aptian.

The lowest 2 m of Subunit IIIB contain two intervals of vitric tuff, the lowermost of which is separated from the underlying basalts by a 25-cm-thick limestone bed. The main component of the tuff intervals is basaltic ash consisting of partly glassy to tachylitic fragments with abundant plagioclase microlites. Texturally, many of the fragments are similar to aphanitic pillow margins in the underlying basalts. Most fragments are nonvesicular, but some have vesicles or scalloped margins. Altered brown glass shards are also present; most are blocky and nonvesicular, but some are moderately vesicular. The tuff is composed of at least eight normally graded beds, several of which have scoured bases. The uppermost layer grades up through parallel-laminated to cross-laminated beds, indicating deposition by turbidity currents or reworking by currents. The minor moderately vesicular basaltic glass shards in these tuff beds indicate formation by relatively shallow submarine eruptions, whereas the partly glassy basaltic ash that constitutes the dominant component could have been derived from shallow-water to subaerial hydroclastic eruptions, or by erosion of a volcanic source somewhere in the summit region of the main Ontong Java Plateau. These beds, and possibly a vitric tuff of similar age just above basement basalt at DSDP Site 289 (Andrews, Packham, et al., 1975) are the only evidence that a portion of the main plateau was relatively shallow and possibly subaerial.

We cored 80.7 m of basaltic basement, from 1130.4 to 1211.1 mbsf, recovering a total of 44.8 m (Table 1) at a low average penetration rate of 1.2 m/hr. We divided the basalt into eight units (Fig. 9), ranging in thickness from 0.36 to 25.70 m, on the basis of the presence of thin interbeds of recrystallized limestone and/or hyaloclastite. Microfossils in the interbeds indicate an age no greater than early Aptian. All eight units contain pillow basalt, defined by quenched glassy rims, grain-size variations from aphanitic near pillow margins to fine grained in the

interiors, and vesicle patterns. Some of the glassy rims appear to be unaltered even though they are laced with calcite veins. The glass is preserved best in Units 4–7. Except near pillow margins, where small (1–2 mm), elongate vesicles are present, the basalt is essentially nonvesicular. Most of it is sparsely olivine ± plagioclase phyric, with a quenched to subophitic groundmass consisting of plagioclase, clinopyroxene, titanomagnetite, glassy mesostasis, and a trace of sulfide. The abundance of olivine phenocrysts increases slightly with depth in the succession, reaching a maximum of ~4%.

Shipboard major and trace element analyses show that the basalt flows at Site 1183 are tholeiitic and very similar in composition to those forming the >2.7-km-thick Kwaimbaita Formation on Malaita, nearly 1000 km to the south (Figs. 10, 11, 12, 13). Kwaimbaita-type basalt also has been sampled 533 km to the north of Site 1183 at Site 807 (Units C–G), in the single flow penetrated at Site 289, 183 km to the northeast, and at Sites 1185 and 1186 (see below). The upper group of basalt flows in Malaita, the ~750-m-thick Singgalo Formation, is compositionally distinct from the Kwaimbaita Formation (Figs. 4, 10, 11, 12, 13); Singgalo-type basalt also is found in Santa Isabel and forms the upper 46 m of flows (Unit A) at Site 807. Its complete absence from Sites 289 and 1183 suggests that basalt of this composition may not be present on the broad crest of the plateau.

Cumulate gabbroic xenoliths and plagioclase megacrysts are present in Units 2–7 at Site 1183 (Fig. 14). They are round to subround and $\leq$3 cm in diameter. Clinopyroxene in the xenoliths is partially to totally resorbed, whereas the plagioclase shows only minimal signs of reaction with its basaltic host. Interestingly, similar xenoliths and megacrysts have been found in lava flows of the Kwaimbaita Formation on Malaita (Tejada et al., 2000) and in the Units C–G flows at Site 807, as well as at Sites 1185 and 1186 (see below).

Pervasive low-temperature interaction of the basaltic basement with seawater-derived fluids under anoxic to suboxic conditions has resulted in alteration ranging from <5% to 20% of the rock. Olivine phenocrysts are completely replaced by smectite (probably saponite with subordinate nontronite and celadonite), Fe oxyhydroxide and, more rarely, calcite. Groundmass glass has been partly to completely replaced by the same secondary minerals, with minor amounts of pyrite. Black halos, ranging from 2 to 50 mm in thickness, are seen in hand specimen along surfaces previously exposed to seawater and, less commonly, along the margins of veins. Such halos are characteristic of an alteration process initiated during cooling of the lava and completed within 1–2 m.y. (e.g., Honnorez, 1981). Pyrite is associated with the black halos and scattered in the groundmass as far as several centimeters beyond the black alteration front. A third stage of alteration, olive halos containing Fe oxyhydroxide and brown smectite, is common in the upper part of the hole and decreases downhole. This stage of alteration corresponds to halmyrolysis or submarine weathering, which takes place at bottom seawater temperature (i.e., around 2°C) in highly oxidizing conditions and with large water:rock ratio.

Veins are relatively abundant (~20 veins/m) in the basaltic basement. Most result from symmetrical infilling of open cracks with minor or no replacement of the wall rock, and the vast majority contain the following succession of secondary minerals from vein wall to center: smectite and/or celadonite, Fe oxyhydroxide or pyrite, and calcite. Rare, small grains of native

copper are present in veins in the upper part of the basement. Veins in the lower part of the basement sequence contain chalcedony and quartz as the final phases precipitated.

The natural remanent magnetization (NRM) of the Miocene ooze and chalk is weak, only slightly above the noise level of the pass-through magnetometer. The Oligocene to Aptian chalk and limestone, with ash layers rich in magnetic minerals, are more strongly magnetized. The NRM of the basalt is strong, but much of the material is broken into small pieces, and reliable magnetic directions are difficult to obtain. However, from detailed sampling of the larger intact pieces, we were able to characterize the intensity and direction of stable remanence. For each core from the hole, we defined magnetic polarity intervals from consistent values of magnetization and calculated a mean paleoinclination. The combination of polarity intervals and biostratigraphic data yields a magnetic stratigraphy for much of the cored interval below 770 mbsf, including the Cretaceous/Tertiary boundary. All basalt samples measured have normal polarity, consistent with formation of basement during the Aptian. Conversion of paleoinclinations to paleolatitudes, combined with age information, allowed us to construct a drift path for Site 1183 for times between ~120 Ma and the present (Fig. 15). The oldest sedimentary rocks indicate a paleolatitude of 25°–30°S. These values are slightly higher than those determined for basement lava flows at ODP Site 807 (Mayer and Tarduno, 1993) but slightly lower than obtained by Hammond et al. (1975) for basal sedimentary rocks and basement at DSDP Site 289. Results for Sites 1185, 1186, and 1187 are within error of those for Site 1183 (see below). Values for all of these sites are significantly less than both the predicted ~40°S early Aptian paleolatitude of the central plateau in the plate reconstruction of Neal et al. (1997) and the ~50°S latitude of the Louisville hot spot today.

The major results of drilling at Site 1183 are summarized as follows:

1. Depositional setting on the seafloor was primarily deep, oxygenated (pervasively bioturbated and no organic-carbon preservation), and quiet (no significant currents or redeposition events after the Aptian).
2. Calcareous microfossil assemblages in ~800 m of uppermost lower Aptian through upper middle Miocene sediments and sedimentary rocks at Site 1183 are for the most part poorly preserved.
3. Planktonic foraminifers and calcareous nannofossils can be used to detect 12 unconformities, of which the most significant are in the inter-Albian (spanning ~10 m.y.) and terminal Albian to upper Coniacian (~13 m.y.).
4. The preserved sediment was deposited above the CCD, and generally above the foraminifer lysocline. However, the regional pattern of the terminal Albian to upper Coniacian (99–86 Ma) condensation or hiatus is consistent with a progressive (relative) rise of the CCD through the Aptian and Albian to a level above the summit of the plateau, followed by a rapid descent of the CCD during the Campanian and early Maastrichtian. These trends may represent the posteruption subsidence history of the plateau coupled with oscillations in the Pacific CCD. Input of volcanic ash into the sedimentary succession is concentrated in two main periods: Paleocene to early Eocene

(65–50 Ma) and late Eocene to Oligocene (40–20 Ma). The latter episode is probably related to the Melanesian arc.

The middle Eocene (50–40 Ma) chalk is chert rich and corresponds to a lull in the input of volcanic ash.

Emplacement of basaltic lava flows was entirely submarine at this site and ceased no later than the middle Aptian. The nonvesicular nature of the flows and the microfossil evidence suggest minimum paleodepths of several hundred meters. Microfossils at Site 807 indicate that basalt emplacement there ended about the same time or slightly earlier. Sedimentary interbeds in the upper levels of basement at both sites yielded microfossils no older than early Aptian. Two thin intervals of vitric tuff in the Aptian limestone at Site 1183 and a vitric tuff just above basement at DSDP Site 289 provide the only evidence that at least a portion of the high plateau was shallow.

The Site 1183 basalt flows are petrographically and chemically similar to those of the Kwaimbaita Formation, the lower of the two basalt formations defined on Malaita, and to the lower basalt units (Units C–G) at Site 807, despite the considerable distances separating Site 1183 from Malaita (~1000 km) and Site 807 (533 km). Very similar basalt is present at Site 1186 and in the lower basement units at Site 1185 (see below).

Site 1184

Site 1184 lies on the unnamed northern ridge of the eastern lobe or salient of the Ontong Java Plateau (Figs. 1, 2). The eastern lobe had not been drilled before Leg 192. As with the dome of the high or main plateau (see “Site 1183" summary above), we thought that this site near the summit of the ridge might be in an area that originally was at relatively shallow water depths. The relationship of the eastern lobe to the high plateau is unknown. It could be contemporaneous with the high plateau or be the trace of the postulated plume tail following the emplacement of the high plateau and, specifically, may be the main locus of 90-Ma eruptions (Tejada et al., 1996). Also, the eastern lobe appears to have been rifted into northern and southern portions that were separated by nearly 300 km of seafloor spreading in the Stewart Basin (Kroenke and Mahoney, 1996). The southern portion, Stewart Arch, is the proposed conjugate feature to the northern ridge. Eruptive products of this poorly understood rifting event may have been preserved along both the northern and southern rift-facing sides of the salient. Furthermore, this part of the plateau passed over the calculated position of the Samoan hot spot around 35–40 Ma (Yan and Kroenke, 1993), and volcanic evidence of this passage might be present.

In the seismic-reflection record for this site (Fig. 16), a sedimentary megasequence laps onto the upper surface of the fault block that forms acoustic basement. Basement reflection character differs from that of basaltic basement on the main plateau (e.g., Site 1183; Fig. 7). Parallel to subparallel, high-frequency, slightly dipping reflections of limited and variable continuity persist to depths as great as 1.0 s of two-way (*P*-wave) traveltime beneath the surface of the fault block. We cored early Miocene pelagic calcareous ooze and chalk (Unit I) from 134.4 mbsf to acoustic basement at 201.1 mbsf and volcaniclastic rocks (Unit II) from 201.1 mbsf to the base of the

hole at 538.8 mbsf. A 1-cm-thick ferromanganese oxide crust represents the contact between the two units. Paleontological data suggest that deposition of the volcaniclastic succession occurred during the middle Eocene (principally nannofossil Zone NP16) and that deposition of the calcareous ooze began during the earliest Miocene. Little, if any, sedimentary record of events during the late Eocene or Oligocene is preserved.

Unit I is dominated by nannofossil foraminifer ooze with as much as 10% siliceous microfossils; volcanic ash is a minor component. Paleodepths appear to have been bathyal. Grain densities generally lie between 2.3 and 2.6 g/cm^3, with a mean of 2.5 g/cm^3; porosity averages 66.1%, and the mean bulk density is 1.5 g/cm^3. The ooze is weakly magnetic and was badly disturbed by drilling; consequently, we were unable to obtain reliable paleomagnetic data. The basement volcaniclastic sequence of Unit II consists of coarse lithic vitric tuff, lapilli tuff, and lapillistone, most of which have a massive texture. Several thin beds of fine ash are also present, but we recovered no pelagic or neritic interbeds. Grain densities in Unit II are significantly more variable than those in Unit I, with a mean of 2.4 g/cm^3; bulk densities maintain a nearly constant value of ~1.9 g/cm^3, and porosities cluster between 31% and 37%. This unit exhibits normal-polarity magnetization and a continuous record of paleosecular variation. The mean inclination (−54°) is much steeper than the expected Eocene inclination and indicates a paleolatitude (35°S) significantly different from that expected for this area in the Eocene (~15°–20°S). Tectonic rotation of the volcaniclastic beds may have taken place after the magnetic remanence was acquired, but a sufficiently large amount of rotation in the direction required appears unlikely to have occurred.

We divided Unit II into five subunits on the basis of changes in grain size, sorting, and sedimentary structures (Fig. 17; Table 2). Wood fragments (Fig. 18) and organic-rich layers were found at the boundaries between four of the subunits (B, C, D and E) and at the base of the cored part of Subunit IIE, perhaps indicating lulls in volcanic activity. Subunit IID contains numerous thin-bedded intervals with inclined bedding. At about 305 mbsf, where a sharp increase in lapilli size marks the boundary between Subunits IIB and IIC, magnetic susceptibility and *P*-wave velocity increase abruptly, and mean thermal conductivity decreases slightly. Below 380 mbsf, where a reduction in lapilli size marks the top of Subunit IID, both magnetic susceptibility and velocity decrease and mean thermal conductivity increases slightly.

All five subunits of Unit II consist predominantly of coarse ash to lapilli-sized glass and volcanic lithic fragments (Fig. 19), with less abundant accretionary and armored lapilli, set in a fine ash matrix (Figs. 20, 21). In most of the sequence, glass fragments are more abundant than lithic fragments. However, both the abundance of lithic fragments relative to glass and the proportion of red, oxidized lithic fragments are greatest in the lapilli tuff and lapillistone of Subunit IIC. Oxidation of lapilli probably accounts for the distinctively high magnetic susceptibility of Subunit IIC, and the presence of both hematite and magnetite has been confirmed by X-ray diffraction analysis.

Glass shards in Unit II volcaniclastic rocks range from <0.1 to ~10 mm and are predominantly subangular, blocky, and nonvesicular. Slightly to highly vesicular glass shards are relatively rare. Tachylite clasts are found throughout Unit II and form the main component of the

upper and lower parts of Subunit IIC. Lithic fragments are mainly subround and subequant to subelongate and principally comprise nonvesicular and vesicular basalt (generally <10 mm), ranging from partly glassy to microcrystalline and fine grained, with rare fragments of diabase (≤20 mm). Rip-up clasts of tuff (≤65 mm) are also common. Plagioclase and clinopyroxene grains are present as phenocrysts in basaltic lithic fragments and as discrete clasts; as clasts, they are generally anhedral, showing signs of mechanical transport and/or fracturing. Accretionary (Fig. 20) and armored lapilli (≤15 mm) are present in all the subunits and are sometimes concentrated in bands.

We interpret the accretionary and armored lapilli, together with abundant blocky glass shards, to indicate that these deposits were formed by explosive hydroclastic eruptions in a shallow-water to emergent eruptive setting (Fig. 22). The presence of nannofossils in finer-grained intervals of tuff suggests primary deposition or reworking in a marine environment, and wood fragments and organic-rich layers indicate proximity to a vegetated island. Several features indicate that a component of the volcaniclastic material was derived from subaerial eruptions. These include the presence of vesicular tachylite lapilli throughout the volcaniclastic sequence, two intervals of well-sorted lapillistone (consisting almost entirely of nonvesicular tachylite at the top and bottom of Subunit IIC), and the abundant red, oxidized lithic fragments in Subunit IIC.

The entire 337.7-m volcaniclastic sequence cored at Site 1184 is altered to varying extents, and the uppermost 8 m are completely altered to pale brown Fe oxyhydroxide, indicative of weathering in an oxidizing (subaerial?) environment. Except for plagioclase and clinopyroxene, almost all of the volcanic components and matrix are heavily altered to smectite, analcime, celadonite, calcite, zeolite, pyrite, and Fe oxyhydroxide. Unaltered glass is present in several cores (most commonly below ~470 mbsf); individual shards are typically rimmed by brown smectite (Fig. 23). From rim to center, the most commonly observed assemblage of secondary minerals in individual glass fragments follows the progression: smectite; analcime and/or other zeolites; rare calcite. The cement between individual clasts is predominantly composed of the same minerals as those replacing glass. Rare pleochroic, blue-green celadonite is also tentatively identified in the cement, filling vesicles in glass and partly replacing individual glassy fragments. The zeolites identified by X-ray diffraction are gmelinite, chabazite, levyne, and natrolite, an assemblage rarely found in submarine basalt but common in subaerial environments. Several generations of white, hairline to >5-mm-wide veins cut the cores; these veins are filled with analcime ± other zeolites ± calcite and lined with minor smectite and/or celadonite. Haloes in the groundmass adjacent to veins are rare, diffuse, and poorly developed; if present, they typically extend <1 cm into the wall rock and contain smectite and bluish celadonite or brown Fe oxyhydroxide.

Despite the middle Eocene biostratigraphic age of the volcaniclastic rocks, their chemical compositions are similar to those of the 122-Ma Kwaimbaita-type basalt flows and many of the 90-Ma lavas, such as those at Site 803 (Figs. 11, 12, 13). This result suggests that a fertile portion of the distinctive mantle source from which much of the Ontong Java Plateau appears to have been derived remained beneath this part of the eastern salient for 50–80 m.y. In the light of

shipboard inductively coupled plasma–atomic emission spectroscopy (ICP-AES) analyses, it now seems unlikely that the Samoan hot spot provided much, if any, material for volcanism at Site 1184, although it potentially could have provided a source of heat for melting.

The major results of drilling at Site 1184 are summarized as follows:

1. Nannofossil evidence suggests a middle Eocene age for the volcaniclastic sequence drilled; much of the sequence appears to have been deposited within zone NP16. The volcanism at Site 1184 could be contemporaneous with the major change in Pacific plate motion at about 43 Ma (e.g., Duncan and Clague, 1985). The volcaniclastic sequence is much younger than the main phase of construction of the Ontong Java Plateau but similar in age to the 44-Ma alkalic Maramasike Formation in Malaita (Tejada et al., 1996). However, shipboard elemental data show that the volcaniclastic rocks at Site 1184 are composed of tholeiitic basalt clasts, the bulk composition of which resembles that of the widespread 122-Ma Kwaimbaita-type basalt or the similar basalts erupted at 90 Ma. A contribution of Samoan hot-spot mantle in Eocene magmatism at Site 1184 appears unlikely.
2. The abundance of blocky, vesicle-free glass shards implies that the volcaniclastic deposit was formed by hydroclastic eruptions, through the interaction of magma with shallow water. The abundant accretionary lapilli support this conclusion because they form only in steam-rich, subaerial eruption columns.
3. The virtual absence of lapilli larger than 20 mm suggests that the tuffs could not have accumulated close to the center of eruption. Deposition on the margin of a shoaling submarine volcano provides the most likely explanation for the volcaniclastic sequence.
4. Deep subaerial weathering at the top of the basement section, coupled with the nonmarine zeolite assemblage, indicates that this part of the eastern salient was above sea level initially. Proximity to land also is suggested by wood fragments found in organic-rich ash layers in the volcaniclastic sequence. However, the presence of nannofossils shows that at least some of the tuff was deposited in seawater.

Site 1185

Site 1185 is on the eastern edge of the main or high Ontong Java Plateau, at the northern side of an enormous submarine canyon system (informally termed the Grand Canyon of the plateau) that extends from Ontong Java and Nukumanu atolls into the Nauru Basin (Fig. 1). This part of the plateau is far from sites where basaltic basement crust was sampled previously, the closest being ODP Site 803 (334 km to the north-northwest) and DSDP Site 289 (351 km to the west). We chose this site for two principal reasons. Firstly, the portion of basement volcanic stratigraphy that we could sample by drilling was likely to be different in this part of the plateau from that in more centrally located areas. In particular, only relatively few, far-traveled lava flows may have reached the edge of the plateau, and it might be possible to sample deeper stratigraphic levels here than atop the plateau. Secondly, the 26 m of lava flows penetrated at ODP Site 803 (the only other basement site on the eastern side of the high plateau) belong to the

90-Ma eruptive event (Mahoney et al., 1993). Basement at other sites drilled on the high plateau (Sites 289, 807, and 1183) formed around 122 Ma. We thought it possible that 90-Ma basement might also be found at Site 1185; indeed, seismic reflection data (Fig. 24) reveal intrabasement reflectors in this part of the plateau, suggesting that a carapace of 90-Ma lava flows might overlie 122-Ma basalt. If so, drilling at Site 1185 would provide further insight into the extent, composition, and mantle sources of the poorly understood 90-Ma event, documented previously at Site 803 and far to the south in lava sequences on the islands of Santa Isabel (Tejada et al., 1996; Parkinson et al., 1996) and San Cristobal (Birkhold-VanDyke et al., 1996) and in ash layers at DSDP Site 288 (Andrews, Packham, et al., 1975).

We drilled two holes at Site 1185 (Table 1), the first of which was a pilot hole to determine the depth to basement and the length of casing necessary to attach to a reentry cone at the second hole. In Hole 1185A, we started coring sediments at 250.6 mbsf, contacted basaltic basement at 308.5 mbsf, and cored basement rocks to 328.7 mbsf. In Hole 1185B (20 m west of Hole 1185A), we started coring at 308.0 mbsf, contacted basaltic basement at 309.5 mbsf, and cored basement to 526.1 mbsf. We recovered 14.1 m of the 57.9-m sedimentary section cored in Hole 1185A (Fig. 25). The dominant lithology is middle to upper Eocene radiolarian nannofossil chalk, which gradually darkens downward from white to light gray. Maximum bulk density is 1.6 g/cm^3. The most distinctive features of the chalk are its abundant siliceous microfossils and a highly variable abundance (in places, a virtual absence) of planktonic foraminifers, suggesting that deposition was often below the foraminifer lysocline. Foraminifers preserved in the chalk indicate a middle to upper Eocene unconformity that may be associated with a rise in the CCD. Eocene siliceous chalk similar to that at Site 1185 has been found at other DSDP and ODP sites on the Ontong Java Plateau.

The basement sequence consists of pillow basalt and massive basalt flows. We did not recover the sediment-basalt contact in either Hole 1185A or 1185B, but rare intercalations of limestone are present between lava flows and in fissures within the basalt. The limestone is composed of micritic calcite with very rare and poorly preserved nannofossils, foraminifers, and radiolarians that provide only rough age control but reveal that limestones of two ages are present. Extremely rare nannofossils in limestone within the upper 15 m of basement indicate a latest Cenomanian to Albian (possibly late Albian) age, whereas recrystallized planktonic foraminifers in thermally metamorphosed limestone 126 m below the top of basement suggest a late Aptian age. This difference in age between the upper and lower parts of the basement section corresponds to differences in basalt petrography, composition, and alteration. The entire basement sequence exhibits normal magnetic polarity, compatible with this range of ages, and paleolatitudes derived from paleoinclination data agree well with those for Site 1183. The ~50-m.y. hiatus between the lower sediments and basement suggests that this site may have been below the CCD much of the time from the Late Cretaceous to middle Eocene.

In Hole 1185A, we cored 20.2 m of pillow basalt (308.5 to 328.7 mbsf; 55% average recovery). The pillows have glassy rims, spherulitic chilled margins, and fine-grained interiors. We divided the basalt into five units (Fig. 26) on the basis of apparent limestone interbeds, some of which may be only interpillow fill. The 216.6 m of basaltic basement penetrated in Hole

1185B (309.5 to 526.1 mbsf; 42% average recovery) exceed the previous maximum on the plateau of 149 m of lava flows penetrated at Leg 130 Site 807 (Kroenke, Berger, Janecek, et al., 1991). We divided the 216.6-m basement section of Hole 1185B into 12 units ranging in thickness from 1 to 65 m. Units 1, 3, 4 and 6–9 were identified as pillow basalt on the basis of glassy rims and grain-size variations, and Units 2 and 5 are more massive lava flows with pillowed tops and bases. Units 1–9 are separated by thick (as much as 70 cm) intervals of hyaloclastite breccia composed of pillow-rim fragments cemented by carbonate and clay. Units 10–12 are massive flows. The flow tops of Units 10 and 12 are marked by carbonate- and clay-cemented breccia; the top of Unit 11 was not recovered but was inferred from the presence of vesicles, a pronounced change in alteration, and a marked increase in drilling rate over an interval of about 3 m.

The basalt in Hole 1185A and in Units 1–9 of Hole 1185B is sparsely to moderately olivine phyric and generally highly veined. Olivine, the only common phenocryst phase, varies from fresh, in the glassy and aphanitic rims of pillows, to completely replaced by smectite, Fe oxyhydroxide, or calcite. Tiny octahedral crystals of chrome spinel are present, often as inclusions in the olivine phenocrysts (Fig. 27). Aphanitic pillow margins display a prominent spherulitic texture (Fig. 28) that grades into variolitic texture in fine-grained pillow interiors. The massive units also have variolitic texture and are less heavily veined. Units 10–12 in Hole 1185B contain small, sparse phenocrysts of plagioclase and clinopyroxene in addition to olivine. These rocks are similar in appearance to the basalt flows at Sites 1183 and 1186 and, like them, contain plagioclase-rich xenoliths. Shipboard ICP-AES analyses show that Units 10–12 are also very similar in composition to basalt at Sites 1183 and 1186 (Figs. 10, 11, 12, 13). For example, all have $TiO_2 \approx 1.1$ wt%, Cr ≈ 200 ppm, and Zr ≈ 60 ppm and appear to belong to the widespread Kwaimbaita magma type. In contrast, the overlying basalt flows (those in Hole 1185A, and Units 1–9 in Hole 1185B) have the lowest concentrations of incompatible elements ($TiO_2 \approx 0.7$ wt%; Zr ≈ 38 ppm; Fig. 12) yet recorded in basalt from the Ontong Java Plateau. Furthermore, Units 1–8 are composed of the most primitive, magnesium-rich basalt (MgO 8–10 wt%; Cr ≈ 460 ppm) yet found on the plateau (Figs. 11, 13). This combination of elemental characteristics appears to indicate that the magmas formed by even higher total fractions of partial melting than other Ontong Java Plateau basalt (see "Background" section above).

Bulk densities are higher (>2.4 g/cm^3) in Units 2, 5, 10, and 11 than in Units 3 and 6–9 (<2.3 g/cm^3). Both grain and bulk density decrease downhole in Units 4–9, corresponding to a change from massive to highly veined pillow basalt, and bulk density increases with the change from veined to massive basalt from Unit 9 to Units 10–12. *P*-wave velocities are generally >5000 m/s in the dense basalts of Units 2 and 10–12 and generally <5000 m/s in the veined basalts of Units 3 and 6–9.

Seawater-derived fluids have interacted pervasively at low temperatures with the basaltic basement, and we can divide the basement section into two groups of flows with different alteration characteristics. One group consists of all the basement units of Hole 1185A and Units 1–9 of Hole 1185B. Alteration in these units occurred under highly oxidizing conditions and with high water:rock ratios, as indicated by light and dark yellow-brown colors near glassy and

aphanitic pillow margins; these colors fade to gray-brown and dark gray in coarser-grained pillow interiors. The yellow-brown colors are a result of the complete replacement of olivine and pervasive alteration of groundmass by smectite (saponite and nontronite) and Fe oxyhydroxide. Although olivine phenocrysts are commonly completely replaced, rare unaltered olivine is present in aphanitic, dark gray to black areas interpreted as pillow rims. These characteristics are significantly different from the style of alteration in basalt at Site 1183.

The other alteration type comprises Units 10–12 at Hole 1185B. The top of Unit 10 marks a dramatic change in alteration character, and the brecciated top of this unit consists of angular basalt fragments that are the most pervasively altered yet observed on Leg 192. Such severe alteration is likely to be the result of exposure of very permeable basaltic seafloor to bottom seawater for an extended period of time (several million years). Groundmass alteration in Units 10–12 is characterized by pervasive celadonite. Unaltered glass is much rarer in these units than in Units 1–9, but this may be a consequence of the greater flow thickness rather than the level of glass alteration. Broad (centimeter scale) green-gray halos developed near veins; wider reduction fronts consisting of scattered pyrite grains in the groundmass extend a few millimeters to a few centimeters beyond these halos. Smaller (millimeter scale) olive halos similar to those at Site 1183 also are developed near veins, both within green-gray halos and where green-gray halos are absent.

Veins throughout the basement sequence predominantly contain calcite, zeolites (phillipsite), smectite, Fe oxyhydroxide, and rare celadonite and pyrite. Some veins were probably produced by sediment filling open fractures in the basalt; these veins are a few centimeters to <5 mm wide, are filled with pink carbonate and Fe oxyhydroxide, and contain recrystallized foraminifers. They are present both near the boundaries and within the interiors of basaltic units.

The major results of drilling at Site 1185 are summarized as follows:

1. The 60 m of white to light-gray radiolarian nannofossil chalk immediately above basement are of middle to upper Eocene age. The most distinctive feature is the abundance of siliceous microfossils and, in places, a nearly complete absence of planktonic foraminifers, suggesting that many of the sediments were deposited below the foraminifer lysocline. Recovered foraminifers indicate a middle-to-upper Eocene unconformity that may be associated with a rise in the CCD.
2. A hiatus on the order of 50 m.y. separates the sedimentary succession from the basaltic basement.
3. Extremely rare calcareous nannofossils recovered from limestone between basalt flows in the upper 15 m of basement indicate an Albian to latest Cenomanian age. Recrystallized planktonic foraminifers found within thermally altered limestone 126 m below the sediment-basement contact in Hole 1185B tentatively suggest a late Aptian age.
4. The basaltic lava flows in Hole 1185B can be divided into two major groups. The upper group appears to have been erupted sometime between the latest Cenomanian and Albian; the lower group is Aptian in age.

5. The two basalt groups have distinct chemical compositions. The older group is very similar to the basalt at Sites 1183 and 1186 and appears to represent the abundant Kwaimbaita magma type. The younger group has much lower concentrations of incompatible elements and includes the most primitive (magnesian) basalt yet found on the plateau.
6. Different styles of alteration in the two groups of basement lava flows suggest that the older group was in contact with seawater for a long period before the eruption of the younger group. This observation is consistent with the paleontological evidence that suggests a >15-m.y. hiatus between the two groups.

Site 1186

The plan for Leg 192 included a site on Stewart Arch within the territorial waters of the Solomon Islands (proposed Site OJ-7; see Fig. 1). However, the Solomons were in a state of civil and political upheaval throughout much of 2000, and ODP and the U.S. State Department were unable to obtain clearance for this site before the cruise. By midcruise, it was evident that clearance would not be forthcoming in time (if at all) to drill the site. We therefore chose Site 1186, on the eastern slope of the main Ontong Java Plateau, 206 km west of Site 1185, 319 km east of Site 1183, and 149 km east-southeast of DSDP Site 289 (Figs. 1, 2). The very different volcanic stratigraphy at Sites 1183 and 1185, particularly our discovery of high-Mg, low-Ti basalt of probable latest Cenomanian to Albian age at Site 1185, highlighted the importance of a site at a location intermediate between the crest and eastern edge of the main plateau.

Approximately 12 km east-northeast of Site 1186 the seismic-reflection data show a small body, interpreted to be an igneous intrusion or small volcanic cone, rising into the sedimentary sequence ~500 m above the surrounding acoustic basement (Fig. 29). Emanating from this body toward the drill site is a package of high-amplitude and continuous reflections that could represent a sill, lava flow, or volcaniclastic sediments. Alternatively, it could represent pelagic sediments altered by hydrothermal fluids derived from the igneous body. A secondary reason for selecting Site 1186 was to core this reflection package. If it proved to represent a sill or lava flow, it would provide information on the poorly known late-stage magmatism seen in seismic reflection records across much of the high plateau (Kroenke, 1972; Nixon, 1980) and in the 34-Ma alnöite intrusions and 44-Ma alkalic Maramasike Formation lavas on Malaita (e.g., Davis, 1977; Nixon and Neal, 1987; Tejada et al., 1996).

We began coring at 697.4 mbsf. The lithologic units recognized at this site parallel those at other sites on the main Ontong Java Plateau, except that the Oligocene–Neogene chalk and ooze, designated as Unit I elsewhere on the plateau (and presumed to be present at Site 1186), were not cored. Recovery of Paleocene–Eocene Unit II (697.4-812.7 mbsf; see Fig. 30) was generally <5%. The rocks recovered are white limestone and chalk with faint burrow mottling and dark reddish gray to olive-brown chert interbeds. The lowest core of Unit II contains numerous thin gray beds of zeolite-rich chalk, which were interpreted to be altered volcanic ash layers at other sites on the main plateau. No material indicative of a late-stage lava flow or sill was recovered.

Despite the low overall recovery in this unit, the abundance of chert suggests that the seismic reflector package mentioned above represents a particulary chert-rich interval of sediment.

Unit III (812.7 mbsf to the contact with basaltic basement at 968.6 mbsf; Fig. 30) is Cretaceous chalk and limestone. The upper 118 m (Subunit IIIA; Campanian–Maastrichtian) consists of white to brownish white chalk, and the lower 38 m (Subunit IIIB; Aptian–Albian) is mottled light gray and dark brown limestone with minor clay beds. The division between the subunits is marked by a clay-rich band at 930.55 mbsf. As at Site 1183, this band marks a major hiatus (~13 m.y.) in carbonate deposition between the upper Albian and upper Coniacian. Other prominent hiatuses common to both Sites 1186 and 1183 are middle Albian (10 m.y.), uppermost Maastrichtian (2 m.y.), and middle Danian through middle Selandian (4 m.y.). Paleoenvironmental differences between Sites 1183 and 1186 are probably mostly a result of the greater paleodepth of Site 1186 and include a longer period of deposition in the Late Cretaceous below the foraminifer lysocline at Site 1186 (late Albian through early Maastrichtian) than at Site 1183 (late Albian through earliest Campanian).

The lowermost three beds above basement are a yellowish brown limestone overlying a bioturbated transition to a 5-cm-thick interval of dark brown ferruginous claystone, which in turn lies atop a 0.5-cm layer of breccia containing angular basaltic glass fragments. The limestone is late early Aptian in age (upper *Leupoldina cabri* Zone) and contains a small hiatus marking the absence of the planktonic foraminifer *Globigerinelloides ferreolensis* and calcareous nannofossil NC7B zones. The 65.4 m of basement penetrated (with 59% average recovery) at Site 1186 consists of basalt lava flows with minor interbeds of yellowish brown sandstone and one interval of reddish brown conglomerate containing rounded limestone clasts (Fig. 31). Fractures in some of the flows are filled with pale brown, partially recrystallized limestone breccia.

Site 1186 was the only hole logged during Leg 192. High-quality logs were acquired in igneous basement and in parts of the cored sedimentary interval. We tentatively interpret a strong seismic reflection in the sedimentary section at 4.57 s two-way traveltime (~720 mbsf; see Fig. 29) as an ~11-m-thick chert or chert-dominated interval. The Aptian–Albian limestone appears to be thinly and regularly bedded. The sharp boundary between sedimentary and igneous rock is well defined on conductivity, porosity, density, and, particulary, Formation MicroScanner logs. Using the same logs, we can distinguish between pillowed and massive intervals within igneous basement.

We divided the basement section (968.6–1034.0 mbsf) into four units on the basis of limestone and hyaloclastite interbeds and downward changes in character from massive to pillowed. The units range from 10 to >26 m in thickness (Fig. 32). Basement Unit 1 consists entirely of pillow lava, whereas Units 2–4 have massive interiors. The basalts are sparsely olivine (± plagioclase) phyric. All olivine is altered and usually replaced by dark green clay. The pillows have glassy rims (commonly containing some unaltered glass), aphanitic outer zones, and fine-grained interiors. In the massive flows forming most of Units 2–4, the transition from aphanitic flow tops to coarser-grained interiors occurs over several meters and is marked by an intermediate zone with a patchy texture varying between fine grained and aphanitic on a scale of

a few millimeters. Olivine phenocrysts are concentrated in the coarser patches and are rare to absent in the aphanitic parts (Fig. 33).

Plagioclase xenocrysts (>2 mm) and, more rarely, plagioclase-rich xenoliths are present throughout the entire basalt section and are more common in the massive intervals. They are similar to the xenocrysts and xenoliths that we reported from Site 1183 and from the lower group of lava flows at Site 1185. Seven bulk-rock lava samples analyzed by shipboard ICP-AES are closely similar in chemical composition to basalt at Site 1183, the lower group at Site 1185B, Units C–G at Site 807, and the Kwaimbaita Formation on the island of Malaita (Figs. 10, 11, 12, 13). The basalt flows all have normal magnetic polarity and give a 23°S paleolatitude, which agrees well with values obtained from basalt of similar age at Sites 1183 and 1185.

The entire section of basaltic basement cored at Site 1186 has undergone low-temperature water-rock interactions resulting in complete replacement of olivine and almost complete replacement of glassy mesostasis. Clinopyroxene and plagioclase are generally unaltered. The overall alteration of the basalt ranges from 5% to 35% by volume, estimated visually by color distribution in hand specimen. On the whole, the alteration is similar to that in the lower group of basalt flows at Site 1185 and especially to that at Site 1183. The effects of the same three main low-temperature alteration processes are clearly seen:

1. Black and dusky green halos resulted from the replacement of olivine phenocrysts and groundmass glass by celadonite, Fe oxyhydroxide, and, to a minor extent, smectite.
2. Brown halos formed by the complete replacement of olivine and glass by smectite and Fe oxyhydroxide as a result of strongly oxidative alteration at high water:rock ratios.
3. Pervasive alteration under anoxic to reducing conditions and low water:rock ratios has affected the basalt in areas outside the colored halos. Smectite, pyrite, and calcite are the principal secondary minerals formed during this process.

Veins in the basement rocks are lined with smectite or celadonite and filled with calcite. Veined basalt has lower bulk density than does unveined basalt (<2.4 g/cm^3 compared with >2.4 g/cm^3), lower *P*-wave velocity (<5000 m/s compared with >5000 m/s), and lower magnetic susceptibility.

The major results of drilling at Site 1186 are summarized as follows:

1. The sedimentary sequence closely parallels those at other sites on the main Ontong Java Plateau.
2. Biostratigraphy indicates a major hiatus (~13 m.y.) in carbonate deposition between the upper Albian and upper Coniacian, as at Site 1183. Other significant hiatuses at both sites are middle Albian (10 m.y.), uppermost Maastrichtian (2 m.y.), and middle Danian through middle Selandian (4 m.y.).

3. Basement at Site 1186 consists of basaltic pillow lava and massive lava flows. It is probably of similar age to basement at Site 1183; both are immediately overlain by upper lower Aptian (~118 Ma in the time scale of Gradstein et al., 1995) limestone.
4. The basalt is similar in chemical composition to basalt from Site 1183, the lower group of flows at Site 1185, Units C–G at Site 807, and the Kwaimbaita Formation on Malaita. The types and amounts of basalt alteration at Site 1186 are very similar to those at Site 1183.
5. The basalt flows have normal magnetic polarity and yield a paleolatitude of 23°S, which agrees well with that obtained from basalt of similar age at Sites 1183 and 1185.

Site 1187

We decided to drill Site 1187 while coring at Site 1186. By the time we had penetrated ~50 m into basement at Site 1186, it was clear from shipboard ICP-AES analyses that the basalt was of the widespread, remarkably homogeneous, ~122-Ma Kwaimbaita magma type found at Site 1183 and in the lower 92 m of basement at Site 1185. The bottom of the Kwaimbaita-type lava sequence has not been reached in any of the locations where such lavas have been encountered. This sequence is >100 m thick at Site 807 (Units C–G) (Kroenke, Berger, Janecek, et al., 1991), and on the island of Malaita the Kwaimbaita Formation is >2.7 km thick (Tejada et al., 2000). Furthermore, our rate of penetration in basement was low, and there was risk involved in reentering (after an imminent drill-bit change) an uncased >900-m-deep hole in chert-rich sediment. These considerations led us to believe that attempting to deepen Site 1186 would be less likely to provide fundamental new information about the age, composition, or mantle sources of the Ontong Java Plateau than would drilling at a new site.

A site somewhere between Site 1185 and Site 803 would be particularly useful because, unlike other sites on the main plateau, Sites 803 and (on the basis of shipboard biostratigraphic data) 1185 contain basalt that is younger than 122 Ma, and the lava flows in the upper 125 m of basement at Site 1185 are compositionally different from any seen elsewhere on the plateau. We therefore selected Site 1187 (Fig. 1), near Site 804 (which did not reach basement) on the eastern edge of the main plateau. Site 1187 is 194 km southeast of Site 803, 146 km north of Site 1185, and <3 km from the easternmost point where Ontong Java Plateau basement can be distinguished easily, on seismic records, from that of the Nauru Basin (Fig. 34). Our principal objectives at Site 1187 were to establish the composition, age, and eruptive environment of the basement volcanic rocks and to compare them with those of lavas sampled at Sites 803 and 1185. In particular, we wanted to determine whether basement in this region was emplaced during the ~122-Ma or later magmatic events, or both.

We encountered basaltic basement at 372.5 mbsf (Table 1), ~40 m shallower than estimated from the seismic record. We had begun coring at 365.5 mbsf and recovered only 1.36 m of the sedimentary succession above basement. The sediment recovered consists of dark brown ferruginous claystone that grades downward from burrow mottled to laminated and overlies an ~2-cm-thick chalk layer. Biostratigraphic analysis of the claystone indicates an age of late Aptian to Albian. The chalk layer, which immediately overlies basalt, contains a late Aptian

foraminiferal assemblage, including the planktonic taxa *Globigerinelloides ferreolensis, Blowiella duboisi* and *Blefuscuiana praetrochoidea,* and a lower-slope benthic assemblage. The calcareous nannofossils *Eprolithus floralis* and *Hayesites irregularis,* present without any Albian-restricted species, are consistent with a late Aptian age for the chalk. Washed residues of the overlying claystone very rarely contain the planktonic foraminifer *Globigerinelloides aptiensis,* indicating an age range of late Aptian to middle Albian. A single, questionable specimen of the Albian taxon *Blefuscuiana albiana* was also recovered. The claystone residues are dominated by fish-bone fragments and small ferromanganese nodules, suggesting slow accumulation below the CCD.

A 70-cm-thick interval of the claystone is reversely magnetized. The late Aptian to Albian biostratigraphic age of the claystone suggests that this interval may be ISEA, a short reverse-polarity subchron (~115 Ma) within the Cretaceous normal superchron. The underlying basalt flows all exhibit normal polarity. Paleoinclination data for the basalt indicate a paleolatitude of 19°S, essentially the same as at Site 1186 and within error of values for Sites 1183 and 1185.

We cored 135.8 m of basaltic basement, which we divided into 12 units (ranging in thickness from 0.7 to 41.3 m; Fig. 35) on the basis of recrystallized limestone, significant (>10 cm thick) hyaloclastite interbeds, and/or downward changes in basalt structure from massive to pillowed (e.g., the contact between Units 6 and 7). Most of the sequence consists of pillow-lava flows. The only unequivocally massive portion is the fine-grained, 9-m-thick base of Unit 6; some basalt interpreted to be from pillows >2 m thick also may be from massive flows.

The rims of the pillows contain both unaltered and altered glass. Basalt inside the rims is aphanitic, generally altered, and often contains spherulitic zones stained by Fe oxyhydroxide. In the larger pillows, the grain size coarsens gradually from aphanitic near the margins to fine grained in pillow interiors. The basalt is aphyric to moderately olivine phyric. Fresh olivine is present in some of the least-altered intervals of fine-grained basalt in pillow interiors and in the massive basalt of Unit 6. Rare, irregular miarolitic cavities (as large as 1 cm × 2 cm) are present in the interiors of pillows and in the massive portion of Unit 6. Shipboard ICP-AES analyses (Figs. 10, 11, 12, 13) show that the basalt is relatively primitive (MgO ≈ 9 wt%; Cr ≈ 485 ppm), like the upper 125 m of lava flows at Site 1185, and virtually identical to them in its unusually low concentrations of incompatible elements (e.g., Zr and Ti). The presence of these distinctive lava flows in >100-m-thick piles at two sites 146 km apart implies that substantial volumes of this type of magma were erupted on the eastern flank of the high plateau after the main plateau-forming eruptions at ~122 Ma.

Seawater-derived fluids have interacted at low temperatures with the basaltic basement, resulting in the most pervasive overall alteration observed on Leg 192. This observation is consistent with the high abundance of relatively small pillows. Alteration occurred under highly oxidizing conditions with high water:rock ratios and resulted in the development of light and dark yellow-brown colors through the complete replacement of olivine and the alteration of groundmass to smectite (saponite and nontronite) and Fe oxyhydroxide near the outer zones of pillow margins. The color grades into dark brown and dark gray in the coarser-grained pillow interiors. Despite the high average level of alteration in the basalt, unaltered glass is relatively

abundant at Site 1187 because of both the large number of individual pillows (i.e., more glassy margins are present per length of core) and the greater thickness of many of the glassy margins compared with those at other Leg 192 sites. Overall, the secondary mineral assemblages and visual characteristics of basalt alteration at all Leg 192 sites are remarkably similar to those seen elsewhere in nonplateau seafloor of varying ages. This similarity indicates that alteration conditions in basement on the Ontong Java Plateau were similar to those operative in typical ocean crust formed at spreading centers.

Veins throughout the basement sequence consist mainly of calcite, zeolites (probably phillipsite with analcime), smectite, Fe oxyhydroxide, and rare celadonite and pyrite. As at Sites 1185 and 1186, the physical properties of basement at Site 1187 strongly reflect the amount of veining and alteration in the basalts. *P*-wave velocities are high (>5300 m/s) in the dense, relatively sparsely veined basalt of Units 6 and 7 and lower (<5300 m/s) in the more abundantly veined basalt of other units. Areas of high magnetic susceptibility also correlate with the presence of dense, unveined basalt, and the mean bulk densities of sparsely veined intervals are >2.7 g/cm^3 vs. <2.7 g/cm^3 in abundantly veined intervals.

The major results of drilling at Site 1187 are summarized as follows:

1. A late Aptian biostratigraphic age for an ~2-cm-thick chalk layer directly above basaltic basement and a late Aptian to Albian age for a ferruginous claystone overlying the chalk suggest that basalt at this site is older than the Albian to latest Cenomanian age indicated for the upper portion of basement at Site 1185.
2. Basement at Site 1187 consists mainly of basaltic pillow lavas, with minor massive flows. Despite the apparent difference in age, the chemical composition of Site 1187 basalt closely resembles that of the upper 125 m of lava flows at Site 1185. Both groups of lavas are significantly less differentiated and poorer in incompatible elements than other Ontong Java Plateau basalts. Relatively large amounts of incompatible element–poor, rather high Mg basalt appear to have been erupted along the eastern edge of the plateau. These rocks represent high total fractions of partial melting, possibly of previously melted mantle.
3. The level of basaltic alteration at Site 1187 is generally greater than at other Leg 192 sites, although fresh glass is present in many of the pillow rims, and unaltered olivine is abundant in some pillow interiors and in the one massive flow. The basalt flows have normal magnetic polarity and yield a paleolatitude of ~19°S, which agrees within error with values obtained for basement at Sites 1183, 1185, and 1186. A 70-cm-thick reversed-polarity interval in the claystone overlying basement may correspond to ISEA, a short reverse-polarity subchron (~115 Ma) within the Cretaceous normal superchron.

DISCUSSION AND SUMMARY

Drilling/Coring Summary

Four of the five sites drilled during Leg 192 are on the main or high plateau, and one is on the northern ridge of the eastern lobe or salient (Fig. 1). The four sites on the main plateau and the three previous DSDP and ODP sites that reached basement form a transect extending eastward from Site 1183 on the crest of the plateau, via Sites 289 and 1186, to Site 1185 on the extreme eastern edge of the plateau. From Site 1185, the transect runs northward along the eastern edge of the plateau to Sites 1187 and 803 and then northwestward to Site 807 on the northern flank. Figure 36, shows the stratigraphic sections drilled at all eight Ontong Java basement sites, with the seven main-plateau sites arranged in order on the transect. Eastern-salient Site 1184 lies off the transect, 586 km to the southeast of Site 1185. The diagram summarizes water depth, sediment thickness, basement penetration, and basement rock types. Basement ages for previously drilled sites are from ^{40}Ar-^{39}Ar dating of basalt and are estimated from biostratigraphic evidence for the Leg 192 sites. Figure 37, shows the present-day water depth to basement at each site, corrected for the effects of sediment loading. Assuming that (1) Aptian basement lies beneath a relatively thin 90-Ma lava sequence at Site 803, (2) all sites (except Site 1184) have subsided by the same amount since the Aptian, and (3) there has been no subsequent tectonic disturbance, Figure 37, should give the relative depths of each site at the time of plateau formation.

Scientific Results

Our principal objectives for this cruise were to establish the composition, age, and eruptive environment of the basement volcanic rocks at each site. We also hoped to determine the early subsidence history from the overlying sedimentary succession at each site and to ascertain the ages of sequence boundaries observed in the seismic record. Many of these objectives were partially met through shipboard studies but will require more comprehensive shore-based work to be achieved fully.

Basement Ages

Shipboard biotstratigraphic analysis brackets the age of basement at Sites 1183 and 1186 between the early and middle Aptian; thus, the upper levels of basement crust at these sites belong to the 122 (±3)-Ma phase of Ontong Java Plateau volcanism. At Site 1185, biostratigraphic age controls on basement are poor but suggest that basalt flows of two ages are present. The upper 15 m (and possibly ~125 m; i.e., the upper group of basalt units in Fig. 26) of lava flows appear to be between latest Cenomanian and Albian, possibly late Albian, in age; that is, micropaleontological data suggest they were emplaced between ~93 and 112 Ma (in the time scale of Gradstein et al., 1995). The lower 92 m of Kwaimbaita-type flows (the lower group in Fig. 26) appear to be late Aptian or older. The simplest interpretation, in the absence of radiometric age data, is that the lower flows belong to the widespread ~122-Ma event and the upper ones to the 90 (±4)-Ma event documented in lava flows at Site 803, on Santa Isabel and

San Cristobal, and in ash layers at DSDP Site 288 (see Fig. 3). The nearly identical, and unusual, low-Ti, high-Mg compositions of the upper group of flows at Site 1185 and the entire lava sequence drilled at Site 1187 suggest that all the low-Ti, high-Mg flows are related and were formed at the same time. However, biostratigraphic data suggest that the Site 1187 flows are late Aptian or older (>115 Ma). Therefore, we have a discrepancy, the resolution of which must await ^{40}Ar-^{39}Ar dating of basalt samples and/or refinement of the biostratigraphic age estimates.

Nevertheless, the evidence now available from Leg 192, combined with age data for Legs 30 and 130 sites, indicates that an immense part of the high plateau was formed in the ~122-Ma event: the central region (Sites 289, 1183, and 1186), northern flank (Site 807), and probably much of the eastern flank (lower group of flows at Site 1185, possibly Site 1187). Basement crust in Malaita and much of Santa Isabel also was formed in this event, and possibly the lowest part of the section exposed in San Cristobal (Neal et al., 2000). With the resolution of existing sampling and ^{40}Ar-^{39}Ar and biostratigraphic ages, the duration of this event could have been as great as ~7 m.y., or much shorter. Importantly, the central region of the main plateau appears to have been largely bypassed by post-122-Ma eruptive episodes. Evidence for these episodes is found exclusively in locations around the eastern margins of the main plateau (Site 803, possibly Site 1187, and the upper group of basalt at Site 1185) and on the eastern salient (Santa Isabel, Malaita, San Cristobal, Site 1184, and in ash layers at Site 288, at the boundary between the salient and main plateau). Thus, the ~90-Ma episode now appears to have been volumetrically minor in relation to the ~122-Ma event and later episodes to have been still less important. This conclusion is one of the major results of Leg 192. In sharp contrast, in the southern and central Kerguelen Plateau and Broken Ridge, substantial volumes of magma appear to have been emplaced over a period of ~30 m.y. (Pringle and Duncan, 2000).

The thick sequence of volcaniclastic rocks at Site 1184 demonstrates that at least locally significant volcanism occurred on the northern part of the plateau's eastern lobe in the middle Eocene (~41–43 Ma in the time scale of Berggren et al., 1995). On the southern part of the eastern lobe, the 44-Ma alkalic lavas of the Maramasike Formation in Malaita (Tejada et al., 1996) reach a maximum thickness of 900 m (Petterson et al., 1997). The age of the Site 1184 volcaniclastic rocks and the Maramasike lavas is close to that of the ~43-Ma major change in Pacific plate motion (e.g., Duncan and Clague, 1985), and it is tempting to suggest that volcanism in one or both cases may have occurred in response to a change in the stress field of the plateau.

Petrology and Geochemistry of Igneous Rocks

Fundamental results of Leg 192 are that Kwaimbaita-type basalt was the only type we encountered at Sites 1183 and 1186 and that it lies below the 125 m of low-Ti, high-Mg basalt at Site 1185. Units C–G at Leg 130 Site 807 on the far northern flank of the high plateau are also of the Kwaimbaita type. Thus, Kwaimbaita-type lava flows cover an immense region of the high plateau. Furthermore, despite the considerable distances separating these sites, the total range of elemental variation is surprisingly small (Figs. 10, 11, 12, 13). Other magma types, whether ~122 Ma or younger, such as the low-Ti, high-Mg basalt discovered on Leg 192 and the

Singgalo type at Site 807, in Santa Isabel, and particularly abundant in Malaita, appear to be present mainly on the margins of the plateau. No Singgalo-type basalt was recovered at any of the Leg 192 sites. We conclude that the Kwaimbaita magma type was by far the most abundant type produced, at least during construction of the upper levels of basement crust. Although shore-based isotopic work on Leg 192 basement samples is needed, the implication from the shipboard elemental data is that the magmas were derived from a very homogeneous and voluminous mantle source.

One of the most exciting discoveries of Leg 192 was the low-Ti, high-Mg basalt of Sites 1185 and 1187, along the eastern edge of the plateau. The Kwaimbaita magma type represents a high total percentage of partial melting, probably on the order of 18%–30% (Mahoney et al., 1993; Tejada et al., 1996; Neal et al., 1997). The low-Ti, high-Mg basalt requires significantly higher total amounts of partial melting. Small amounts of basalt with rather similar elemental characteristics are found along some oceanic spreading axes and in Iceland (Hemond et al., 1993; Hardarson and Fitton, 1997), but understanding how the apparently large volume of these flows on the eastern Ontong Java Plateau originated poses a formidable challenge. An explanation of their origin and of the relationship of their mantle source region to the Kwaimbaita and Singgalo sources awaits more precise knowledge of their age, and comprehensive elemental and isotopic data from shore-based studies.

By the Eocene, the plateau had drifted thousands of kilometers from its 90- and 122-Ma positions (e.g., Yan and Kroenke, 1993). Yet, surprisingly, the mantle source of the Eocene volcanism at Site 1184 appears to have been compositionally similar to the source of the Kwaimbaita-type ~122- and ~90-Ma basalts (e.g., Fig. 12). The same is true of the Paleocene and Eocene tholeiitic basalts in San Cristobal, which closely resemble the older basalt groups both elementally and isotopically (Birkhold-VanDyke et al., 1996; Neal et al., 2000). Although late-stage tholeiitic magmatism could have been caused by upwelling of mantle completely unrelated to the source that formed most of the plateau, the compositional similarity of the later tholeiitic basalts and those formed many tens of millions of years earlier argues that the sources of the later basalts were rather closely related to the mantle that formed the bulk of the plateau. Our working hypothesis is that the sources of such late-stage tholeiitic volcanism resided in fertile portions of the plateau's lithospheric mantle root that did not melt, or possibly were veined (i.e., refertilized) by migrating melts, at 122 (and/or 90) Ma. Such regions would be capable of melting to form tholeiitic magma if heated sufficiently, but the specific causes of melting remain obscure at present.

Basement Paleolatitude

Estimates of basement paleolatitude at Sites 1183, 1185, 1186, and 1187 are in the 19°–25°S range, well to the north of the ~35°–42°S location suggested for the central high plateau between 125 and 90 Ma in the plate reconstruction of Neal et al. (1997) and even farther from the present position of the Louisville hot spot (~50°S) proposed by several workers to be the source of the plateau. Part of the difference may be explained by flexuring and faulting of the plateau's crust associated with postconstructional subsidence, although this possibility remains to be evaluated.

Likewise, the amount of true polar wander and the distance the Louisville hot spot has drifted since the Early Cretaceous (if it existed then) are unknown. Presently, in agreement with Nd-Pb-Sr isotopic data for pre–Leg 192 basement samples and the lack of a postplateau seamount chain corresponding to a plume tail (e.g., Neal et al., 1997; Tejada et al., 2000), the paleolatitude data do not appear to support a Louisville hot-spot origin for the Ontong Java Plateau.

Site 1184 presents a paradox in that the −54° mean magnetic inclination of the volcaniclastic sequence implies a paleolatitude of ~35°S. Assuming the middle Eocene biostratigraphic age is accurate, this value is much farther south than the expected Eocene paleolatitude of ~15°–20°S for this part of the plateau. At this site, postdepositional tilting of the sequence appears unlikely to explain a difference of this magnitude, and we currently have no satisfactory explanation for the discrepancy.

Eruptive Environment and Paleoenvironmental Impact

The volcaniclastic sequence at Site 1184 formed in shallow water but represents magmatism that occurred long after the Aptian phase of plateau construction. Basement rocks at the four Leg 192 sites on the main plateau were emplaced well below sea level, as were those of Sites 289, 803, and 807, and the Ontong Java Plateau basement sections in the eastern Solomon Islands (see “Background” section above). Site 1183, on the crest of the main plateau, appears to have been by far the shallowest site originally (Fig. 37), but the virtually vesicle-free pillow lava flows there were probably erupted at a depth of at least several hundred meters. Indeed, the only evidence that any part of the main plateau was at least briefly shallow or emergent in the Aptian is provided by the two thin (<1 m recovered) layers of laminated vitric tuff deposited as turbidites at the base of the sedimentary sequence at Site 1183, a vitric tuff immediately above basement at Site 289 and, possibly, abundant glass shards in Aptian limestone at Site 288 (Andrews, Packham, et al., 1975). If a large proportion of Ontong Java Plateau magmas were erupted under shallow water or subaerially, then the flux of climate-modifying volatiles (particularly SO_2, Cl, and F) to the atmosphere would have been considerable (e.g., Michael, 1999). Because our results indicate that most of the plateau formed substantially below sea level, its large-scale environmental effects were probably quite limited. The magnitude of hydrothermal exchanges between seawater and the plateau’s magmatic systems is unknown; all of the basement rocks recovered on Leg 192 have been affected only by low-temperature alteration processes. Overall, the types and amounts of alteration at all of the sites are similar to those found in normal (nonplateau) seafloor formed at spreading centers. The only evidence from Leg 192 sediments of relatively short-lived biological "deserts" that might be associated with the huge amount of Aptian volcanism on the plateau is in the thin, barren ferruginous claystone layers immediately above basement at Sites 1183 and 1187.

REFERENCES

Abbott, D., and Mooney, W., 1995. The structural and geochemical evolution of the continental crust: support for the oceanic plateau model of continental growth. *Rev. Geophys. Suppl.,* US Natl. Rept. to IUGG 1991–1994, 231–242.

Albarède, F., 1998. The growth of continental crust. *Tectonophysics,* 296:1–14.

Anderson, D.L., 1996. Enriched lithosphere and depleted plumes. *Int. Geol. Rev.,* 38:1–21.

Andrews, J.E., Packham, G., et al., 1975. *Init. Repts., DSDP,* 30: Washington (U.S. Govt. Printing Office).

Babbs, T.L., 1997. Geochemical and petrological investigations of the deeper portions of the Ontong Java Plateau: Malaita, Solomon Islands [Ph.D. dissertation]. Leicester University, U.K.

Bercovici, D., and Mahoney, J., 1994. Double flood-basalt events and the separation of mantle-plume heads at the 660 km discontinuity. *Science,* 266:1367–1369.

Berger, W.H., Kroenke, L.W., Mayer, L.A., Backman, J.T., Janecek, R., Krissek, L., Leckie, M., Lyle, M., and Shipboard Scientific Party, 1992. The record of Ontong Java Plateau: main results of ODP Leg 130. *Geol. Soc. Am. Bull.,* 104:954–972.

Berggren, W.A., Kent, D.V., Swisher, C.C., III, and Aubry, M.P., 1995. A revised Cenozoic geochronology and chronostratigraphy. *In* Berggren, W.A., Kent, D.V., Aubry, M.P., and Hardenbol, J. (Eds.), *Geochronology, Time Scales and Global Stratigraphic Correlation,* Spec. Publ.- Soc. Econ. Paleontol. Mineral., 54:129–212.

Birkhold-VanDyke, A.L., Neal, C.R., Jain, J.C., Mahoney, J.J., and Duncan, R.A., 1996. Multi-stage growth for the Ontong Java Plateau (OJP)? A progress report from San Cristobal (Makira), Solomon Islands. *Eos,* 77F:714.

Blum, P., 1997. Physical properties handbook: a guide to the shipboard measurement of physical properties of deep-sea cores. *ODP Tech. Note,* 26 [Online]. Available from World Wide Web: <http://www-odp.tamu.edu/publications/tnotes/tn26/INDEX.HTM>. [Cited 2000-10-15]

Campbell, I.H., 1998. The mantle‘s chemical structure: insights from the melting products of mantle plumes. *In* Jackson, I. (Ed.), *The Earth’s Mantle: Composition, Structure, and Evolution:* Cambridge University Press, 259–310.

Castillo, P., Pringle, M.S., and Carlson, R.W., 1994. East Mariana Basin tholeiites: Jurassic ocean crust or Cretaceous rift basalts related to the Ontong Java plume? *Earth Planet. Sci. Lett.,* 123:139–154.

Cloos, M., 1993. Lithospheric buoyancy and collisional orogenesis: subduction of oceanic plateaus, continental margins, island arcs, spreading ridges, and seamounts. *Geol. Soc. Am. Bull.,* 105:715–737.

Coffin, M.F., and Eldholm, O., 1993. Scratching the surface: estimating dimensions of large igneous provinces. *Geology,* 21:515–518.

————, 1994. Large igneous provinces: crustal structure, dimensions, and external consequences. *Rev. Geophys.,* 32:1–37.

Coffin, M.F., and Gahagan, L.M., 1995. Ontong Java and Kerguelen Plateaux: Cretaceous Icelands? *J. Geol. Soc. London,* 152:1047–1052.

Coffin, M.F., Frey, F.A., Wallace, P.J., et al., 2000. *Proc. ODP, Init. Repts.,* 183 [CD-ROM]. Available from: Ocean Drilling Program, Texas A&M University, College Station TX 77845–9547, USA.

Coleman, P.J., 1965. Stratigraphical and structural notes on the British Solomon Islands with reference to the first geological map, 1962. *Report No. 29, British Solomon Islands Geological Record,* 2 (1959–1962):17–33.

Crough, S.T., 1983. The correction for sediment loading on the seafloor. *J. Geophys. Res.,* 88, 6449–6454.

Davis, G.L., 1977. The ages and uranium contents of zircon from kimberlites and associated rocks. *Extended Abstracts 2nd Intl. Kimberlite Conf.,* Santa Fe, New Mexico.

Dick, H.J.B., Mével, C.A., et al., 1996. Report of the ODP-InterRidge-IAVCEI workshop on "The Oceanic Lithosphere and Scientific Drilling into the 21st Century", 26–29 May, 1996, Woods Hole, MA.

Duncan, R.A., 1985. Radiometric ages from volcanic rocks along the New Hebrides-Samoa lineament. *In* Brocher, T.M. (Ed.), *Geological Investigations of the Northern Melanesian Borderland.* Circum-Pac. Coun. Energy and Miner. Resour., Earth Sci. Ser., 3:67–76.

Duncan, R.A., and Clague, D.A., 1985. Pacific plate motion recorded by linear volcanic chains. *In* Nairn, A.E.M., Stehli, F.G., and Uyeda, S. (Eds.), *The Ocean Basins and Margins, 7A:*

New York (Plenum), 89–121.

Furumoto, A.S., Webb, J.P., Odegard, M.E., and Hussong, D.M., 1976. Seismic Studies on the Ontong Java Plateau, 1970. *Tectonophysics,* 34:71–90.

Gladczenko, T.P., Coffin, M., and Eldholm, O., 1997. Crustal structure of the Ontong Java Plateau: modeling of new gravity and existing seismic data. *J. Geophys. Res.,* 102:22711–22729.

Gradstein, F.M., Agterberg, F.P., Ogg, J.G., Hardenbol, J., van Veen, P., Thierry, J., and Huang, Z., 1995. A Triassic, Jurassic and Cretaceous time scale. *In* Berggren, W.A., Kent, D.V., Aubry, M.-P., and Hardenbol, J. (Eds.), *Geochronology, Time Scales and Global Stratigraphic Correlation,* Spec. Publ.[0150] Econ. Paleontol. Mineral., 54:129–212.

Hammond, S.R., Kroenke, L.W., and Theyer, F., 1975. Northward motion of the Ontong Java Plateau between 110 and 30 m.y.: a paleomagnetic investigation of DSDP Site 289. *In* Andrew, J.E., Packham, G., et al., *Init. Repts. DSDP,* 30: Washington (U.S. Govt. Printing Office), 415–418.

Hardarson, B.S. and Fitton, J.G., 1997. Mechanisms of crustal accretion in Iceland. *Geology,* 25:1043–1046.

Hèmond, C., Arndt, N., Lichtenstein, U., Hofmann, A.W., Oskarsson, N., and Steinthorsson, S., 1993. The heterogeneous Iceland plume: Nd–Sr–O isotopes and trace element constraints. *J. Geophys. Res.,* 98:15833–15850.

Hilde, T.W.C., Uyeda, S., and Kroenke, L.W., 1977. Evolution of the western Pacific and its margin. *Tectonophysics,* 38:145–165.

Hill, R.L., 1991. Starting plumes and continental break-up. *Earth Planet. Sci. Lett.,* 104:398–416.

Honnorez, J., 1981. The aging of the oceanic crust at low temperature. *In* Emiliani, C. (Ed.), *The Sea (Vol. 7): The Oceanic Lithosphere*: New York, (Wiley), 525–587.

Hooper, P.R., 1997. The Columbia River flood basalt province: current status. *In* Mahoney, J.J., and Coffin, M.F. (Eds.), *Large Igneous Provinces: Continental, Oceanic and Planetary Flood Volcanism.* Geophys. Monogr., Am. Geophys. Union, 100:1–28.

Hussong, D.M., Wipperman, L.K., and Kroenke, L.W., 1979. The crustal structure of the Ontong Java and Manihiki oceanic plateaus. *J. Geophys. Res.,* 84:6003–6010.

International Hydrographic Organization / Intergovernmental Oceanographic Commission (IHO/IOC), 1997. General Bathymetric Chart of the Ocean (GEBCO) Digital Atlas. *British Oceanographic Data Centre,* London.

Ito, G., and Clift, P.D., 1998. Subsidence and growth of Pacific Cretaceous plateaus. *Earth Planet. Sci. Lett.,* 161:85–100.

Ito, G., and Taira, A., 2000. Compensation of the Ontong Java Plateau by surface and subsurface loading. *J. Geophys. Res.,* 105:11,171–11,183.

Jones, C.E, Jenkyns, H.C., Coe, A.L., and Hesselbo, S.P., 1995. Strontium isotopic variations in Jurassic and Cretaceous seawater. *Geochim. Cosmochim. Acta,* 58:3061–3075.

Kerr, A.C., 1998. Oceanic plateau formation: a cause of mass extinction and black shale deposition around the Cenomanian-Turonian boundary? *J. Geol. Soc. London,* 155:619–626.

Kroenke, L.W., 1972. Geology of the Ontong Java Plateau. *Hawaii Inst. Geophys. Rep.* HIG 72–75.

Kroenke, L.W., 1974. Origin of continents through development and coalescence of oceanic flood basalt plateaus. *Eos,* 55:443.

Kroenke, L.W., Berger, W.H., Janecek, T.R., et al., 1991. *Proc. ODP, Init. Repts.,* 130: College Station, TX (Ocean Drilling Program).

Kroenke, L.W., and Mahoney, J.J., 1996. Rifting of the Ontong Java Plateau‘s eastern salient and seafloor spreading in the Ellice Basin: relation to the 90 Myr eruptive episode on the plateau. *Eos,* 77F:713.

Larson, R.L., and Kincaid, C., 1996. Onset of mid-Cretaceous volcanism by elevation of the 670-km thermal boundary layer. *Geology,* 24:551–554.

Le Bas, M.J., Le Maitre, R.W., Streckeisen, A., and Zanettin, B., 1986. A chemical classification of volcanic rocks based on the total alkali-silica diagram. *J. Petrol.,* 27:745–750.

Macdonald, G.A. and Katsura, T., 1964. Chemical composition of Hawaiian lavas. *J. Petrol.,* 5:82–133.

Mahoney, J.J., 1987. An isotopic survey of Pacific oceanic plateaus: implications for their nature and origin. *In* Fryer, P., Keating, B., Batiza, R., Boehlert, G. (Eds.), *Seamounts, Islands, and Atolls.* Geophys.Monogr., Am. Geophys. Union, 43:207–220.

Mahoney, J.J. and Spencer, K.J., 1991. Isotopic evidence for the origin of the Manihiki and Ontong Java oceanic plateaus. *Earth Planet. Sci. Lett.,* 104:196–210.

Mahoney, J.J., Storey, M., Duncan, R.A., Spencer, K.J., and Pringle, M., 1993. Geochemistry and geochronology of the Ontong Java Plateau. *In* Pringle, M., Sager, W., Sliter W., and Stein, S. (Eds.), *The Mesozoic Pacific: Geology, Tectonics, and Volcanism.* Geophys. Monogr., Am. Geophys. Union, 77:233–261.

Mann, P., Gahagan, L., Coffin, M., Shipley, T., Cowley, S., and Phinney, E. 1996. Regional tectonic effects resulting from the progressive east-to-west collision of the Ontong Java Plateau with the Melanesian arc system. *Eos,* 77F:712.

Mayer, H., and Tarduno, J.A., 1993. Paleomagnetic investigation of the igneous sequence, Site 807, Ontong Java Plateau, and a discussion of Pacific true polar wander. *In* Berger, W.H., Kroenke, L.W., Mayer, L.A., et al., *Proc. ODP, Sci. Results,* 130: College Station, TX (Ocean Drilling Program), 51–59.

McNutt, M. et al., 1996. Intraplate Marine Geoscience: Hot Lips and Cracked Plates. Report of an NSF-sponsored planning workshop, Steamboat Springs, Colorado.

Michael, P.J., 1999. Implications for magmatic processes at Ontong Java Plateau from volatile and major element contents of Cretaceous basalt glasses. *Geochemistry, Geophysics, Geosystems,* 1.

Miura, S., Shinohara, M., Takahashi, N., Araki, E., Taira, A., Suyehiro, K., Coffin, M., Shipley, T., and Mann, P. 1996. OBS crustal structure of Ontong Java Plateau converging into Solomon Island arc. *Eos,* 77F:713.

Neal, C.R., Mahoney, J.J., Kroenke, L.W., Duncan, R.A., and Petterson, M.G., 1997. The Ontong Java Plateau. *In* Mahoney J.J., and Coffin M.F. (Eds.), *Large Igneous Provinces: Continental, Oceanic and Planetary Flood Volcanism.* Geophys. Monogr., Am. Geophys. Union, 100:183–216.

Neal, C.R., Birkhold, A.L., Mahoney, J.J., and Duncan, R.A., 2000. Episodic growth of the Ontong Java Plateau through a single plume event and lithospheric extension. *Geol. Soc. Am. Penrose Conf. On Volcanic Rifted Margins,* London.

Nixon, P.H., 1980. Kimberlites in the south-west Pacific. *Nature,* 287:718–720.

Nixon, P.H., and Neal, C.R., 1987. Ontong Java Plateau: deep-seated xenoliths from thick oceanic lithosphere. *In* Nixon, P.H. (Ed.), *Mantle Xenoliths*: London (John Wiley and Sons, Ltd.), 335–345.

Parkinson, I.J., Arculus, R.J., and Duncan, R.A., 1996. Geochemistry of Ontong Java Plateau basalt and gabbro sequences, Santa Isabel, Solomon Islands. *Eos,* 77F:715.

Petterson, M.G., Neal, C.R., Mahoney, J.J., Kroenke, L.W., Saunders, A.D., Babbs, T.L., Duncan, R.A., Tolia, D., and McGrail, B., 1997. Structure and deformation of north and central Malaita, Solomon Islands: tectonic implications for the Ontong Java Plateau-Solomon arc collision, and for the fate of oceanic plateaus. *Tectonophysics,* 283:1–33.

Petterson, M.G., Babbs, T., Neal, C.R., Mahoney, J.J., Saunders, A.D., Duncan, R.A., Tolia, D., Magu, R., Qopoto, C., Mahoa, H., and Natogga, D., 1999. Geological-tectonic framework of Solomon Islands, SW Pacific: crustal accretion and growth within an intra-oceanic setting. *Tectonophysics,* 301:35–60.

Polat, A., Kerrich, R., Wyman, D.A., 1999. Geochemical diversity in oceanic komatiites and basalts from the late Archean Wawa greenstone belts, Superior Province, Canada. *Precambrian Res.,* 94:139–173.

Pringle, M.S., and Duncan, R.A., 2000. Basement ages from the Southern and Central Kerguelen Plateau: initial products of the Kerguelen large igneous province. *Eos,* 81:424.

Richards, M.A., Jones, D.L., Duncan, R.A., and DePaolo, D.J., 1991. A mantle plume initiation model for the Wrangellia flood basalt and other oceanic plateaus. *Science,* 254:263–267.

Richardson, W.P., Okal, E., Van der Lee, S., 2000. Rayleigh-wave tomography of the Ontong Java Plateau. *Phys. Earth Planet. Inter.,* 118:29–51, 2000.

Sandwell, D.T., and Smith, W.H.F., 1997. Marine gravity anomaly from Geosat and ERS 1 satellite altimetry. *J. Geophys. Res.,* 102:10,039–10,054.

Saunders, A.D., Storey, M., Kent, R.W., and Norry, M.J., 1992. Consequences of plume-lithosphere interactions. *In* Storey, B., Alabaster, T., and Pankhurst, R. (Eds.), *Magmatism and the Causes of Continental Break-up.* Geol. Soc. Spec. Publ. London, 68:41–60.

Saunders, A.D., Tarney, J., Kerr, A.C., and Kent, R.W., 1996. The formation and fate of large oceanic igneous provinces. *Lithos,* 37:81–89.

Smith, A.D., 1993. The continental mantle as a source for hotspot volcanism. *Terra Nova,* 5:452–460.

Smith, W.H.F., and Sandwell, D.T., 1997. Global sea floor topography from satellite altimetry and ship depth soundings. *Science,* 277:1956–1962.

Stein, M., and Hofmann, A.W., 1994. Mantle plumes and episodic crustal growth. *Nature,* 372:63–68.

Stoeser, D.B., 1975. Igneous rocks from Leg 130 of the Deep Sea Drilling Project. *In* Andrews, J.E., Packham, G., et al., *Init. Repts., DSDP,* 30: Washington (U.S. Govt. Printing Office) 401–414.

Storey, M., Mahoney, J.J., Kroenke, L.W., and Saunders, A.D., 1991. Are oceanic plateaus sites of komatiite formation? *Geology,* 19:376–379.

Tarduno, J.A., Sliter, W.V., Kroenke, L., Leckie, M., Mahoney, J.J., Musgrave, R., Storey, M., and Winterer, E.L., 1991. Rapid formation of Ontong Java Plateau by Aptian mantle plume volcanism. *Science,* 254:399–403.

Tarduno, J.A., Brinkman, D.B., Renne, P.R., Cottrell, R.D., Scher, H., and Castillo, P., 1998. Evidence for extreme climatic warmth from Late Cretaceous Arctic vertebrates. *Science,* 282:2241–2244.

Tejada, M.L.G., Mahoney, J.J., Duncan, R.A., and Hawkins, M., 1996. Age and geochemistry of basement rocks and alkalic lavas of Malaita and Santa Isabel, Solomon Islands, southern margin of Ontong Java Plateau. *J. Petrol.,* 37:361–394.

Tejada, M.L., Mahoney, J.J., Neal, C.R., Duncan, R.A., and Petterson, M.G., submitted. Basement geochemistry and geochronology of central Malaita, Solomon Islands, with implications for the origin and evolution of the Ontong Java Plateau. *J. Petrol.*

Wessel, P., and Kroenke, L.W., 1999. Cenozoic changes in Pacific absolute plate motion: cause and effect of Pacific basin tectonism? *Eos,* 80F:979.

Winterer, E.L., 1976. Bathymetry and regional tectonic setting of the Line Islands chain. *In* Schlanger, S.O., Jackson, E.D., et al., *Init. Repts., DSDP,* 33: Washington (U.S. Govt. Printing Office), 731–748.

Winterer, E.L., and Nakanishi, M., 1995. Evidence for a plume-augmented, abandoned spreading center on Ontong Java Plateau. *Eos,* 76F:617.

White, R.S., and McKenzie, D.P., 1989. Magmatism at rift zones: the generation of volcanic continental margins and flood basalts. *J. Geophys. Res.,* 94:7685–7729.

Yan, C.Y., and Kroenke, L.W., 1993. A plate techtonic reconstruction of the Southwest Pacific, 0–100 Ma. *In* Berger, W.H., Kroenke, L.W., Janecek, T.R., et al., *Proc. ODP, Sci. Results,* 130: College Station, TX (Ocean Drilling Program), 697–709.

TABLE CAPTIONS

Table 1. Hole summary for Leg 192.

Table 2. Volcaniclastic facies in Unit II at Site 1184.

FIGURE CAPTIONS

Figure 1. Predicted bathymetry (after Smith and Sandwell, 1997) of the Ontong Java Plateau showing the locations of sites drilled on Leg 192. Solid stars = sites penetrating lava sections. Open star = Site 1184, where a volcaniclastic sequence was recovered. Solid circles = previous ODP and DSDP drill sites that reached basement. Open circles = Site 288, which did not reach basement but bottomed in Aptian limestone, and Site OJ-7, which was proposed for Leg 192 but not drilled (see text). The bathymetric contour interval is 1000 m.

Figure 2. Satellite-derived free-air gravity field of the Ontong Java Plateau region (after Sandwell and Smith, 1997). Solid stars = sites penetrating lava sections. Open star = Site 1184, where a volcaniclastic sequence was recovered. Solid circles = previous ODP and DSDP drill sites that reached basement. Open circles = Site 288, which did not reach basement but bottomed in Aptian limestone, and Site OJ-7, which was proposed for Leg 192 but not drilled (see text). Black lines indicate multichannel seismic surveys on the plateau: *Hakuho Maru* KH98-1 Leg 2 (1998) and *Maurice Ewing* EW95-11 (1995). White lines indicate single-channel seismic surveys: *Glomar Challenger* GC07 (1969), GC30 (1973), and GC89 (1983); *Thomas Washington* TW88-11 (1988); and *JOIDES Resolution* JR130 (1990). The bathymetric contour interval is 1000 m.

Figure 3. Summary of pre–Leg 192 age data for Ontong Java Plateau basement basalt, later lava flows and intrusions on Malaita and San Cristobal, and ash or glass-shard-rich layers within the sedimentary section at Sites 288 and 289 (Tejada et al., 2000). Ages derived from biostratigraphy are shown with error bars; the others are ^{40}Ar-^{39}Ar plateau or, for the Malaitan alnöites, U–Pb zircon ages.

Figure 4. Total alkalis vs. silica diagram (after Le Bas, 1986) for basement rocks recovered at DSDP Site 289 and ODP Sites 803 and 807 on the Ontong Java Plateau. Data are from Stoeser (1975), Mahoney et al. (1993), and Tejada et al. (1996, 2000). The broken line separates Hawaiian alkalic and tholeiitic basalts (Macdonald and Katsura, 1964).

Figure 5. Primitive mantle–normalized incompatible-element averages for basalts of Malaita, Santa Isabel (plus Ramos), and ODP Sites 803 and 807. Shaded fields indicate range of values for central Malaita. From Tejada et al. (2000).

Figure 6. Initial $\varepsilon_{Nd}(t)$ vs. $(^{206}Pb/^{204}Pb)_t$ data for basement lava flows of Santa Isabel and Malaita. Heavily outlined fields encompass data for ODP Site 807 basement Unit A and Sites 803 and 807,

Units C–G. Data for the Site 289 basalt lie in the latter field. Data fields for the Manihiki Plateau (for dredged and DSDP Site 317 lava flows), Nauru Basin, Pacific midocean-ridge basalts (MORB), the Koolau and Kilauea volcanoes of Hawaii, and the Mangaia Group islands of the South Pacific are shown by light outlines (from Tejada et al., 2000).

Figure 7. *Hakuho Maru* KH98-1 Leg 2, line 404, multichannel seismic reflection profile across Site 1183 (see Fig. 2, for location). Vertical exaggeration = ~4.2 at seafloor. CDP = common depth point, UTC = Universal Time Coordinated.

Figure 8. Site 1183 log showing core recovery, lithostratigraphic divisions, schematic lithology, color reflectance, magnetic susceptibility, and carbonate content.

Figure 9. Lithologic log of the basement units at Site 1183 showing the distribution of plagioclase-rich xenoliths, glassy pillow margins, and phenocrysts. Basalt units with the suffix B were delineated by the presence of thin sedimentary interbeds, which are designated as Subunit A (not shown).

Figure 10. Total alkalis vs. silica diagram (after Le Bas, 1986) for basement rocks recovered at all Leg 192 sites. The broken line separates Hawaiian alkalic and tholeiitic basalts (Macdonald and Katsura, 1964).

Figure 11. TiO_2 vs. Mg# for basement rocks recovered at all Leg 192 sites and ODP Sites 803 and 807. The fields for basaltic lava flows of the >2.7-km-thick Kwaimbaita Formation and the overlying ~750-m-thick Singgalo Formation on Malaita (Tejada et al., 1996, 2000) are shown for comparison. Data for Sites 803 and 807 are from Mahoney et al. (1993).

Figure 12. Zr vs. TiO_2 for basement rocks recovered at all Leg 192 sites, DSDP Site 289, and ODP Sites 803 and 807. Data for Sites 803 and 807 are from Mahoney et al. (1993). The fields for basaltic lava flows of the >2.7-km-thick Kwaimbaita Formation and the overlying ~750-m-thick Singgalo Formation on Malaita (Tejada et al., 1996, 2000) are shown for comparison.

Figure 13. Cr vs. TiO_2 for basement rocks recovered at all Leg 192 sites, DSDP Site 289, and ODP Sites 803 and 807. Data for Sites 803 and 807 are from Mahoney et al. (1993). The fields for basaltic lava flows of the >2.7-km-thick Kwaimbaita Formation and the overlying ~750-m-thick Singgalo Formation on Malaita (Tejada et al., 1996, 2000) are shown for comparison.

Figure 14. Close-up photograph showing a 1.5 cm × 3 cm plagioclase-rich xenolith on the outer surface of the core (interval 192-1183A-59R-2 [Piece 10A, 112–119 cm]) .

Figure 15. Paleolatitude, calculated from paleomagnetic inclination, for cores from Hole 1183A. Data are plotted against biostratigraphic age.

Figure 16. Seismic reflection record for Site 1184. *Hakuho Maru* KH98-1 Leg 2, line 101, multichannel seismic reflection profile across Site 1184 (see Fig. 2, for location). Vertical exaggeration = ~4.2 at seafloor. CDP = common depth point, UTC = Universal Time Coordinated.

Figure 17. Summary of lithologic characteristics in the subunits of Unit II at Site 1184, based on the facies defined in Table 2. "Wood" indicates approximate intervals in which pieces of wood were found. The uppermost interval is represented by two pieces, 1–2 cm long and <2 mm thick. At the other three wood-bearing levels, pieces of wood are as long as 6 cm. In the chromaticity plot, a = the variation between green (negative) and red (positive), and b = the variation between blue (negative) and yellow (positive) (Blum, 1997).

Figure 18. Close-up photograph of wood fragments in lithic vitric tuff near the base of Subunit IIE (interval 192-1184A-45R-7, 48–65 cm).

Figure 19. Photomicrograph showing a wide range of lithic and vitric clast types present in a lithic vitric tuff from Subunit IID (Sample 192-1184A-31R-7, 40–43 cm). The clasts include glass shards (light brown), basalt, and tachylite (black). The glass is completely altered to smectite, and the matrix is composed mainly of zeolite (field of view = 5.5 mm wide; plane-polarized light).

Figure 20. Close-up photograph of accretionary lapilli, both whole (round) and broken fragments, in gray lithic vitric tuff, Subunit IIA (interval 192-1184A-14R-1, 58–66 cm).

Figure 21. Close-up photograph of coarse (≤2 cm) angular clasts in lapilli tuff, Subunit IIB (interval 192-1184A-21R-6, 60–80 cm). The large pale clast is diabase.

Figure 22. Schematic interpretation of the eruptive setting of the volcaniclastic rocks at Site 1184. These reworked pyroclastic deposits probably formed on top of a large seamount as it grew to within ~200 m of the sea surface. The presence of basalt at depth is conjectural. A = the presence of blocky, nonvesicular glass shards, suggests fragmentation of rapidly quenched magma in hydromagmatic eruptions under shallow water; abundant tachylite clasts in parts of the succession suggest that this process occurred in an environment that was at times subaerial. B = accretionary and armored lapilli form in the atmosphere, in steam-rich columns of volcanic ash. C = the absence of blocks, bombs, or lapilli >20 mm suggests that the primary pyroclastic deposits did not form close to the eruption center(s). D = wood fragments found at the bases of four of the five subunits indicate proximity to land. E = deposition or redeposition of the volcaniclastic material in a marine setting is indicated by the presence of nannofossils throughout the unit. F = redeposition by turbidity currents is suggested by the presence of rip-up clasts and broken accretionary lapilli and by the absence of the layering that would be expected from material settling through water.

Figure 23. Photomicrograph of lithic vitric tuff from Subunit IIE (Sample 192-1184A-42R-1, 147–150 cm). Rims of glass shards are altered to smectite (field of view = 2.8 mm wide; plane-polarized light).

Figure 24. *Hakuho Maru* KH98-1 Leg 2, line 401, multichannel seismic reflection profile across Site 1185 (see Fig. 2, for location). Vertical exaggeration = ~4.2 at seafloor. CDP = common depth point, UTC = Universal Time Coordinated.

Figure 25. Site 1185 log showing core recovery, lithostratigraphic divisions, schematic lithology, color reflectance, carbonate content, and components of sediments. In the color column, L = the total reflectance and indicates lighter shades to the right; a and b quantify the hue as chromaticity, where a = variation between green (negative) and red (positive) and b = variation between blue (negative) and yellow (positive) (Blum, 1997). Component percentages are from observation of smear slides and thin sections.

Figure 26. Lithologic log of basement units at Site 1185. The upper and lower groups of units in Hole 1185B are distinct in their petrography, composition, state of alteration, and biostratigraphic age (see text for details).

Figure 27. Photomicrograph of olivine phenocrysts and tiny octahedral crystals of chrome spinel in a quenched pillow margin (Sample 192-1185A-8R-1 [Piece 2, 15–18 cm]). The groundmass consists of glass with dendritic microlites (field of view = 0.28 mm wide; plane-polarized light).

Figure 28. Close-up photograph showing spherulitic texture in an aphanitic pillow margin, basement Unit 1 (interval 192-1185B-3R-1, 54–63 cm). The spherulites are highlighted by alteration.

Figure 29. *Hakuho Maru* KH98-1 Leg 2, line 403, multichannel seismic reflection profile across Site 1186 (see Fig. 2). Vertical exaggeration = ~4.2 at seafloor. CDP = common depth point, UTC = Universal Time Coordinated.

Figure 30. Lithologic log and selected properties of sediments at Site 1186. There was no coring from 0 to 697.4 mbsf. In the color column, L = the total reflectance and indicates lighter shades to the right; a and b quantify the hue as chromaticity, where a = the variation between green (negative) and red (positive) and b = the variation between blue (negative) and yellow (positive) (Blum, 1997). Component percentages are from observation of smear slides and thin sections. Higher values of magnetic susceptibility generally correlate with bands rich in volcanic ash (e.g., Core 192-1186A-13R) or with claystone (e.g., Core 192-1186A-26R and base of sedimentary sequence in Core 192-1186A-30R). Natural gamma-radiation intensity is from the Formation MicroScanner tool run; medium-penetration resistivity and caliper of borehole diameter are from the geophysical tool run.

Figure 31. Close-up photograph of limestone conglomerate between lava flows in Hole 1186A (interval 192-1186A-32R-3, 65–93 cm).

Figure 32. Lithologic log of basement units at Site 1186 showing the distribution of plagioclase-rich xenoliths, glassy pillow rims, and vesicles. Dashed line = unit boundary. The location of the Unit 3/Unit 4 boundary is uncertain because of poor recovery. However, formation microscanner logging tool images suggest that the top of Unit 4 consists of ~9 m of pillow basalt.

Figure 33. Photomicrograph of plagioclase laths and sprays of clinopyroxene crystals in basalt from the interior of massive flow Unit 2 (see Fig. 32) (Sample 192-1186A-34R-2, 143–146 cm; field of view = 2.8 mm wide; crossed polars).

Figure 34. *Thomas Washington* 88-11 single-channel seismic-reflection profile across Site 1187 (see Fig. 2, for location). Vertical exaggeration = ~6.67 at seafloor. CDP = common depth point, UTC = Universal Time Coordinated.

Figure 35. Lithologic log of basement units at Site 1187 showing the thickness of individual cooling units defined by the presence of glassy or aphanitic margins. Cooling units <1.5 m thick are probably pillows, but the four units that are 2–3 m thick could be thin massive flows.

Figure 36. Stratigraphic sections drilled during Leg 192 and at the three previous DSDP and ODP Ontong Java Plateau basement sites. Seven sites are arranged on a transect from the crest of the main plateau (Site 1183) eastward to the plateau rim (Site 1185) and then north and northwestward to Site 807 on the northern flank. Site 1184 lies off the transect, 590 km to the southeast of Site 1185. Basement ages for the previously drilled sites are from ^{40}Ar-^{39}Ar dating of basalt (Mahoney et al., 1993). For the Leg 192 sites, basement ages are estimated from biostratigraphic evidence.

Figure 37. Basement sections drilled during Leg 192 and at the three previous DSDP and ODP Ontong Java Plateau basement sites (as in Fig. 36), with water depths corrected for sediment loading. The corrected basement depth (D_c) is obtained from the equation of Crough (1983): $D_c = d_w + t_s (\rho_s - \rho_m)/(\rho_w - \rho_m)$, in which d_w is water depth in meters, t_s is sediment thickness in meters, ρ_s is average sediment density (1.90 g/cm^3), ρ_m is upper mantle density (3.22 g/cm^3), and ρ_w is seawater density (1.03 g/cm^3).

Table 1. Hole summary for Leg 192.

Site/Hole	Latitude	Longitude	Water depth (m)	Sediment thickness (m)	Sediment cored (m)	Sediment recovery (m)	Basement depth (mbsf)	Basement penetration (m)	Basement recovery (m)	Total penetration (m)	Oldest sediment (Ma)*
1183	1 10.6189 S	157 0.8988 E	1804.7	1130.4	503.10	216.50	1130.4	80.7	44.20	1211.1	118
1184	5 0.6653 S	164 13.9771 E	1661.5	201.1	66.70	49.80	201.1	337.7	278.90	538.8	41-43
1185A	0 21.4560 S	161 40.0619 E	3898.9	312	57.94	14.08	308.54/312**	20.2	11.17	328.7	93-112
1185B	0 21.4559 S	161 40.0511 E	3898.9	309.5	1.50	1.50	309.5	216.6	90.68	526.1	112
1186	0 40.7873 S	159 50.6519 E	2740.0	968.6	271.20	49.33	966.82/968.6†	65.4	39.36	1034.0	118
1187	0 56.5518 N	161 27.0784 E	3803.6	372.5	1.47	1.47	366.97/372.5**	135.8	100.87	508.3	115

Notes: * = Time scales of Berggren et al. (1995) and Gradstein et al. (1995). ** = Depths of basement contact noted by the driller. All other basement depths are curated depths. † = Driller noted basement at 969 m. However, 1.4 m of basalt was recovered from a cored interval that bottomed at 970 mbsf, yielding a basement depth of 968.6 mbsf.

Table 2. Volcaniclastic facies in Unit II at Site 1184.

Facies	Sedimentary structure	Grain size	Sorting	Thickness	Lithology	Interpretation
1	Massive with some subtle gradations in grain size; includes thin layers of very coarse sand to granules	Very fine sand to pebble	Very poor	20 cm to >10 m	Lithic vitric lapilli tuff	Muddy debris flow deposit
2	Massive, grain size oscillations	Coarse sand to pebble	Very poor	2-30 m	Lithic vitric lapilli tuff to lapillistone	Stony debris flow deposit
3	Inclined granule lamination	Medium sand to granule	Poor	2-5 m	Lithic vitric lapilli tuff	Current-reworked deposit
4	Grading, parallel lamination, traction carpet	Fine to very coarse sand	Moderate	5-200 cm	Lithic vitric tuff	Turbidite
5	Massive, clast supported	Granule to pebble	Moderate	20 cm to10 m	Tachylitic lapillistone	Quenched subaerial eruptive products
6	Chaotic bedding	Fine sand to pebble	Very poor	>3 m	Lithic vitric lapilli tuff	Slump deposit
7	Inverse grading, mud drape	Clay, very fine to coarse sand	Good	~20 cm	Lithic vitric tuff and mudstone	Fluvial deposit?
8	Massive	Silt to very fine sand	Good	5 cm	Lithic vitric tuff	Air-fall ash

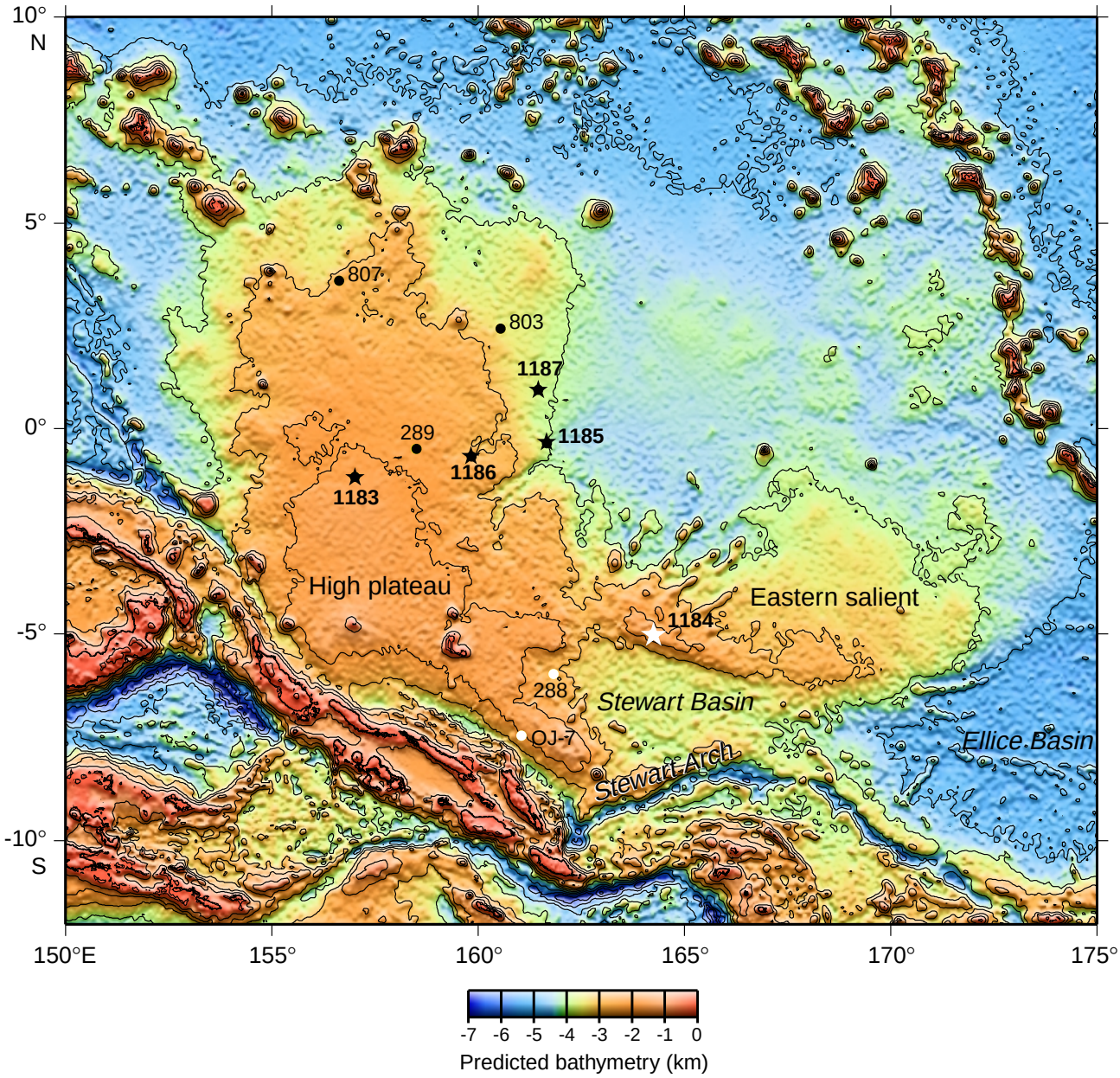
10° N
5°
0°
-5°
-10° S
150°E
155°
160°
165°
170°
175°
807
803
1187
289
1185
1186
1183
High plateau
Eastern salient
1184
288
Stewart Basin
OJ-7
Ellice Basin
Stewart Arch
-7 -6 -5 -4 -3 -2 -1 0
Predicted bathymetry (km)

Figure 1

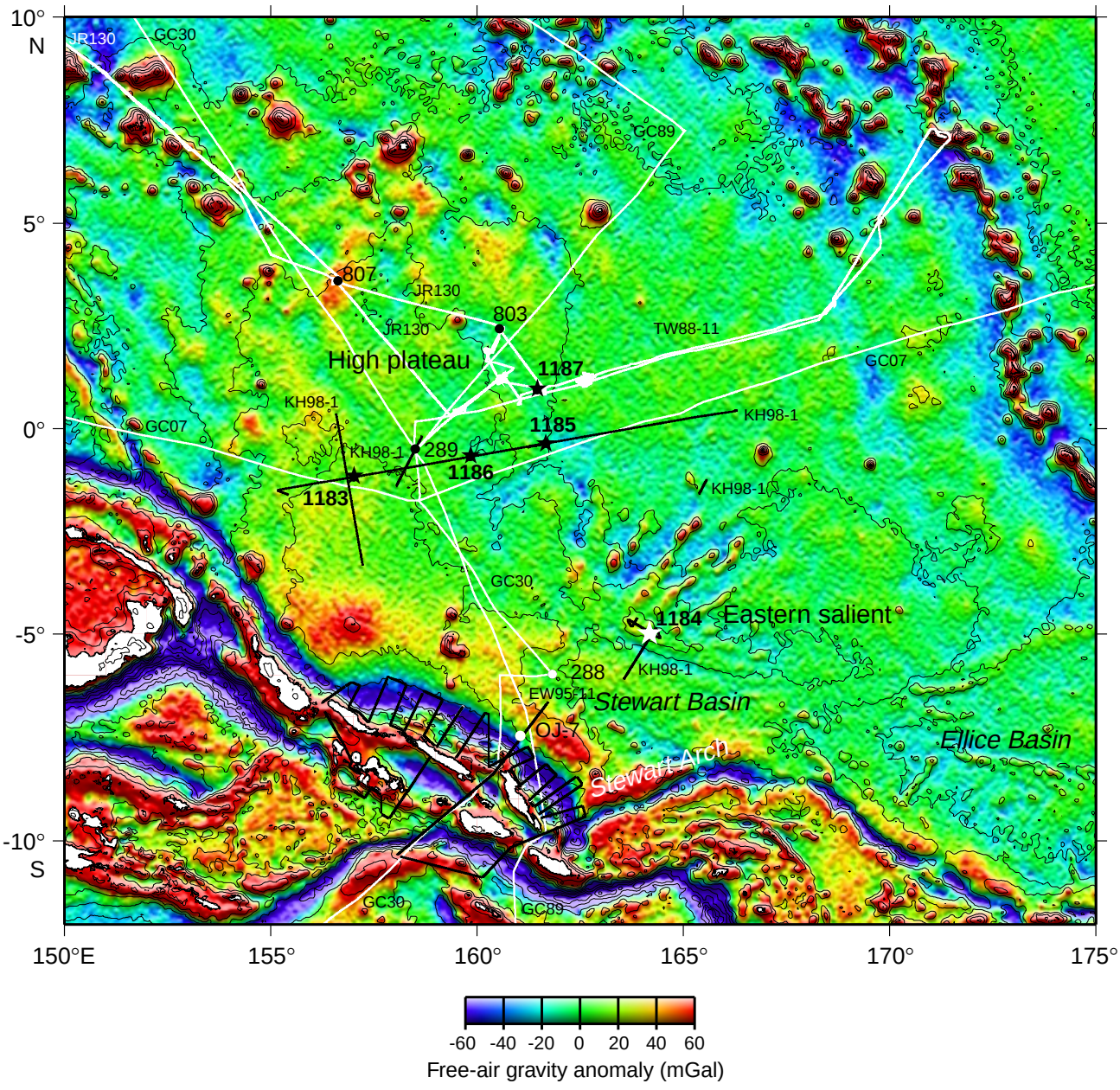
10° N
5°
0°
-5°
-10° S
150°E
155°
160°
165°
170°
175°
JR130
GC30
GC89
807
803
JR130
JR130
TW88-11
High plateau
1187
GC07
KH98-1
KH98-1
GC07
1185
KH98-1
KH98-1
289
1186
1183
KH98-1
GC30
1184
Eastern salient
288
KH98-1
EW95-11
Stewart Basin
OJ-7
Ellice Basin
Stewart Arch
GC30
GC89
-60 -40 -20 0 20 40 60
Free-air gravity anomaly (mGal)

Figure 2

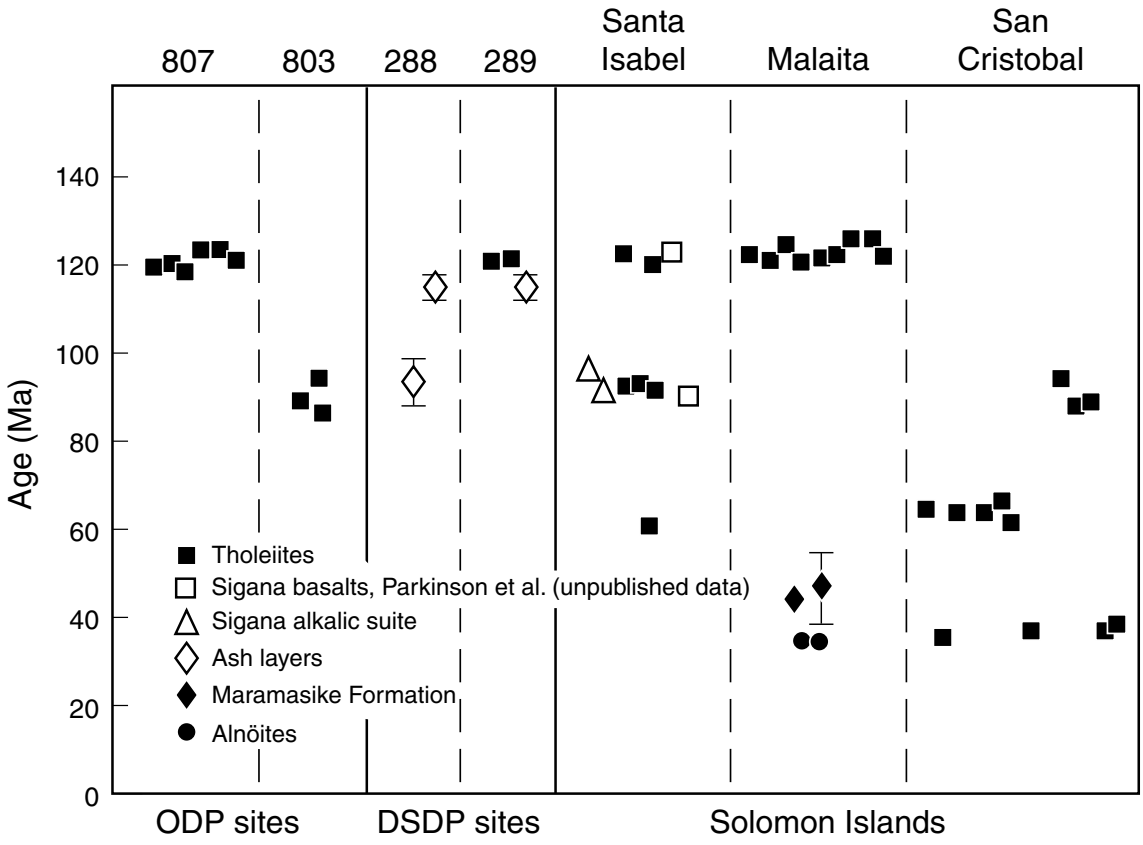
807
803
288
289
Santa Isabel
Malaita
San Cristobal
Age (Ma)
0
20
40
60
80
100
120
140
Tholeiites
Sigana basalts, Parkinson et al. (unpublished data)
Sigana alkalic suite
Ash layers
Maramasike Formation
Alnöites
ODP sites
DSDP sites
Solomon Islands

Figure 3

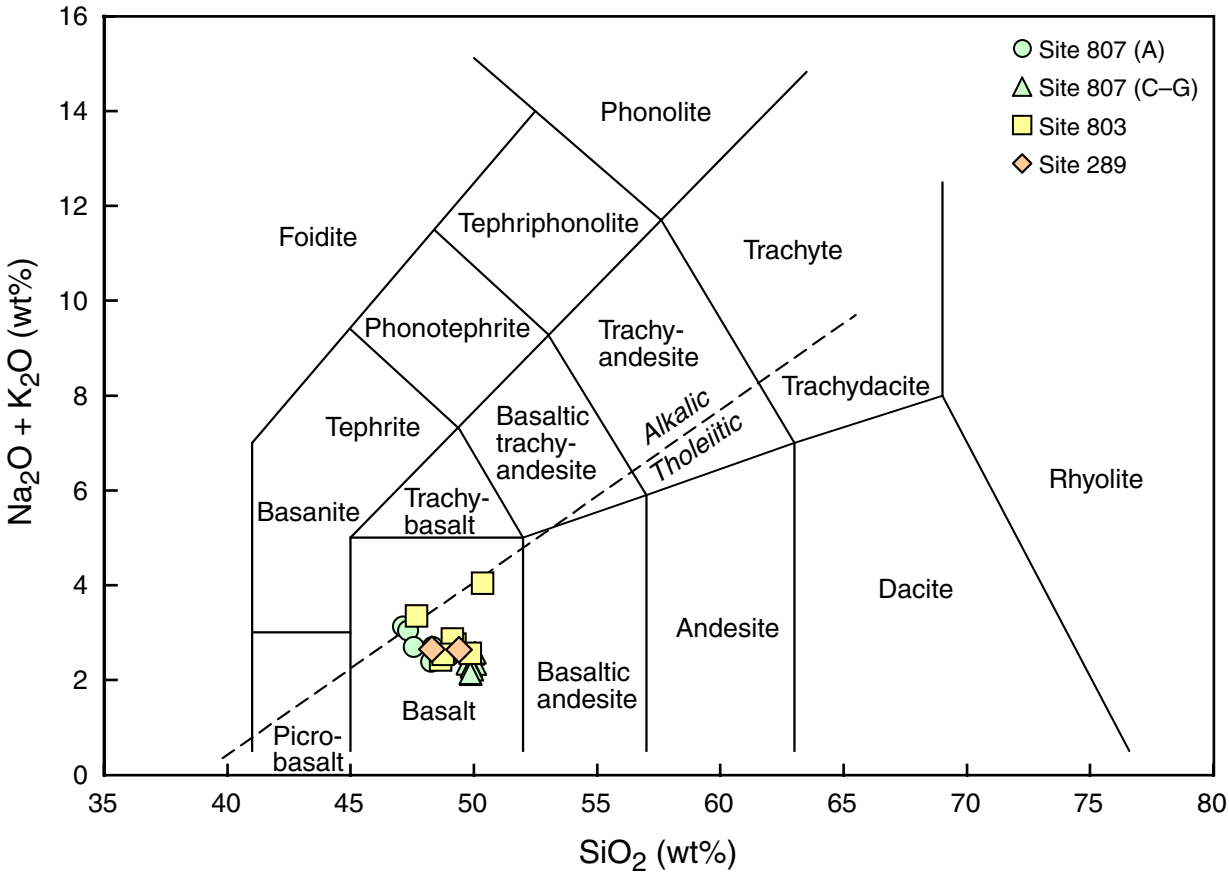
Site 807 (A)
Site 807 (C–G)
Site 803
Site 289
Phonolite
Foidite
Tephriphonolite
Trachyte
Phonotephrite
Trachy-
andesite
Trachydacite
Tephrite
Basaltic
trachy-
andesite
Alkalic
Tholeiitic
Rhyolite
Basanite
Trachy-
basalt
Dacite
Andesite
Basaltic
andesite
Basalt
Picro-
basalt
Na2O + K2O (wt%)
SiO2 (wt%)
0
2
4
6
8
10
12
14
16
35
40
45
50
55
60
65
70
75
80

Figure 4

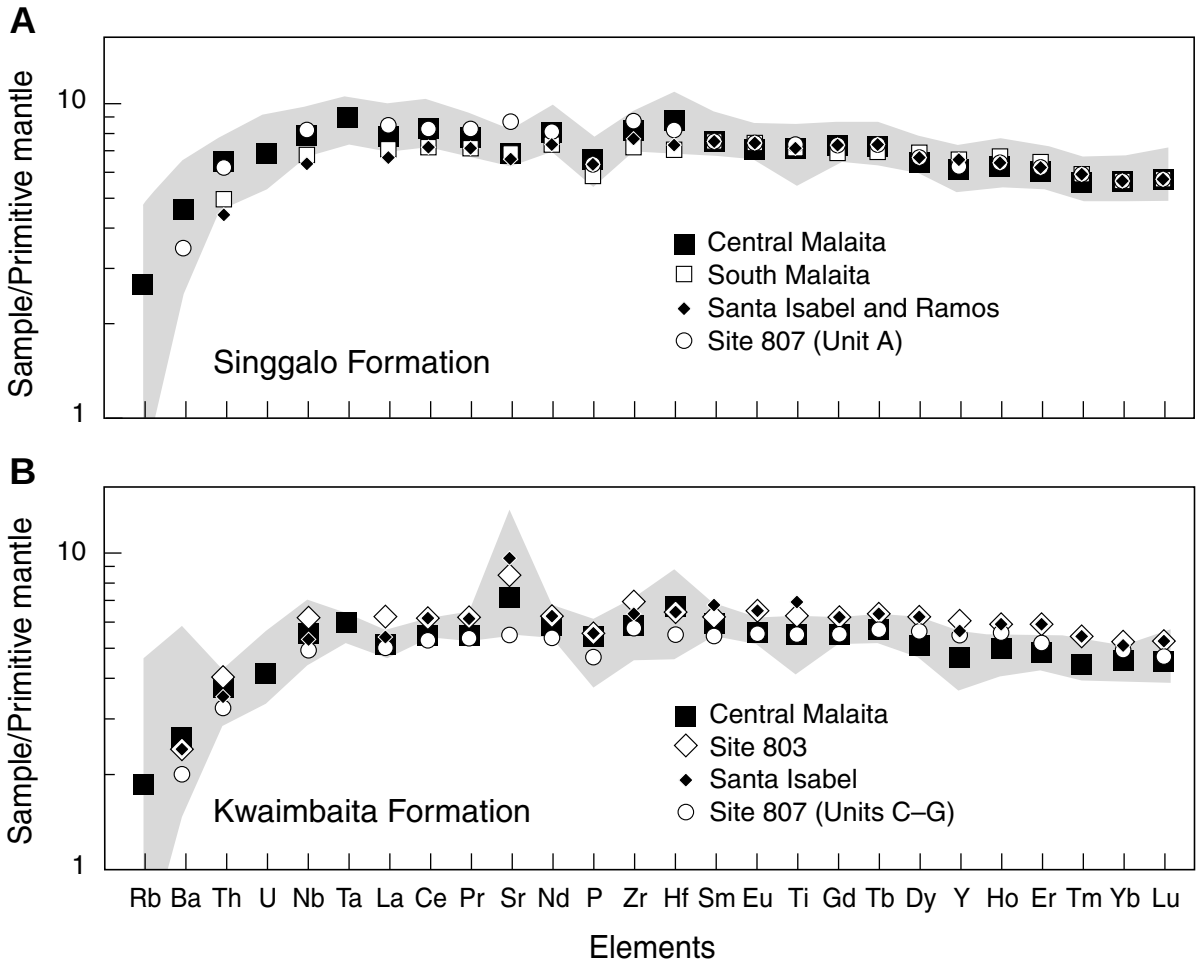
A
Sample/Primitive mantle
10
1
Central Malaita
South Malaita
Santa Isabel and Ramos
Site 807 (Unit A)
Singgalo Formation
B
Sample/Primitive mantle
10
1
Central Malaita
Site 803
Santa Isabel
Site 807 (Units C–G)
Kwaimbaita Formation
Rb Ba Th U Nb Ta La Ce Pr Sr Nd P Zr Hf Sm Eu Ti Gd Tb Dy Y Ho Er Tm Yb Lu
Elements

Figure 5

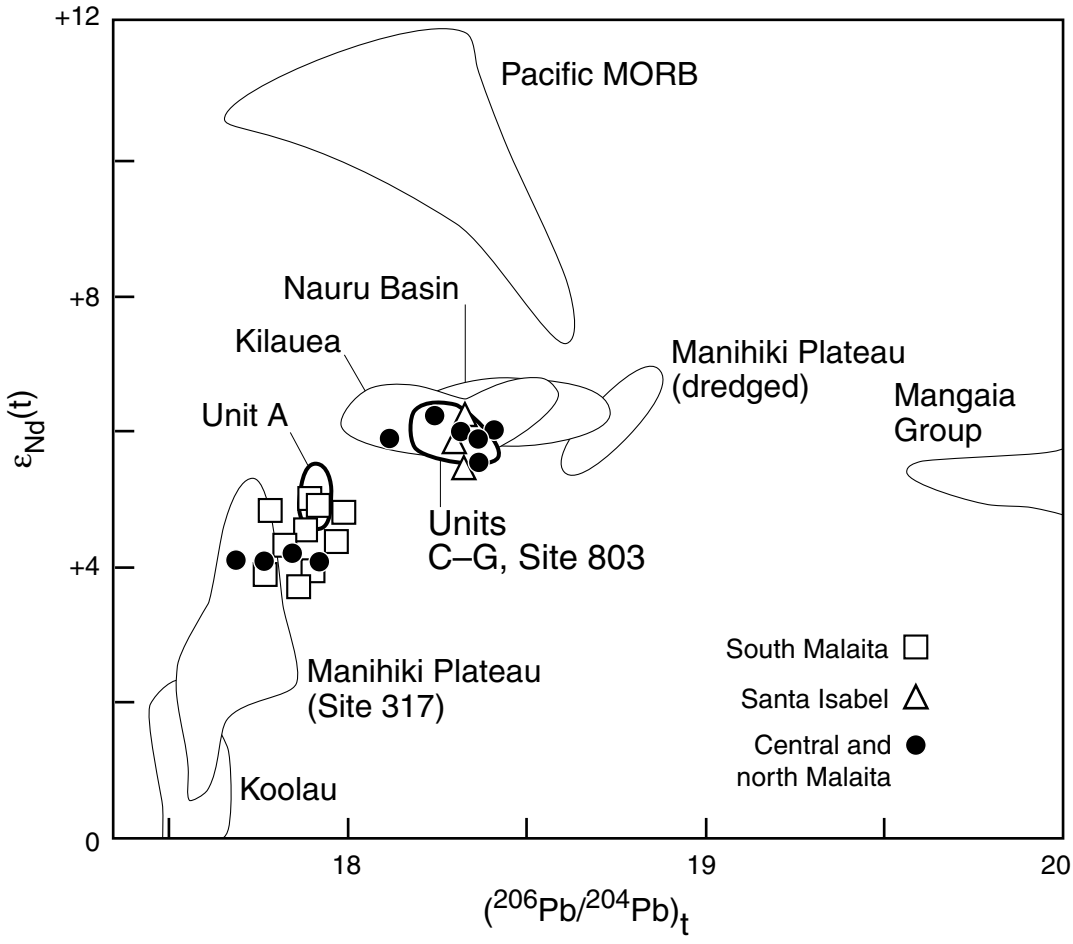
+12
+8
+4
0
18
19
20
$\varepsilon_{Nd}(t)$
$(^{206}Pb/^{204}Pb)_t$
Pacific MORB
Nauru Basin
Kilauea
Manihiki Plateau
(dredged)
Mangaia
Group
Unit A
Units
C–G, Site 803
Manihiki Plateau
(Site 317)
Koolau
South Malaita
Santa Isabel
Central and
north Malaita

Figure 6

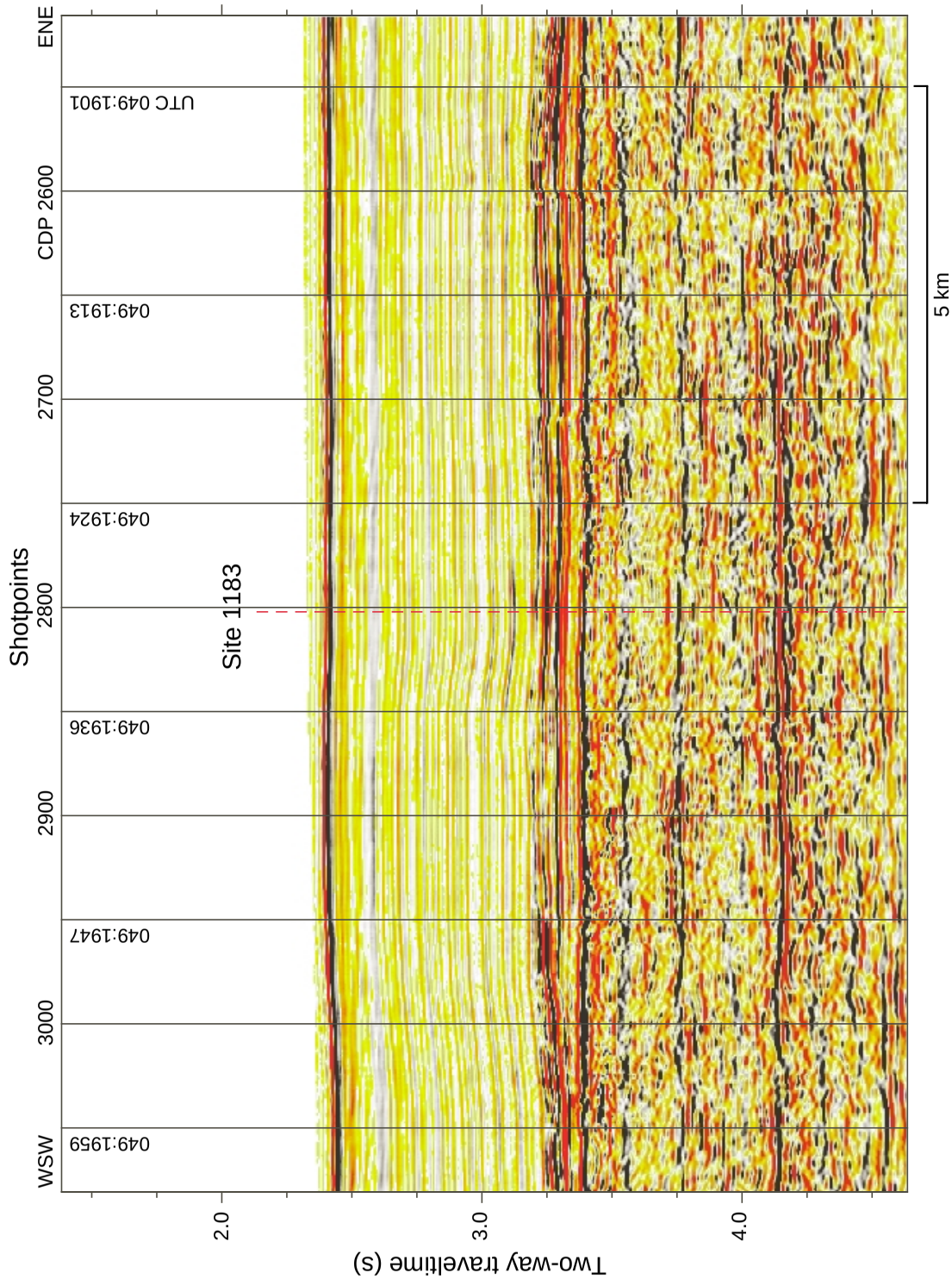
WSW
ENE
Shotpoints
2800
2900
3000
2700
CDP 2600
049:1959
049:1947
049:1936
049:1924
049:1913
UTC 049:1901
Site 1183
5 km
Two-way traveltime (s)
2.0
3.0
4.0

Figure 7

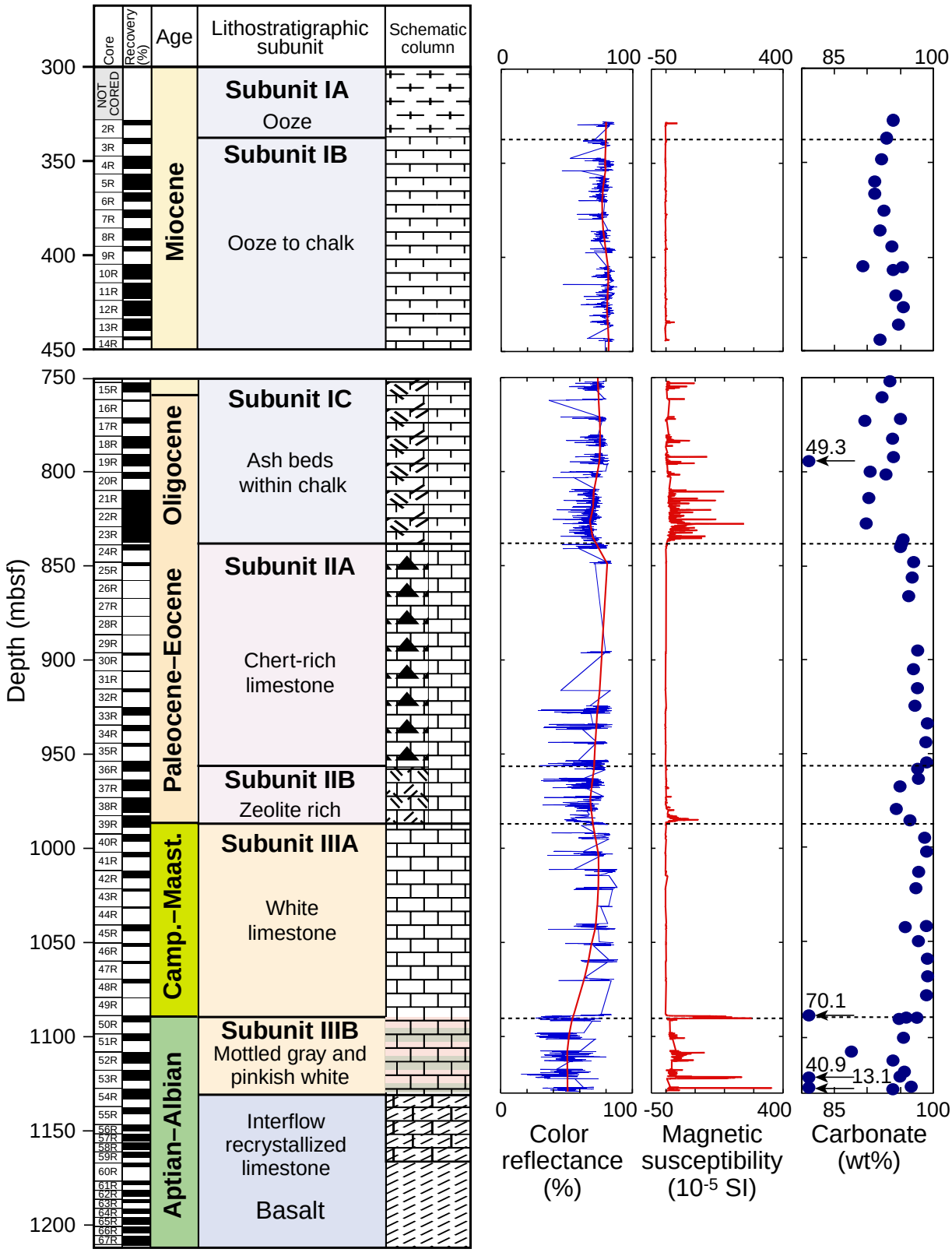
Core
Recovery (%)
Age
Lithostratigraphic subunit
Schematic column
Depth (mbsf)
NOT CORED
Miocene
Subunit IA
Ooze
Subunit IB
Ooze to chalk
Oligocene
Paleocene–Eocene
Subunit IC
Ash beds within chalk
Subunit IIA
Chert-rich limestone
Subunit IIB
Zeolite rich
Camp.–Maast.
Subunit IIIA
White limestone
Aptian–Albian
Subunit IIIB
Mottled gray and pinkish white
Interflow recrystallized limestone
Basalt
49.3
70.1
40.9
13.1
Color reflectance (%)
Magnetic susceptibility (10-5 SI)
Carbonate (wt%)

Figure 8

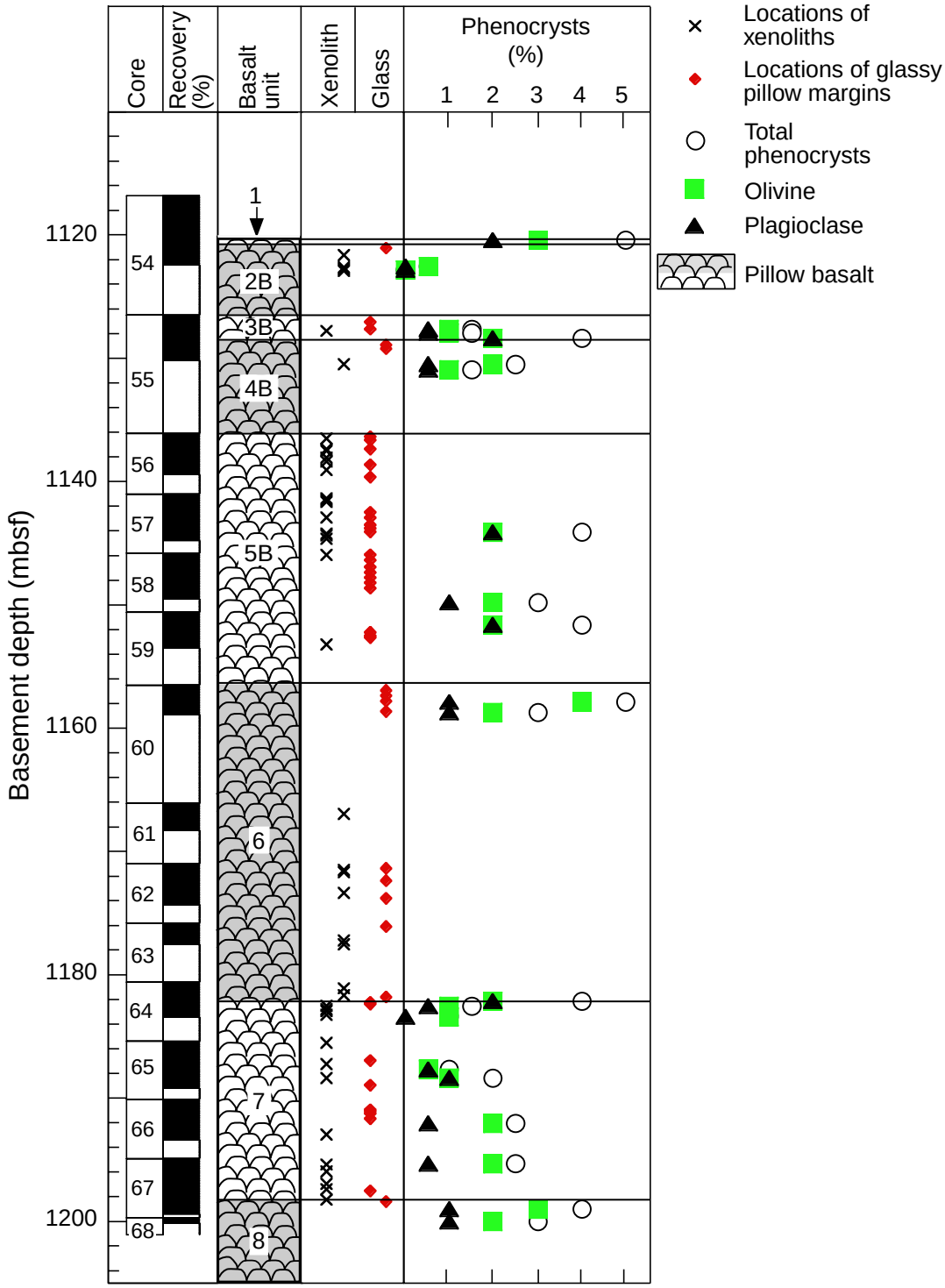
Core
Recovery (%)
Basalt unit
Xenolith
Glass
Phenocrysts (%)
1
2
3
4
5
Locations of xenoliths
Locations of glassy pillow margins
Total phenocrysts
Olivine
Plagioclase
Pillow basalt
Basement depth (mbsf)
1120
1140
1160
1180
1200
54
55
56
57
58
59
60
61
62
63
64
65
66
67
68
1
2B
3B
4B
5B
6
7
8

Figure 9

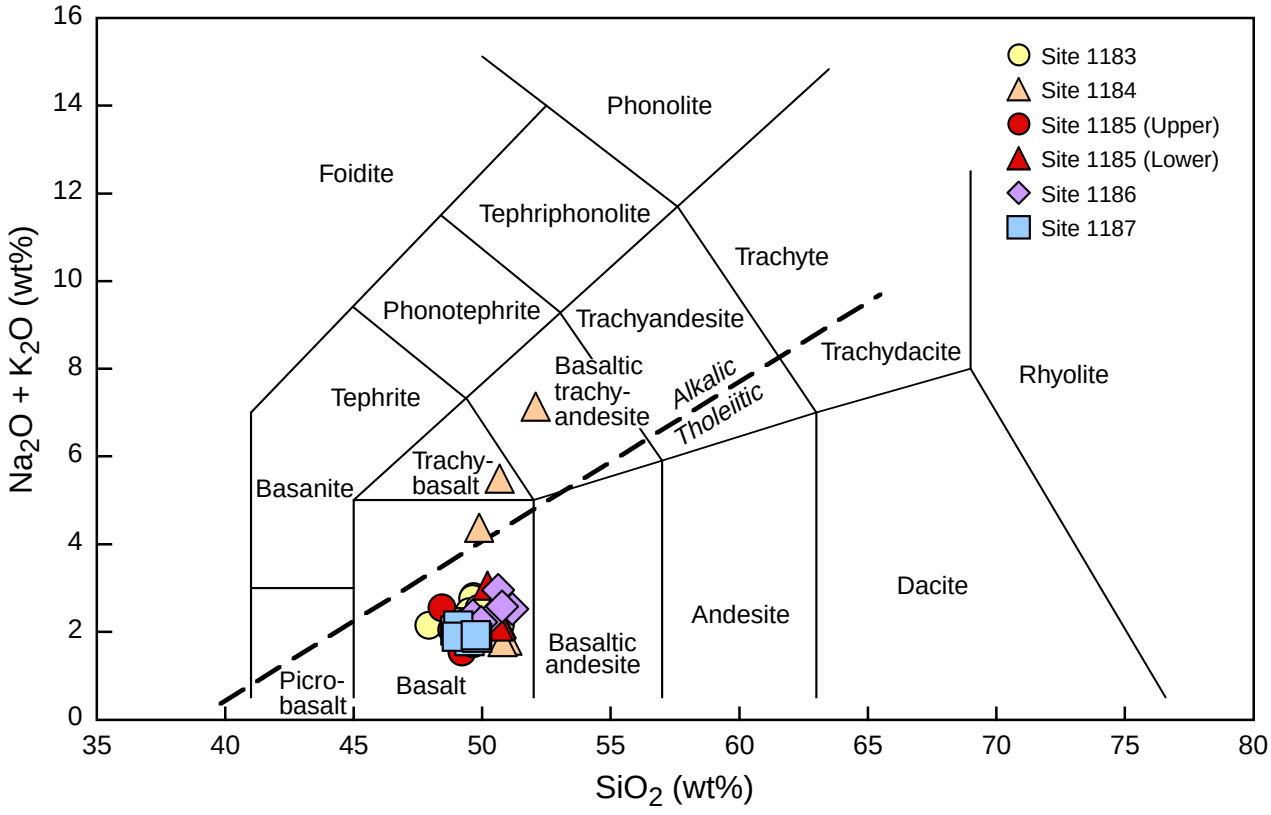
Site 1183
Site 1184
Site 1185 (Upper)
Site 1185 (Lower)
Site 1186
Site 1187
Phonolite
Foidite
Tephriphonolite
Trachyte
Phonotephrite
Trachyandesite
Trachydacite
Rhyolite
Basaltic trachy-andesite
Alkalic
Tholeiitic
Tephrite
Trachy-basalt
Basanite
Dacite
Andesite
Basaltic andesite
Picro-basalt
Basalt
Na2O + K2O (wt%)
SiO2 (wt%)
0
2
4
6
8
10
12
14
16
35
40
45
50
55
60
65
70
75
80

Figure 10

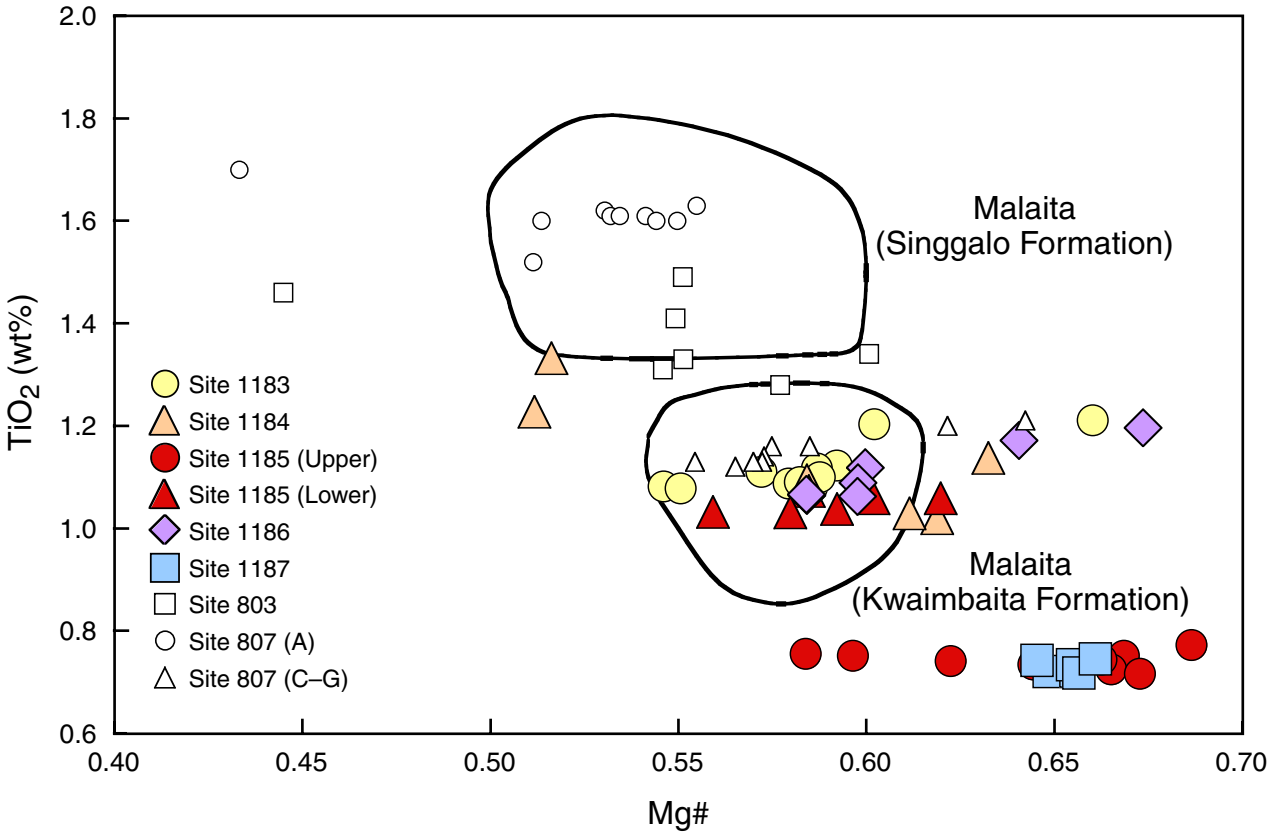
2.0
1.8
1.6
1.4
1.2
1.0
0.8
0.6
TiO2 (wt%)
0.40
0.45
0.50
0.55
0.60
0.65
0.70
Mg#
Malaita
(Singgalo Formation)
Malaita
(Kwaimbaita Formation)
Site 1183
Site 1184
Site 1185 (Upper)
Site 1185 (Lower)
Site 1186
Site 1187
Site 803
Site 807 (A)
Site 807 (C–G)

Figure 11

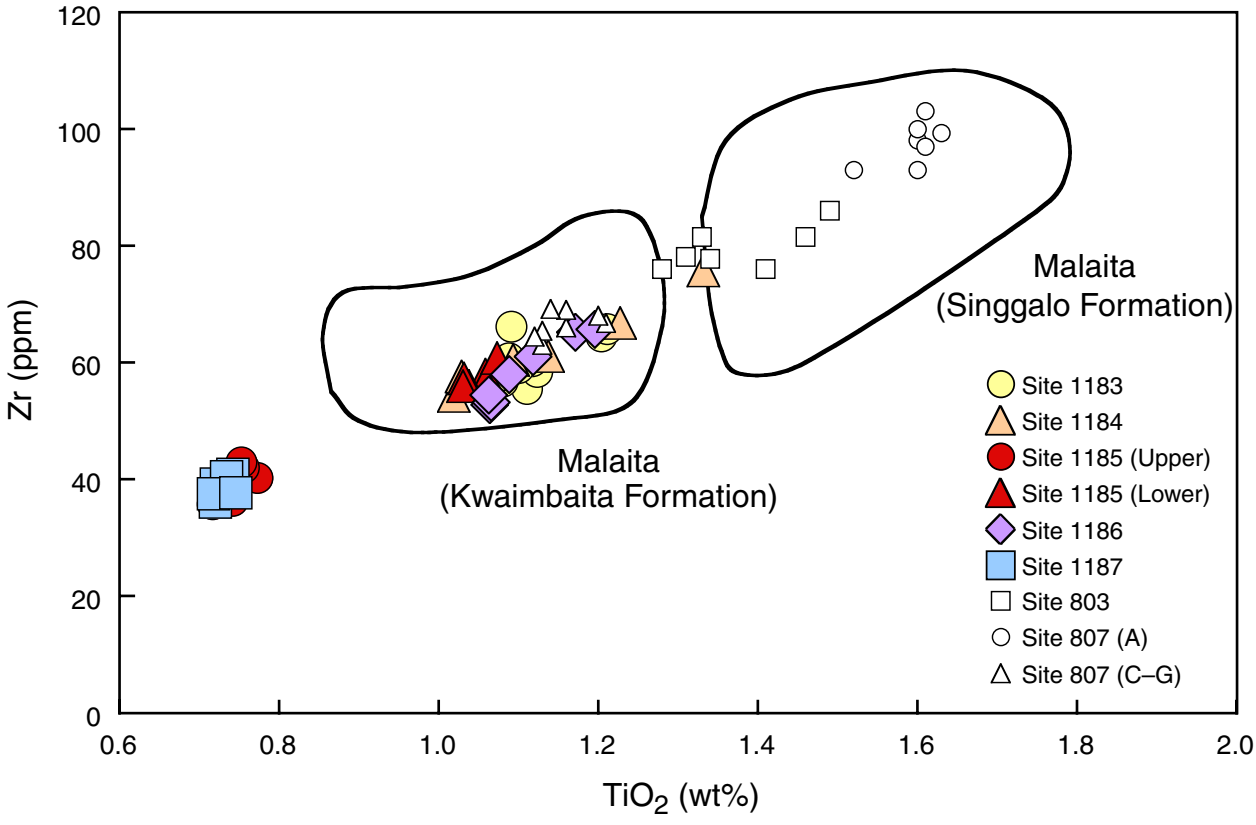
120
100
80
60
40
20
0
Zr (ppm)
0.6
0.8
1.0
1.2
1.4
1.6
1.8
2.0
TiO2 (wt%)
Malaita
(Singgalo Formation)
Malaita
(Kwaimbaita Formation)
Site 1183
Site 1184
Site 1185 (Upper)
Site 1185 (Lower)
Site 1186
Site 1187
Site 803
Site 807 (A)
Site 807 (C–G)

Figure 12

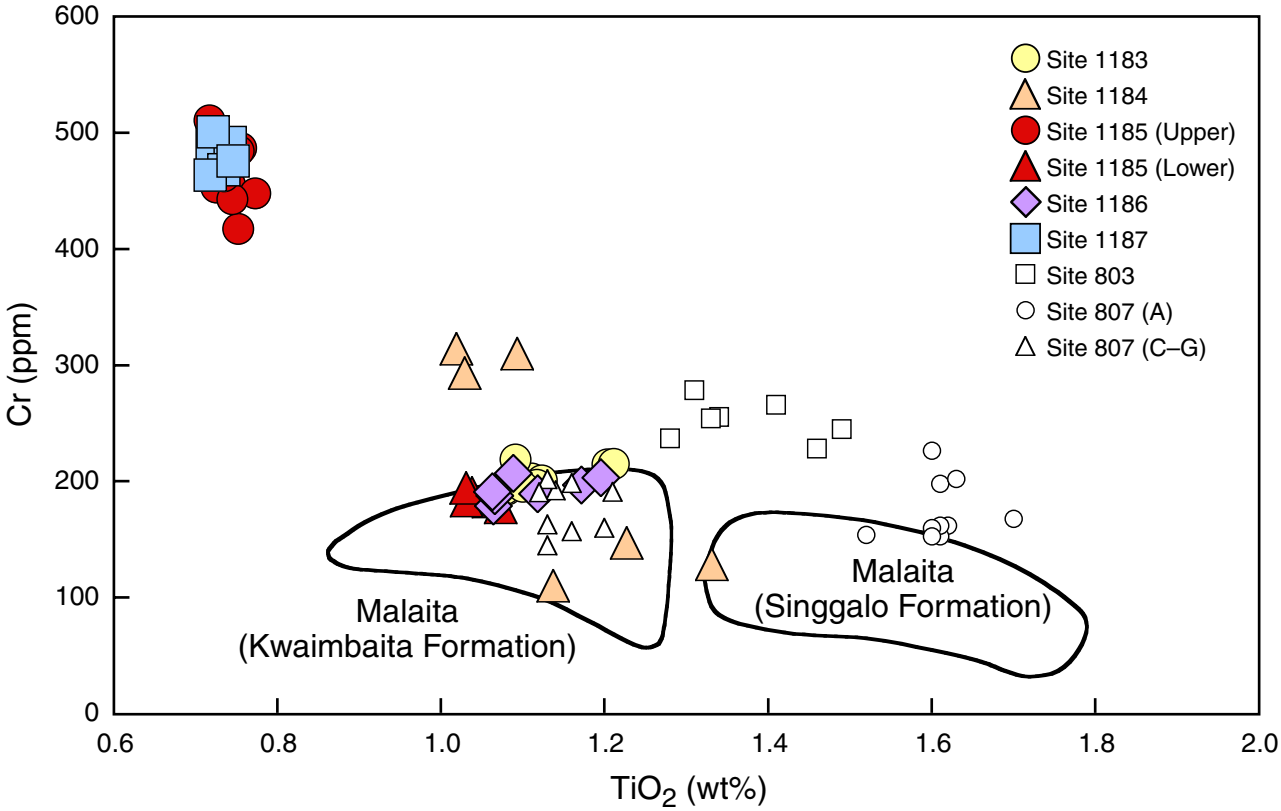
Site 1183
Site 1184
Site 1185 (Upper)
Site 1185 (Lower)
Site 1186
Site 1187
Site 803
Site 807 (A)
Site 807 (C–G)
Malaita
(Kwaimbaita Formation)
Malaita
(Singgalo Formation)
Cr (ppm)
TiO2 (wt%)
0
100
200
300
400
500
600
0.6
0.8
1.0
1.2
1.4
1.6
1.8
2.0

Figure 13

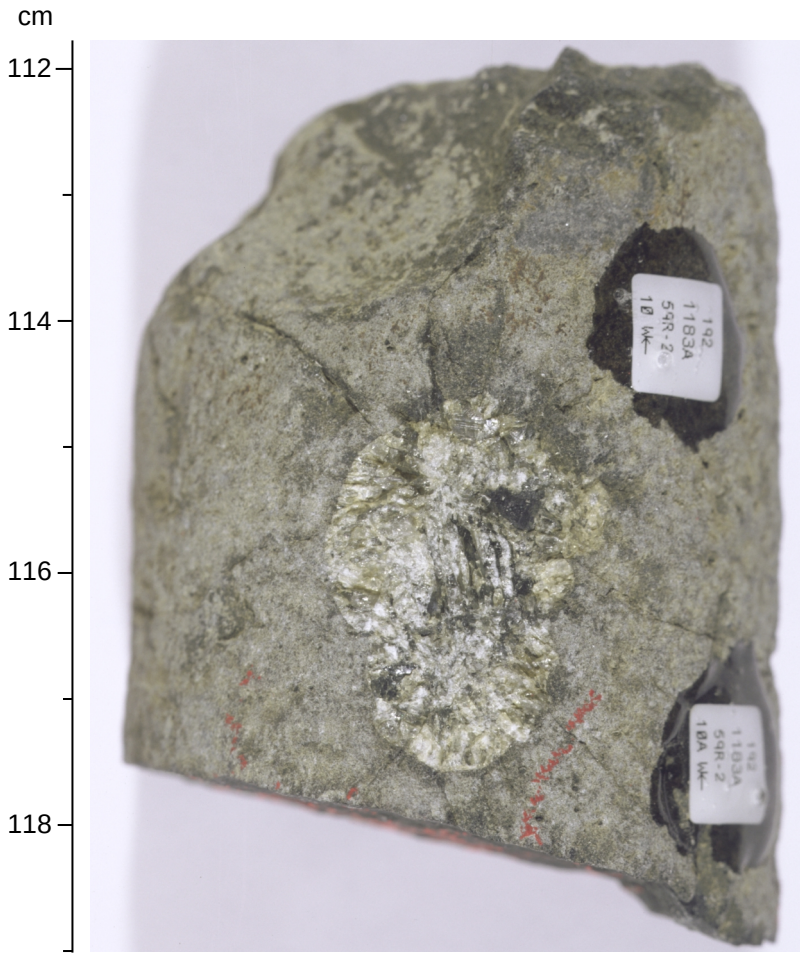

Figure 14

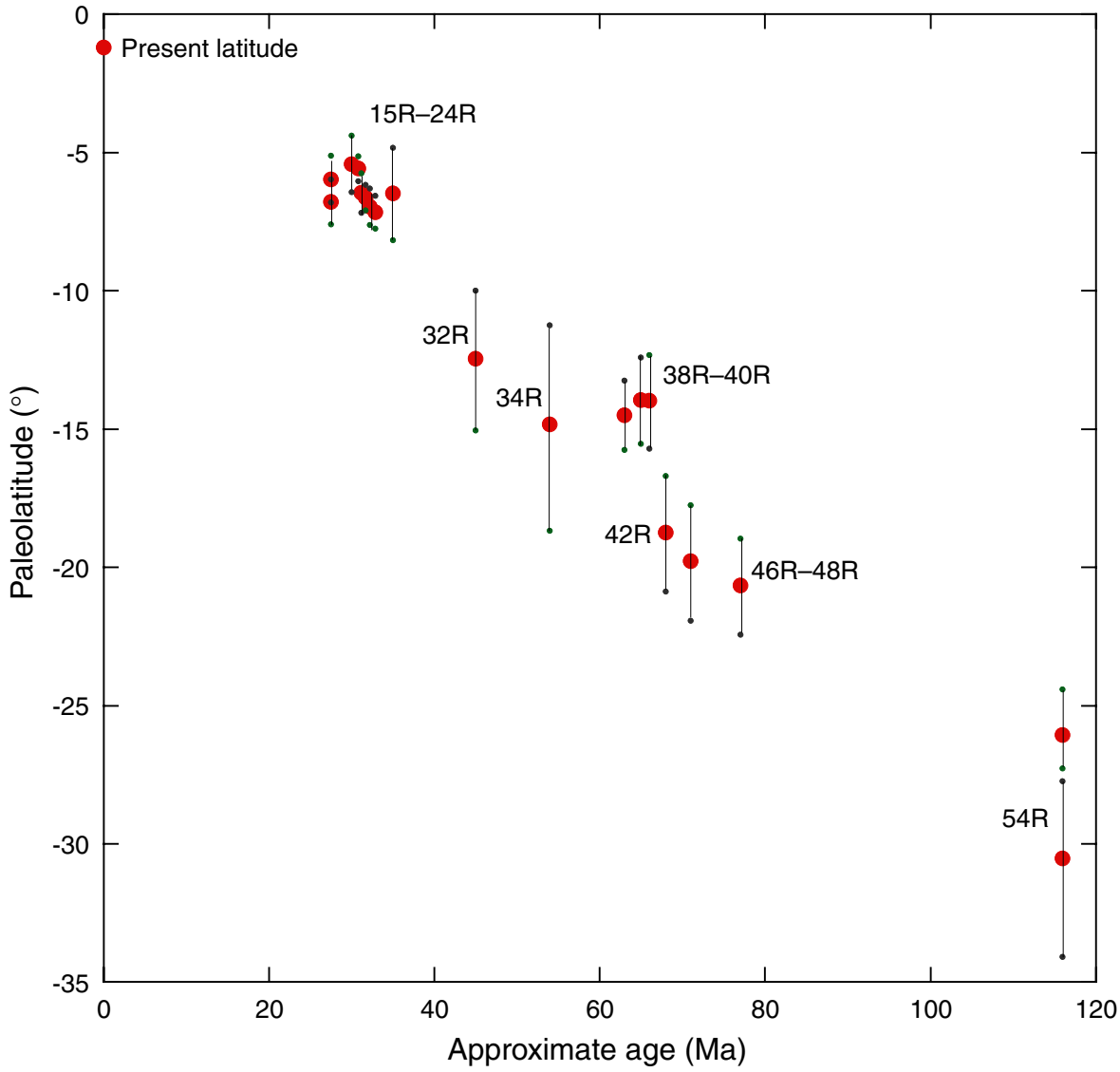
Present latitude
15R–24R
32R
34R
38R–40R
42R
46R–48R
54R
Paleolatitude (°)
Approximate age (Ma)
0
-5
-10
-15
-20
-25
-30
-35
0
20
40
60
80
100
120

Figure 15

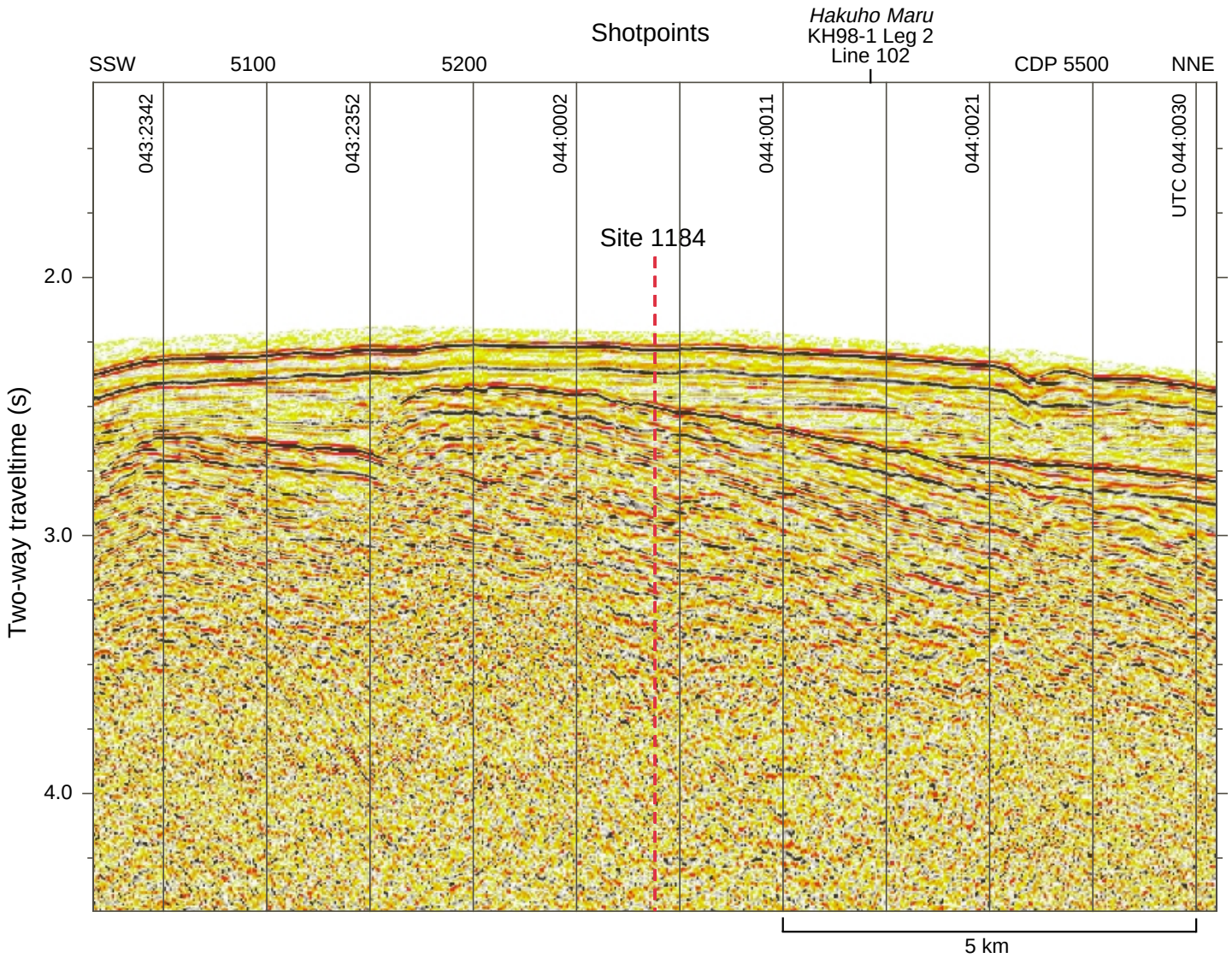
Shotpoints
Hakuho Maru
KH98-1 Leg 2
Line 102
SSW
5100
5200
CDP 5500
NNE
043:2342
043:2352
044:0002
044:0011
044:0021
UTC 044:0030
Site 1184
2.0
3.0
4.0
Two-way traveltime (s)
5 km

Figure 16

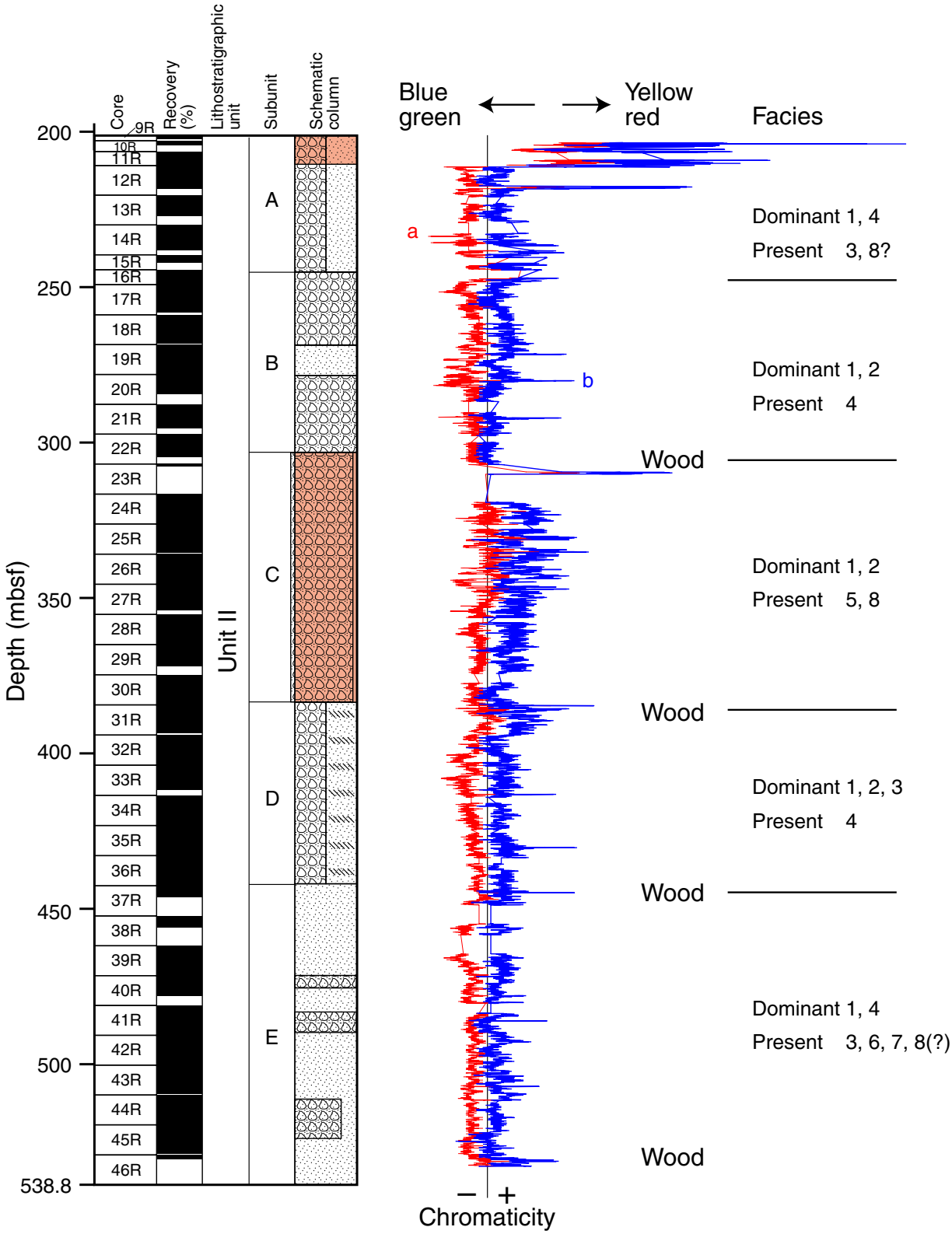
Core
Recovery (%)
Lithostratigraphic unit
Subunit
Schematic column
Depth (mbsf)
200
250
300
350
400
450
500
538.8
9R
10R
11R
12R
13R
14R
15R
16R
17R
18R
19R
20R
21R
22R
23R
24R
25R
26R
27R
28R
29R
30R
31R
32R
33R
34R
35R
36R
37R
38R
39R
40R
41R
42R
43R
44R
45R
46R
Unit II
A
B
C
D
E
Blue green
Yellow red
Facies
a
b
Dominant 1, 4
Present 3, 8?
Dominant 1, 2
Present 4
Wood
Dominant 1, 2
Present 5, 8
Wood
Dominant 1, 2, 3
Present 4
Wood
Dominant 1, 4
Present 3, 6, 7, 8(?)
Wood
−
+
Chromaticity

Figure 17

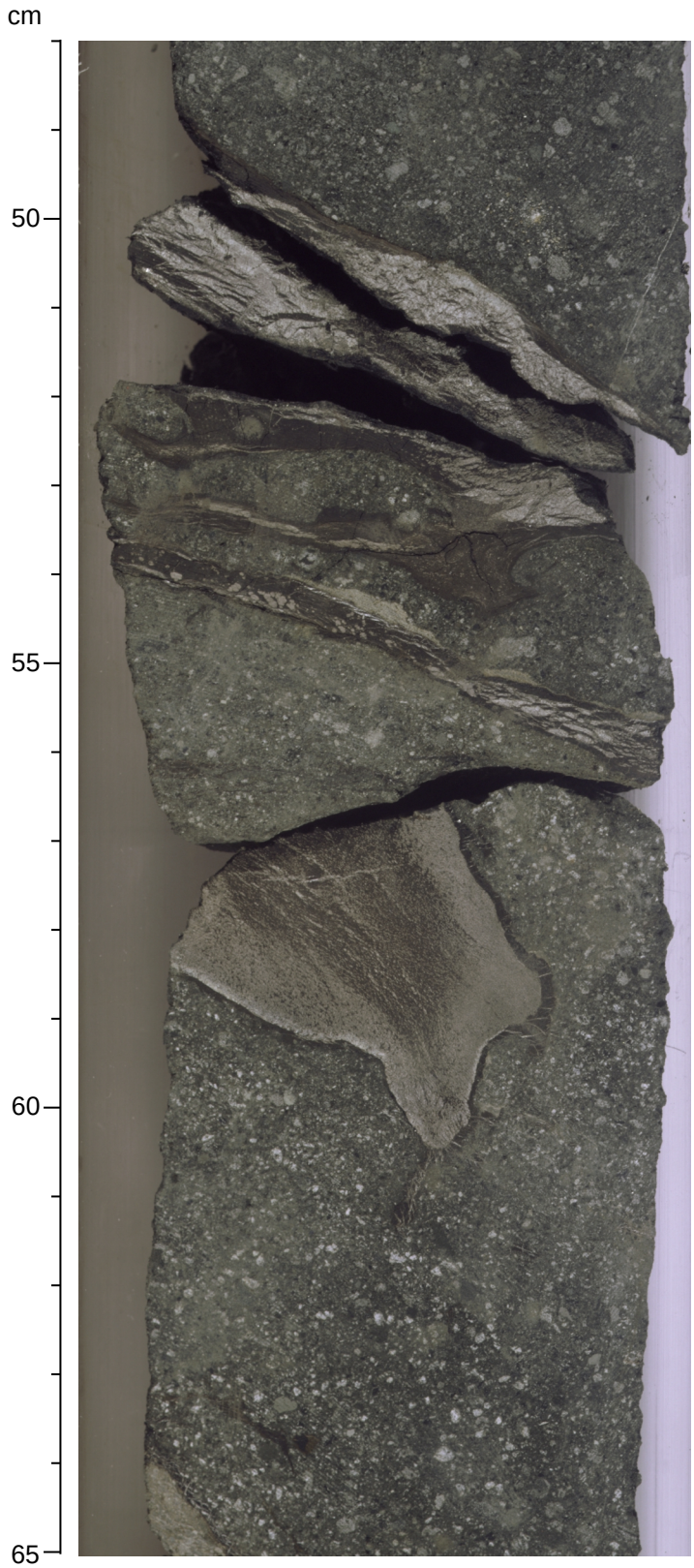

Figure 18

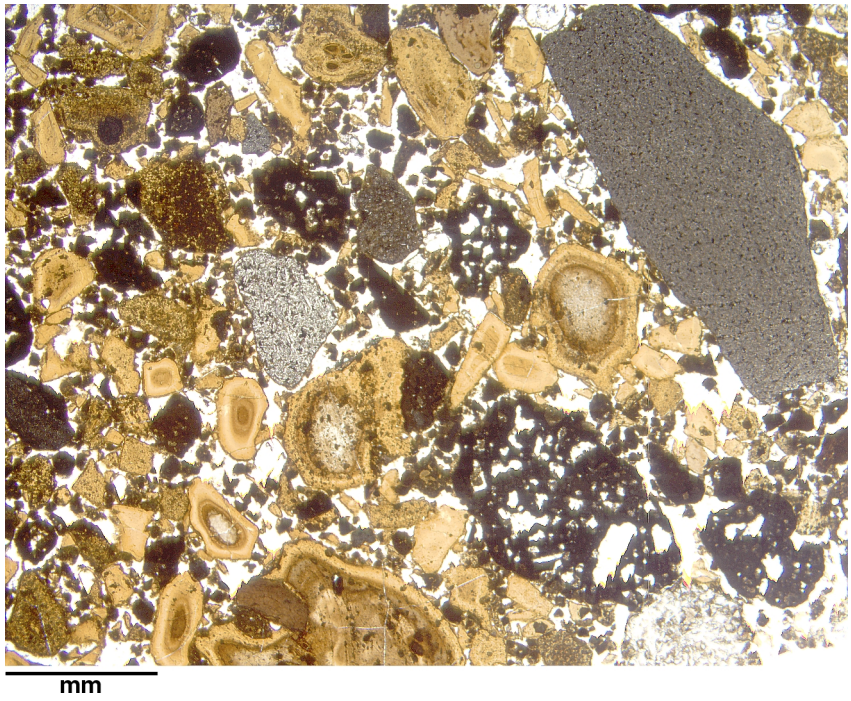

Figure 19

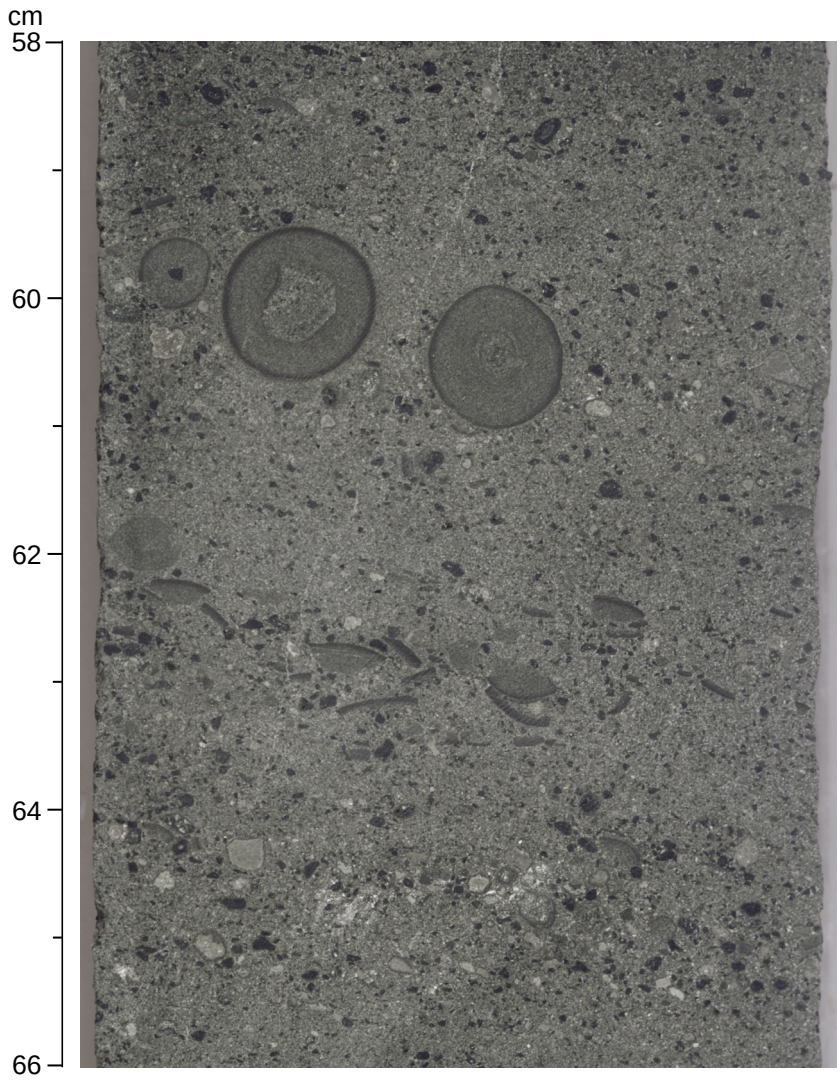

Figure 20

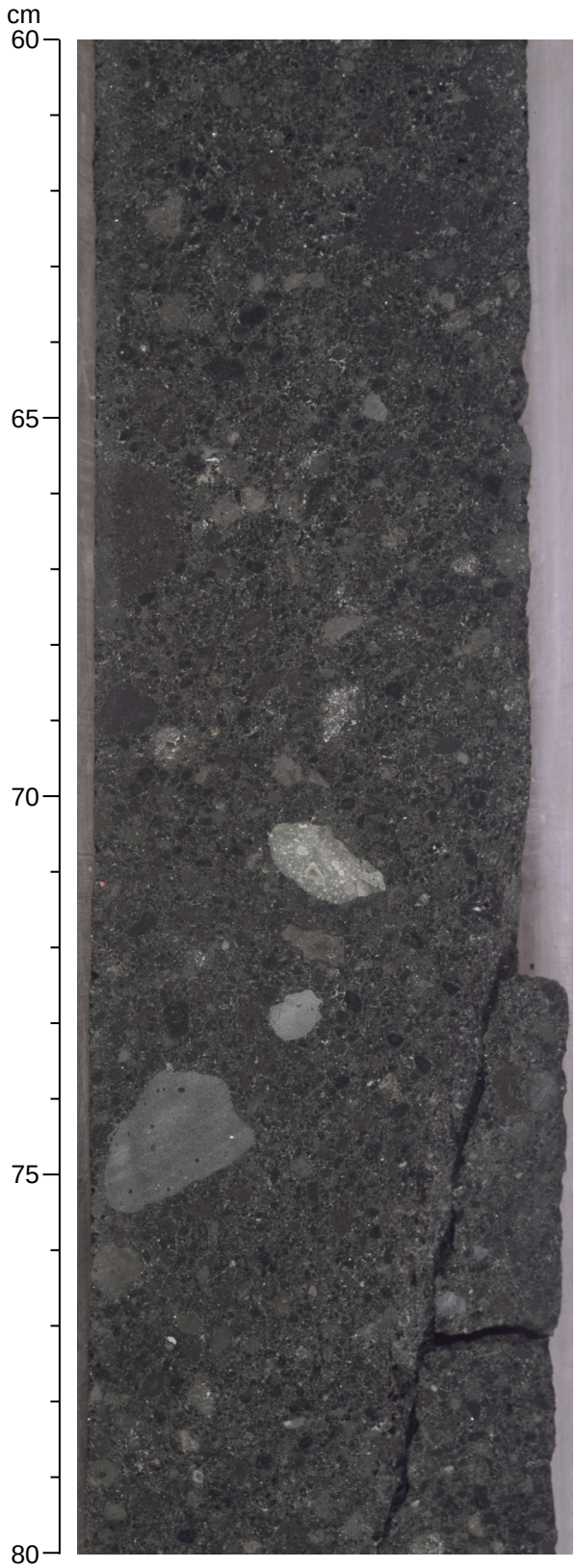

Figure 21

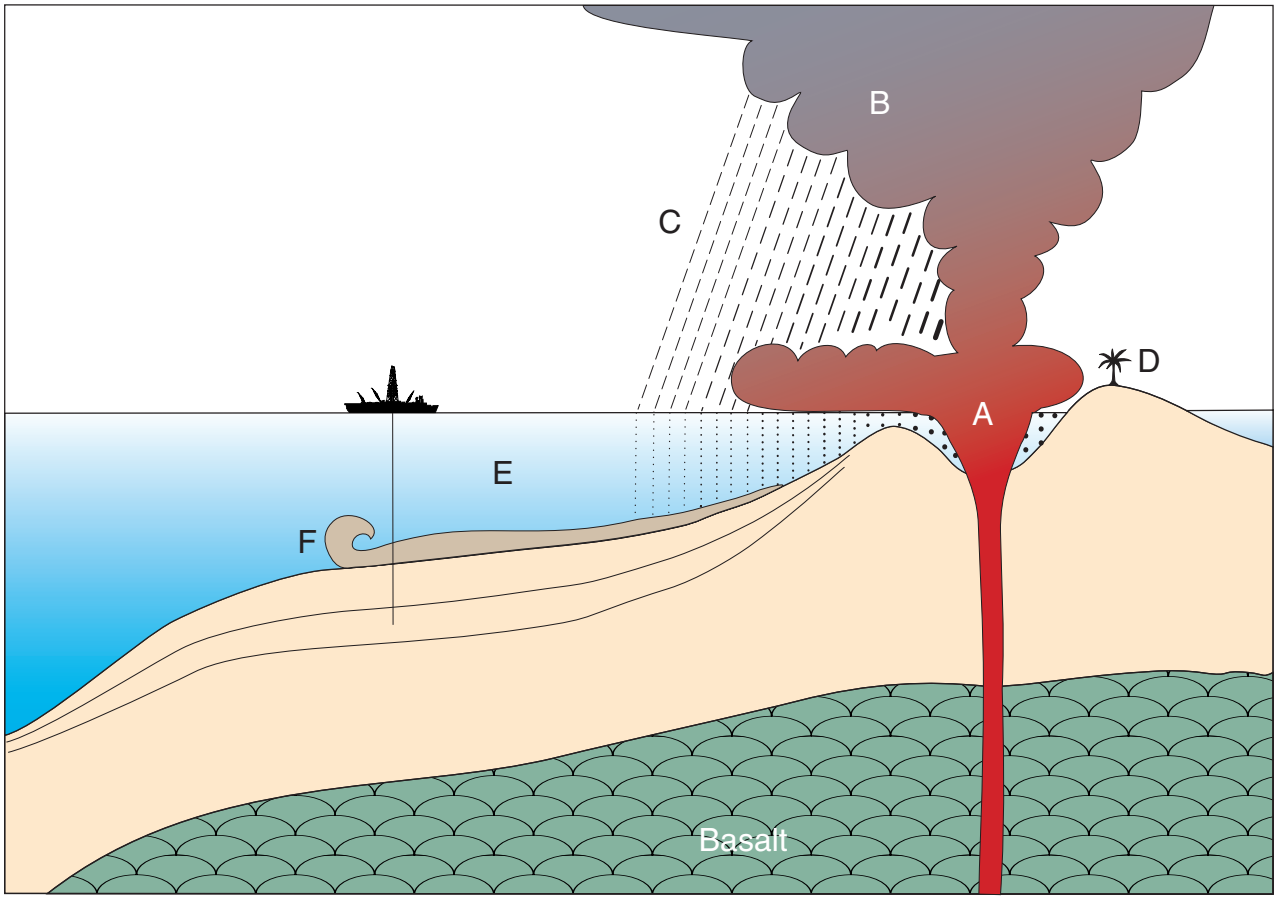

Figure 22

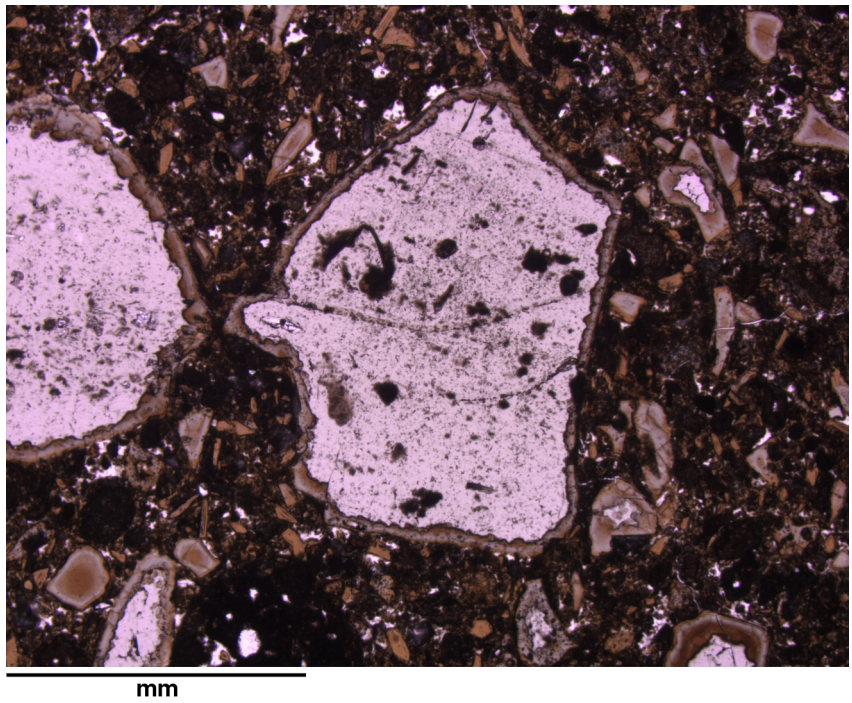

Figure 23

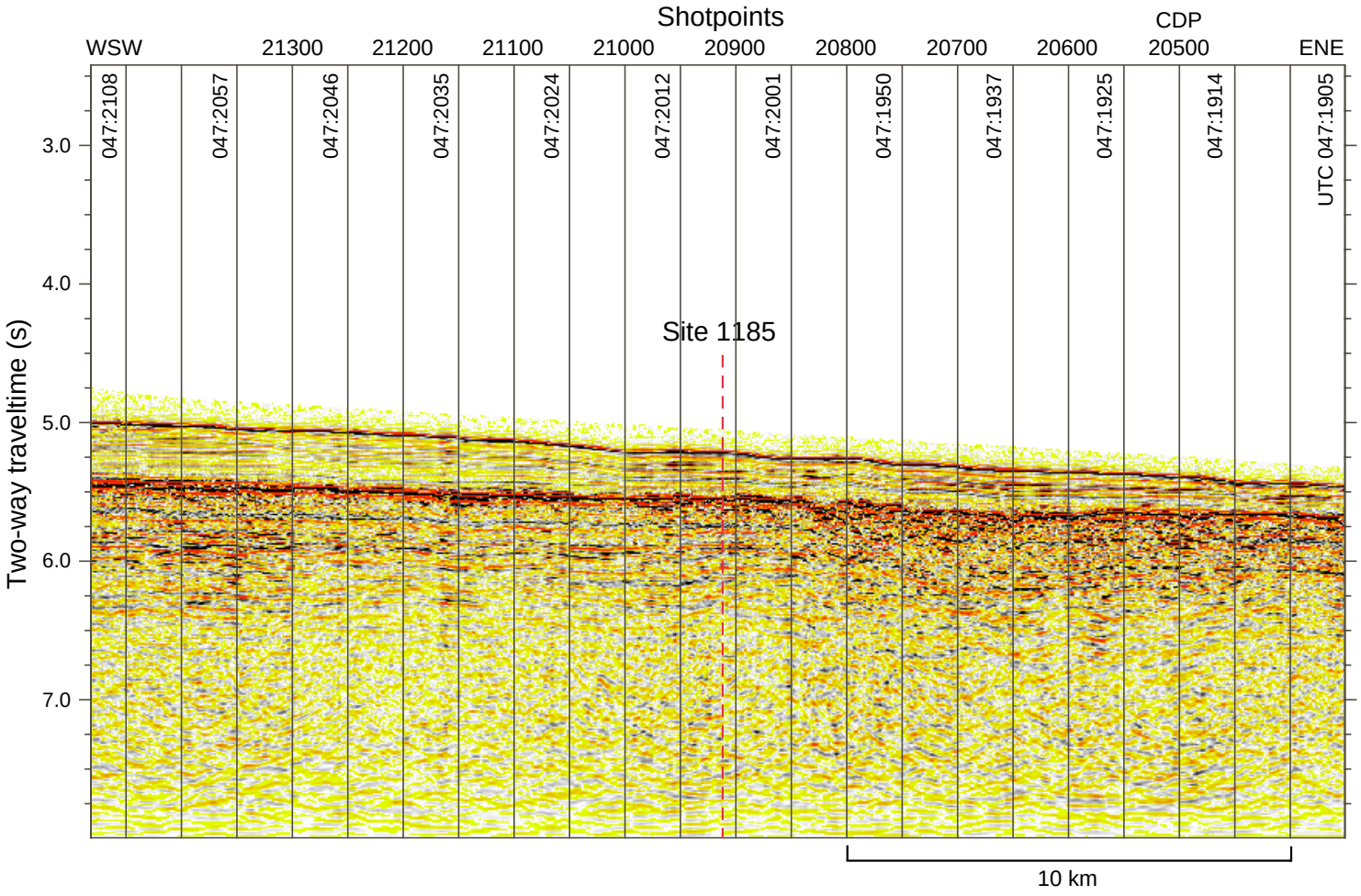
Shotpoints
CDP
WSW
21300
21200
21100
21000
20900
20800
20700
20600
20500
ENE
047:2108
047:2057
047:2046
047:2035
047:2024
047:2012
047:2001
047:1950
047:1937
047:1925
047:1914
UTC 047:1905
3.0
4.0
5.0
6.0
7.0
Two-way traveltime (s)
Site 1185
10 km

Figure 24

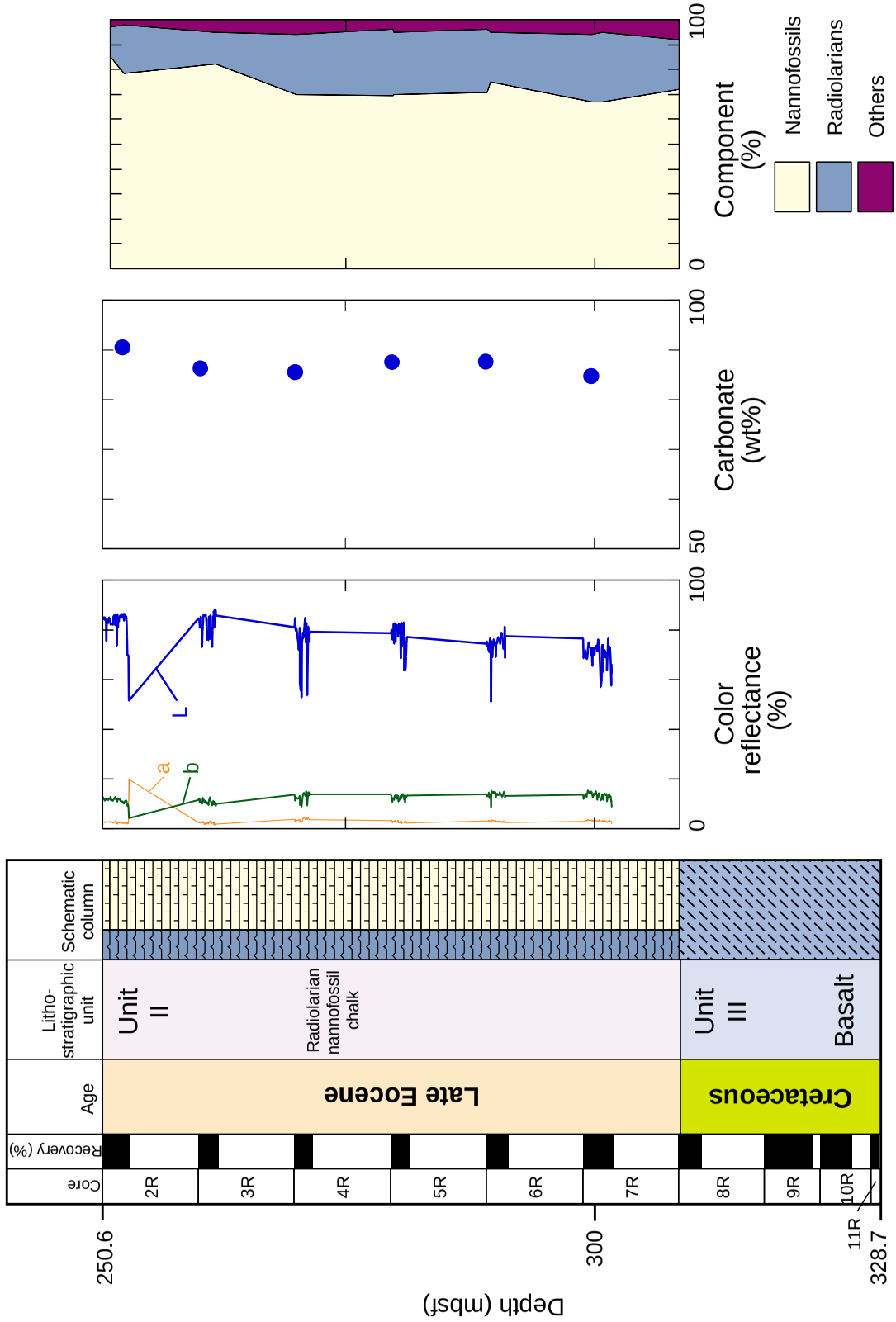
Depth (mbsf)
250.6
300
328.7
Core
Recovery (%)
Age
Litho-stratigraphic unit
Schematic column
2R
3R
4R
5R
6R
7R
8R
9R
10R
11R
Late Eocene
Cretaceous
Unit II
Radiolarian nannofossil chalk
Unit III
Basalt
Color reflectance (%)
a
b
L
0
100
Carbonate (wt%)
50
100
Component (%)
0
100
Nannofossils
Radiolarians
Others

Figure 25

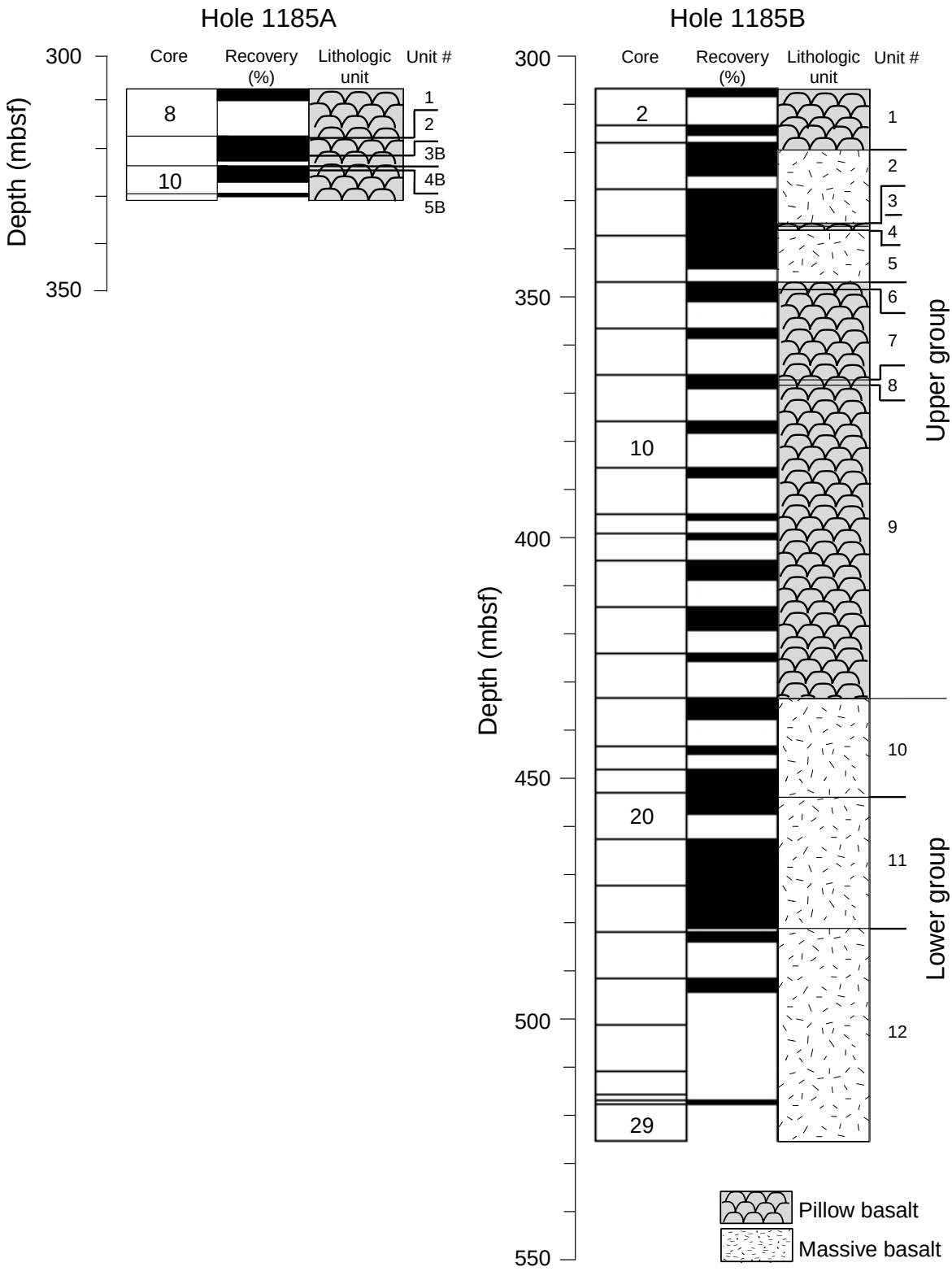
Hole 1185A
Hole 1185B
Depth (mbsf)
Core
Recovery (%)
Lithologic unit
Unit #
300
350
400
450
500
550
8
10
2
20
29
1
2
3B
4B
5B
3
4
5
6
7
8
9
10
11
12
Upper group
Lower group
Pillow basalt
Massive basalt

Figure 26

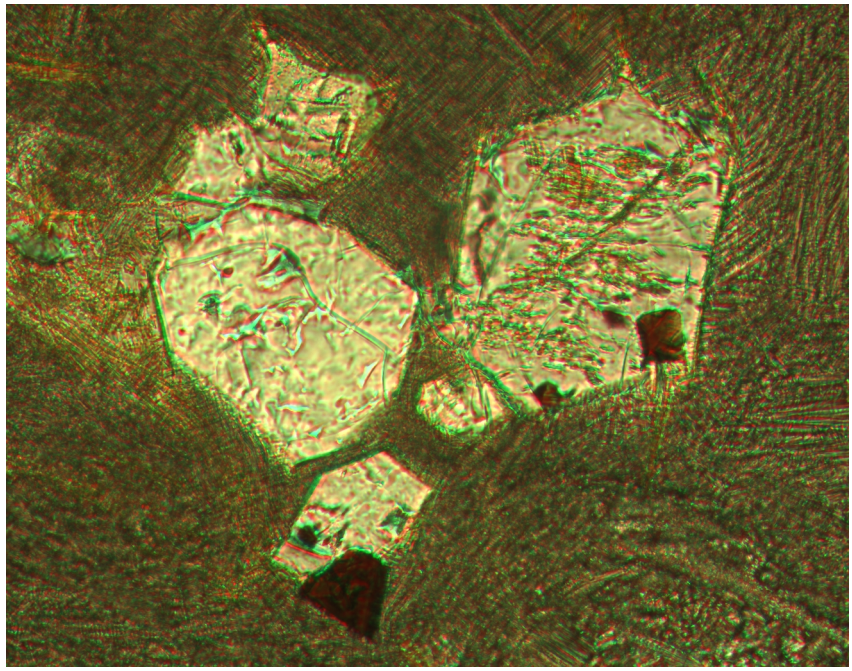

Figure 27

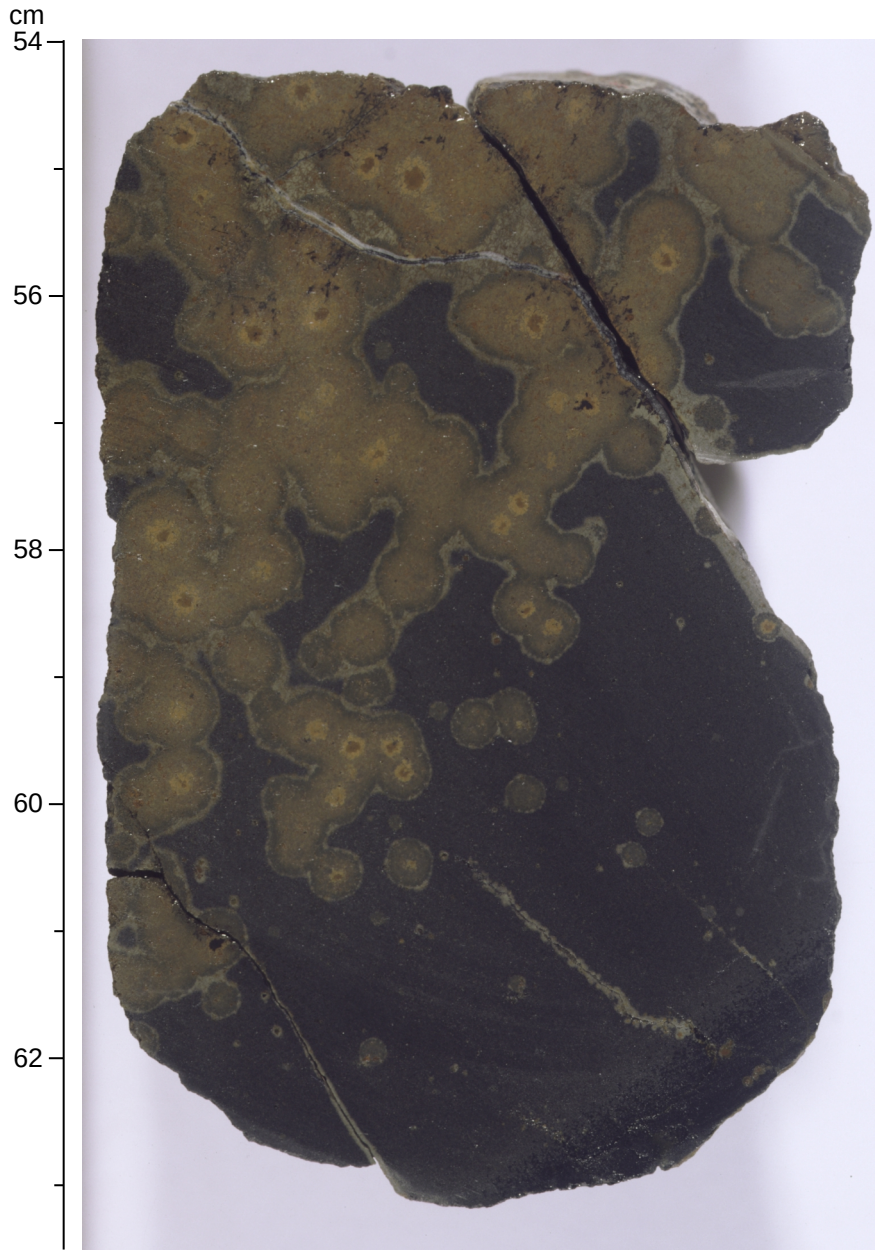

Figure 28

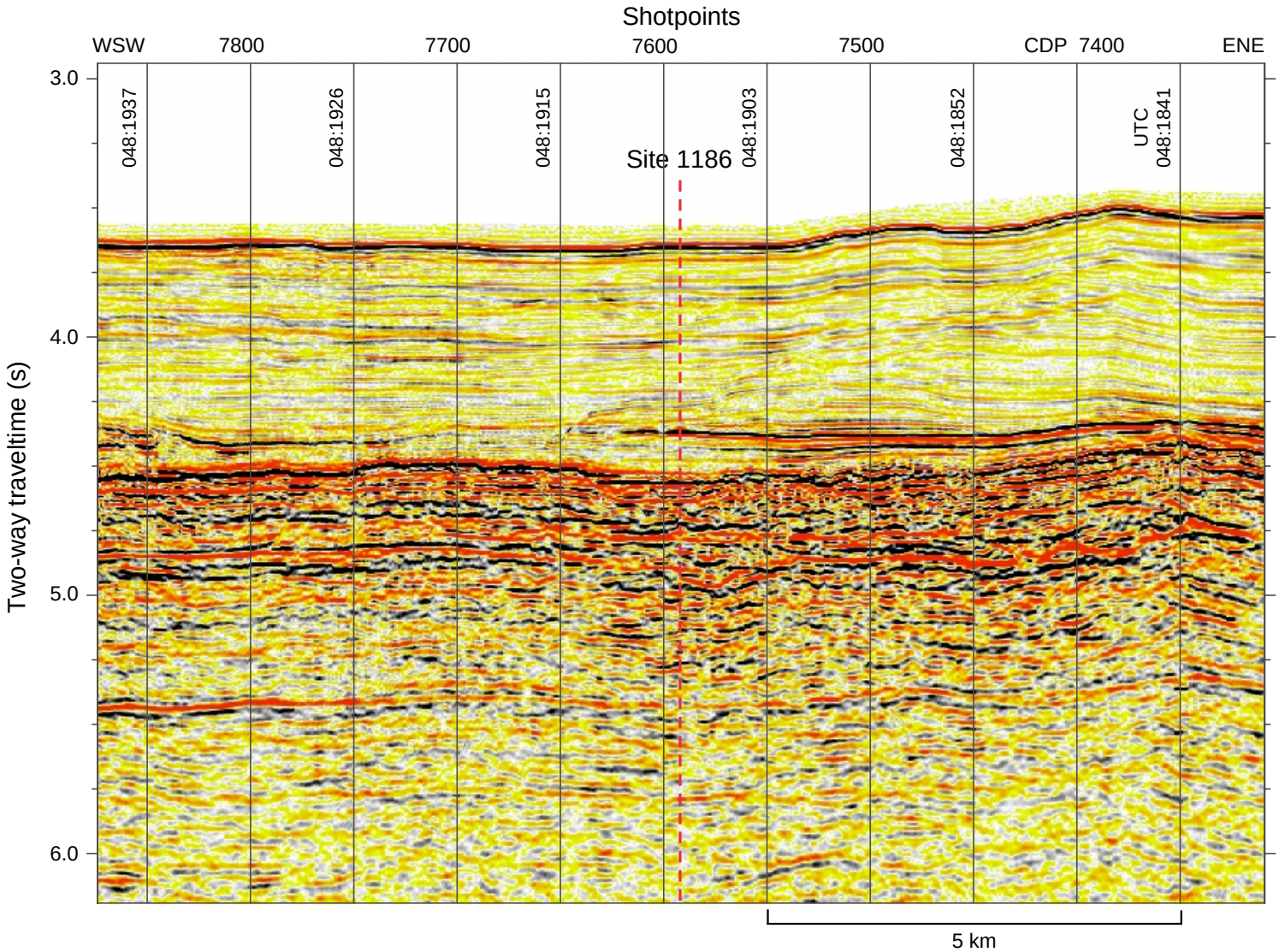
Shotpoints
WSW
7800
7700
7600
7500
CDP 7400
ENE
3.0
4.0
5.0
6.0
Two-way traveltime (s)
048:1937
048:1926
048:1915
Site 1186
048:1903
048:1852
UTC
048:1841
5 km

Figure 29

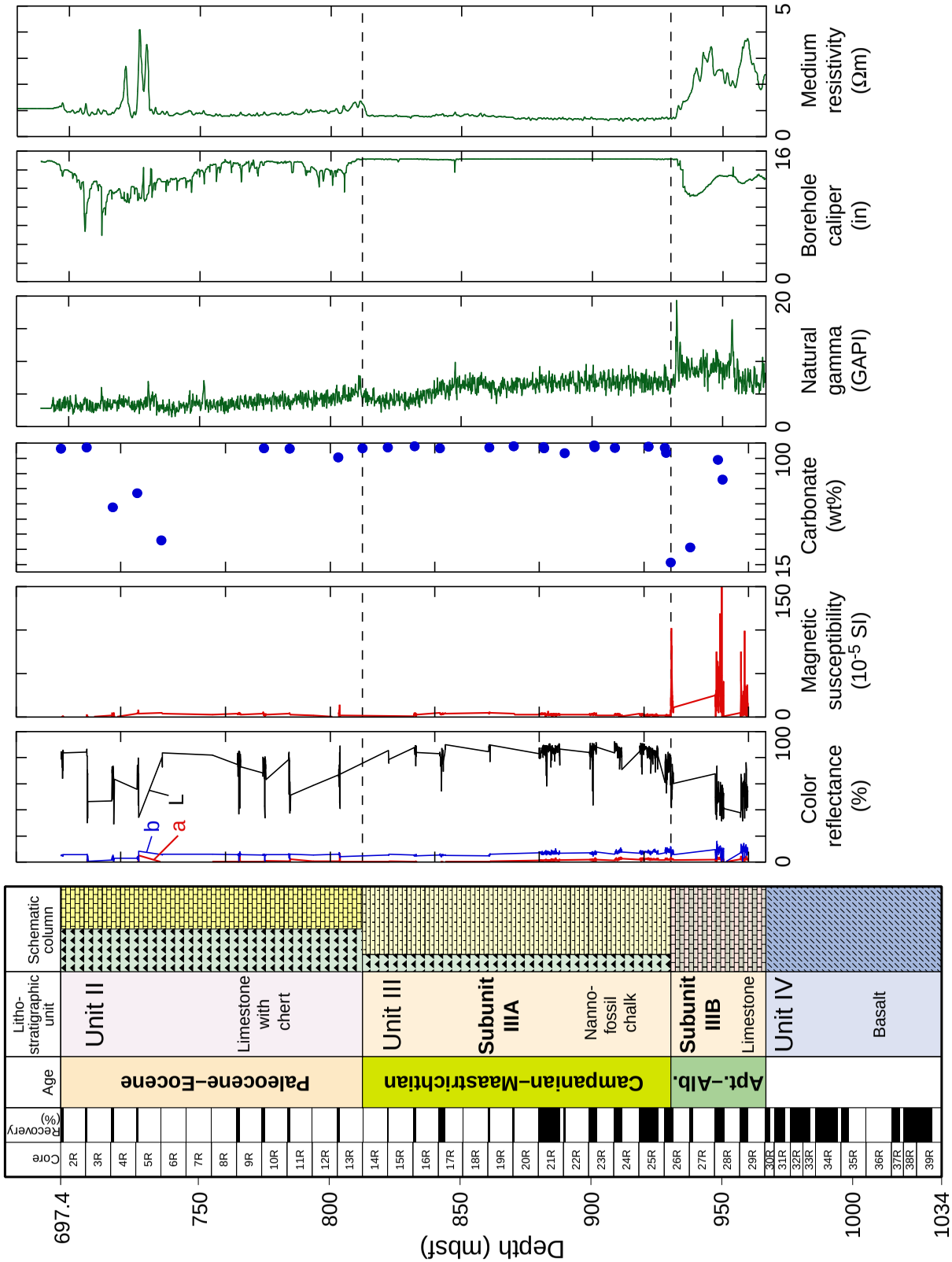
Depth (mbsf)
697.4
750
800
850
900
950
1000
1034
Core
Recovery (%)
Age
Litho-stratigraphic unit
Schematic column
Paleocene–Eocene
Campanian–Maastrichtian
Apt.–Alb.
Unit II
Limestone with chert
Unit III
Subunit IIIA
Nanno-fossil chalk
Subunit IIIB
Limestone
Unit IV
Basalt
Color reflectance (%)
Magnetic susceptibility (10-5 SI)
Carbonate (wt%)
Natural gamma (GAPI)
Borehole caliper (in)
Medium resistivity (Ωm)

Figure 30

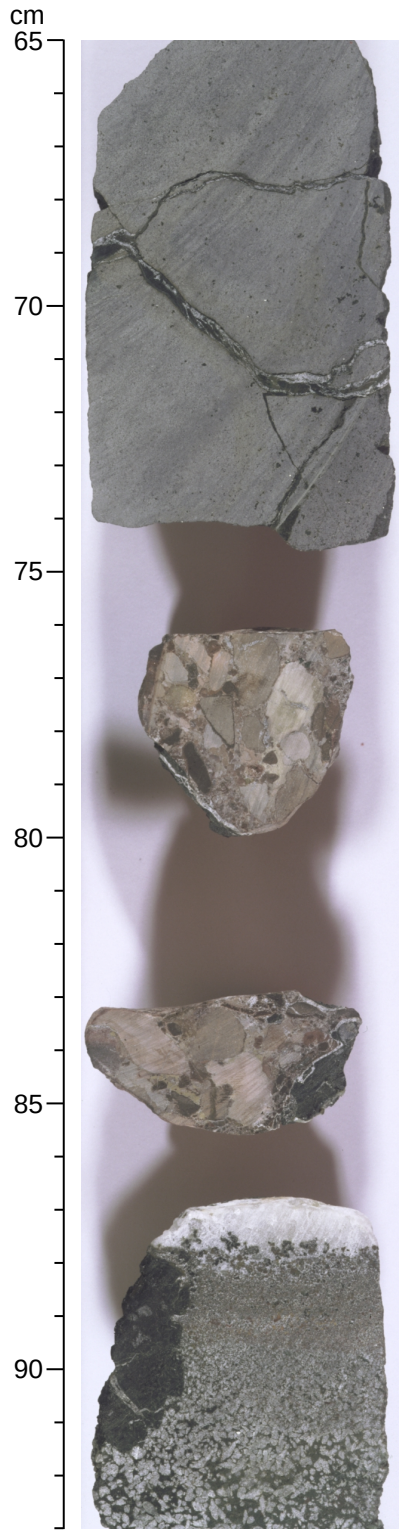

Figure 31

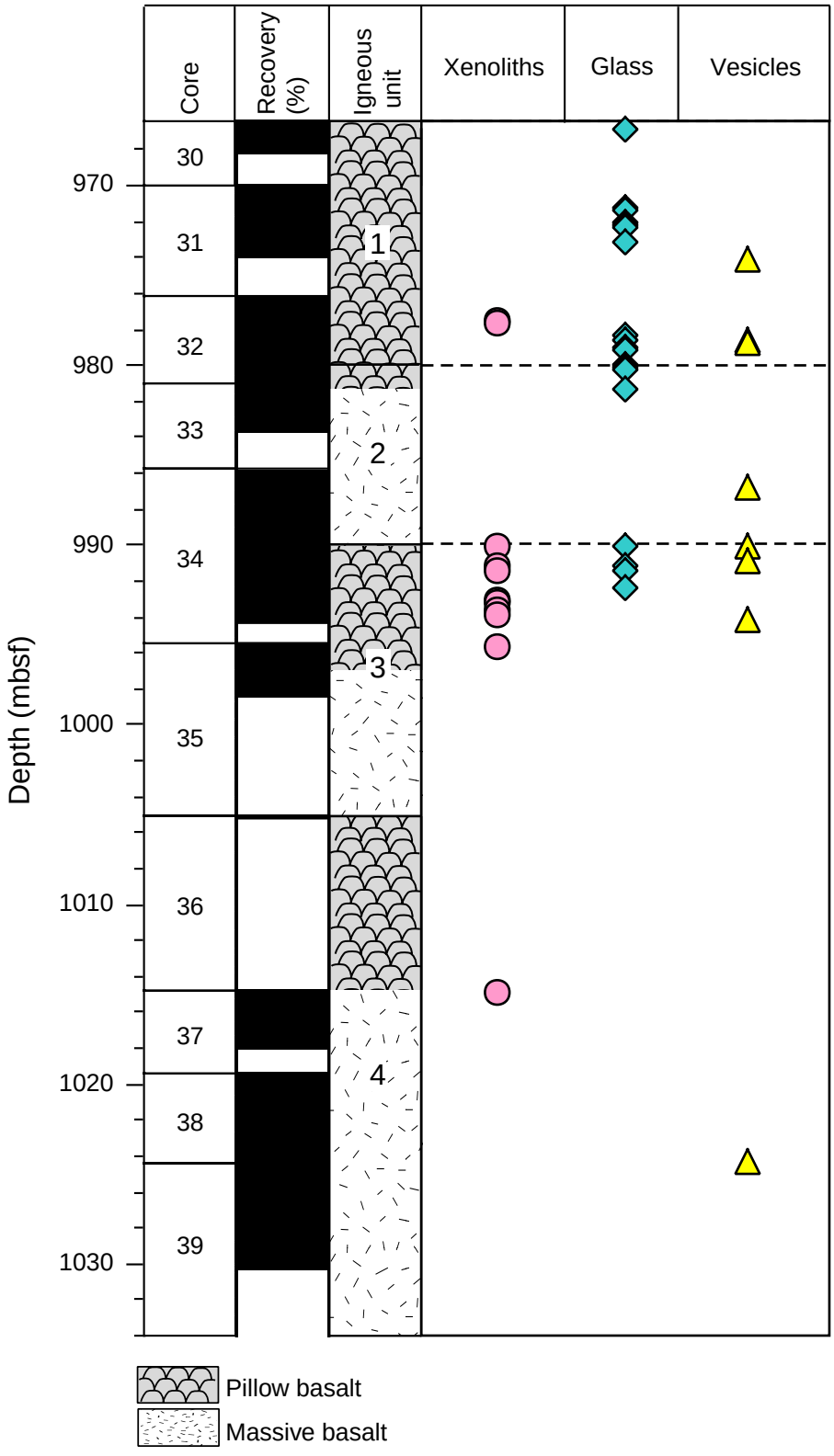
Core
Recovery (%)
Igneous unit
Xenoliths
Glass
Vesicles
Depth (mbsf)
970
980
990
1000
1010
1020
1030
30
31
32
33
34
35
36
37
38
39
1
2
3
4
Pillow basalt
Massive basalt

Figure 32

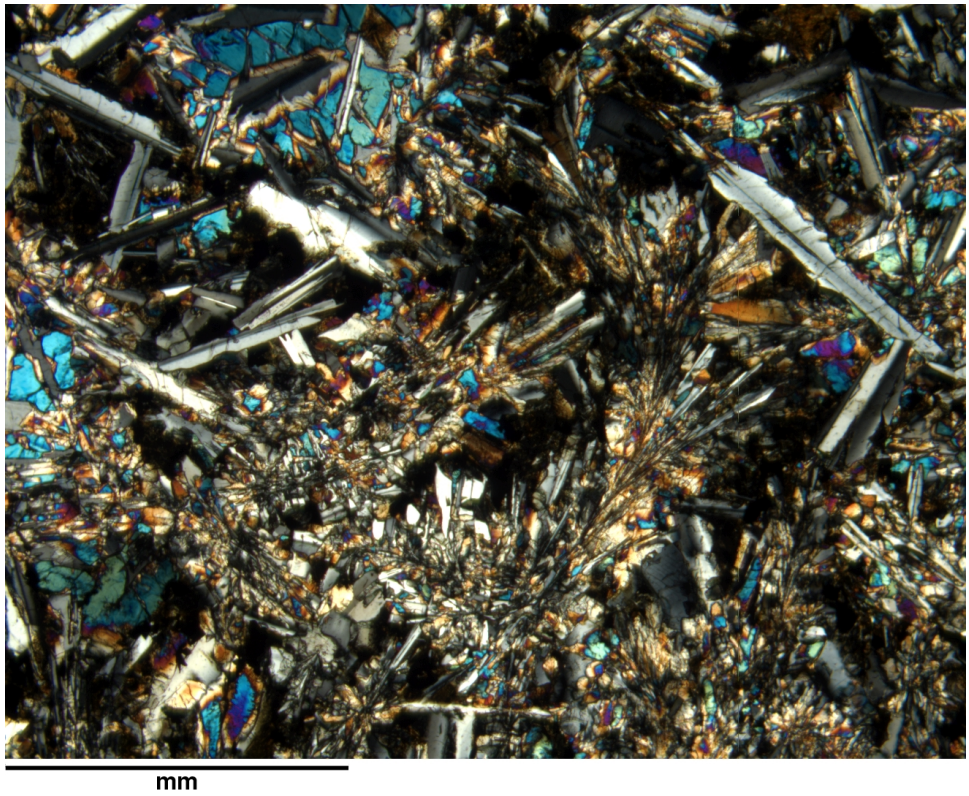

Figure 33

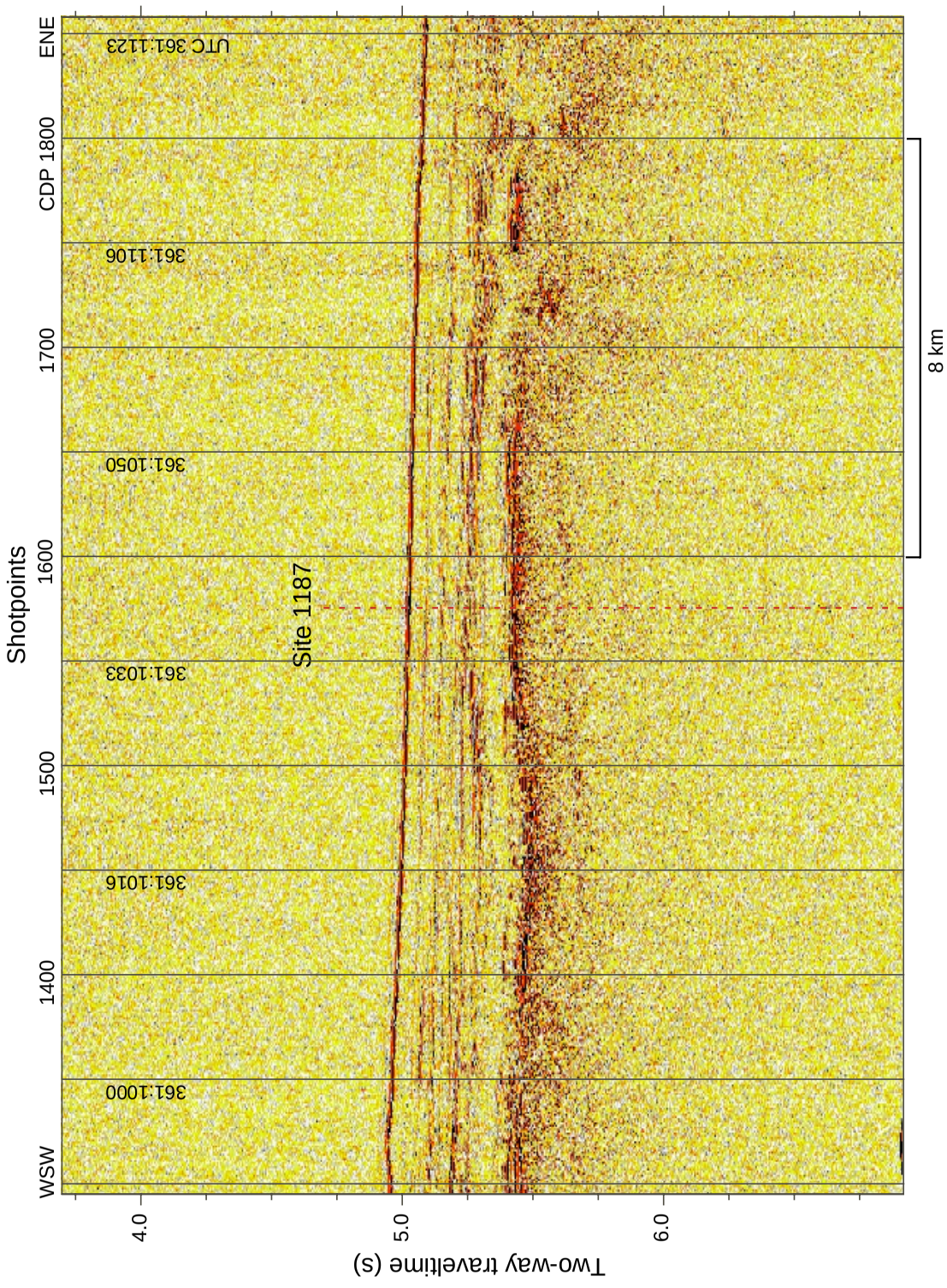
WSW
ENE
Shotpoints
1400
1500
1600
1700
CDP 1800
361:1000
361:1016
361:1033
361:1050
361:1106
UTC 361:1123
Site 1187
8 km
Two-way traveltime (s)
4.0
5.0
6.0

Figure 34

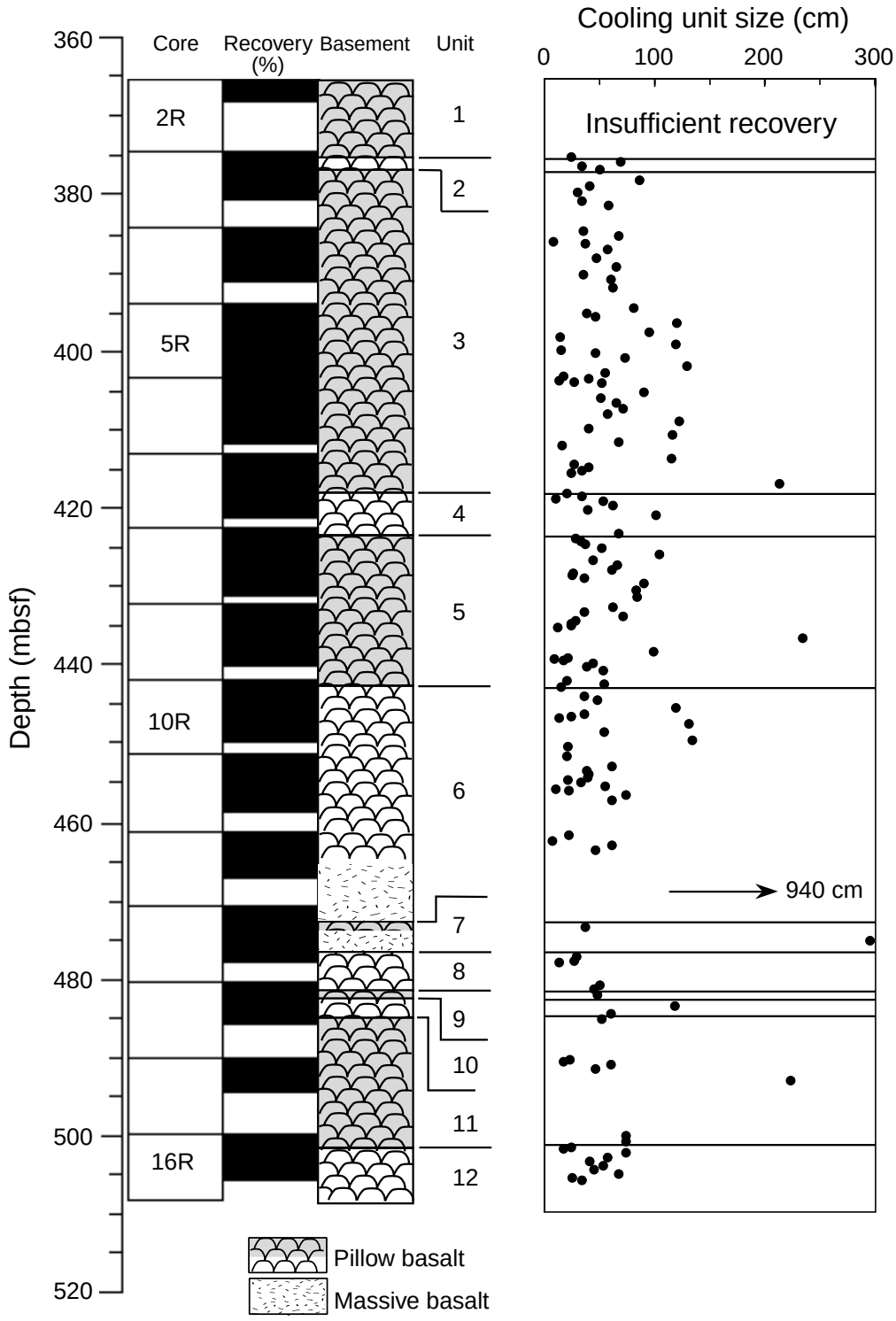
Cooling unit size (cm)
0
100
200
300
Core
Recovery (%)
Basement
Unit
Depth (mbsf)
360
380
400
420
440
460
480
500
520
2R
5R
10R
16R
1
2
3
4
5
6
7
8
9
10
11
12
Insufficient recovery
940 cm
Pillow basalt
Massive basalt

Figure 35

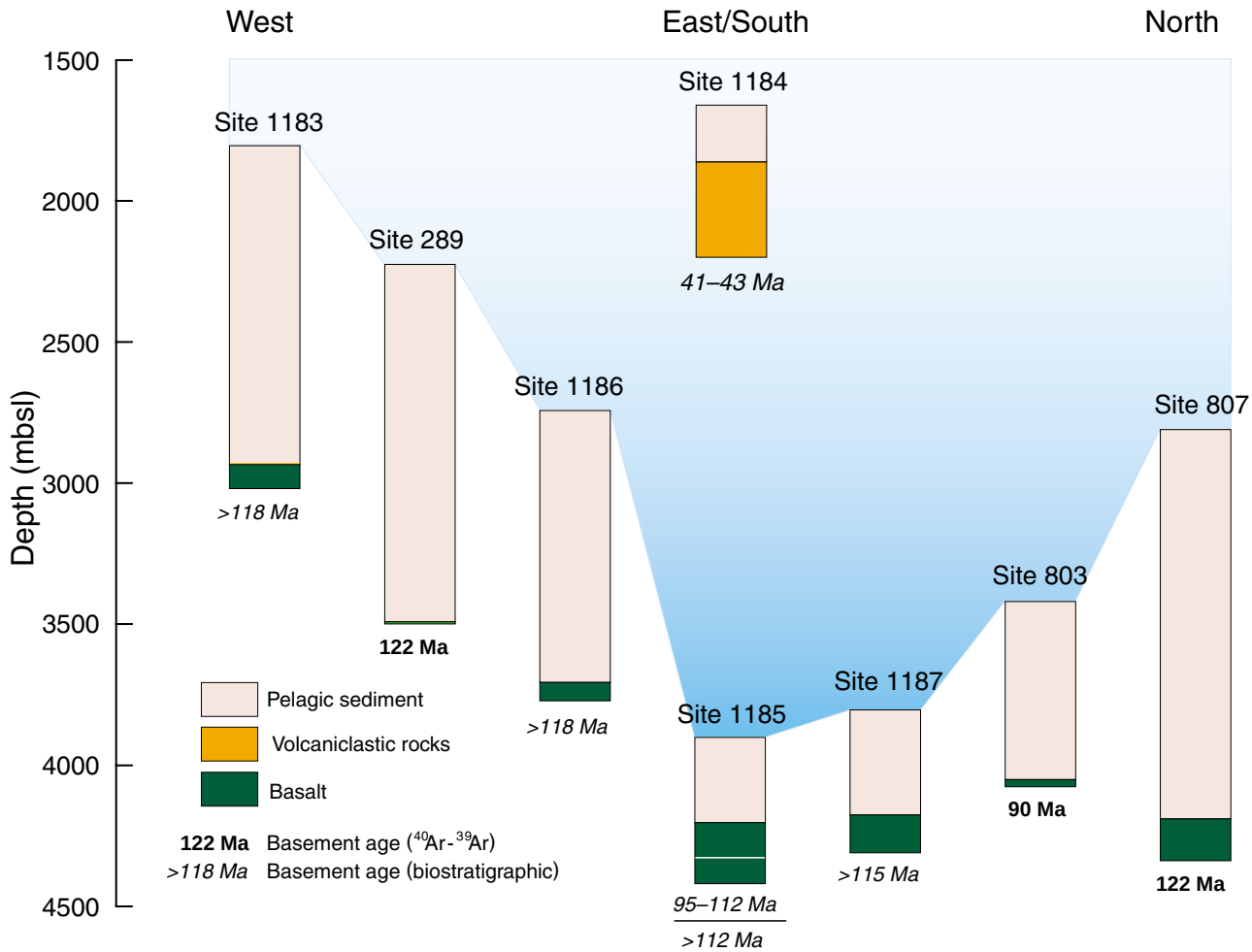
West
East/South
North
1500
2000
2500
3000
3500
4000
4500
Depth (mbsl)
Site 1183
>118 Ma
Site 289
122 Ma
Site 1186
>118 Ma
Site 1184
41–43 Ma
Site 1185
95–112 Ma
>112 Ma
Site 1187
>115 Ma
Site 803
90 Ma
Site 807
122 Ma
Pelagic sediment
Volcaniclastic rocks
Basalt
122 Ma Basement age (40Ar-39Ar)
>118 Ma Basement age (biostratigraphic)

Figure 36

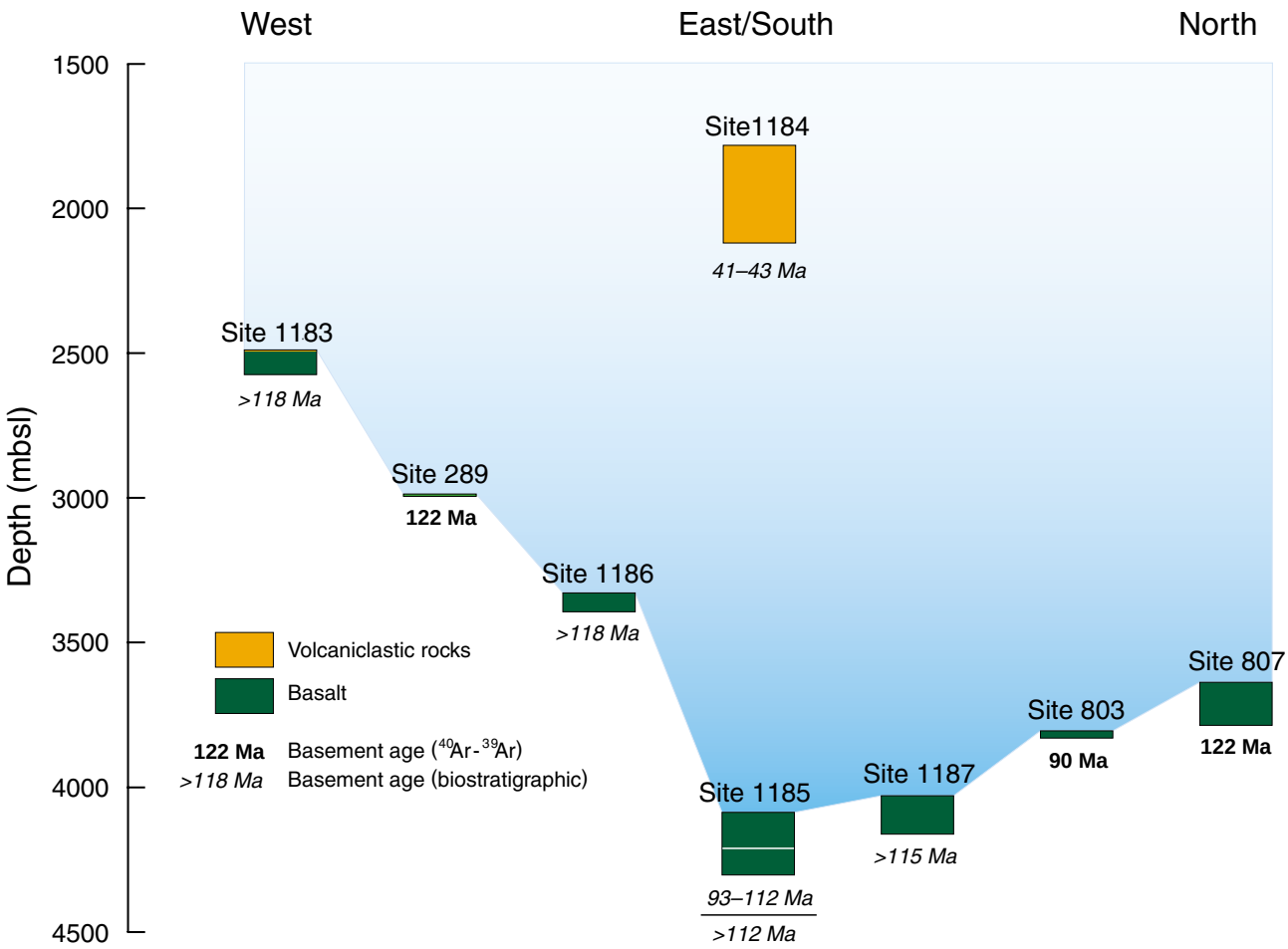
West
East/South
North
Depth (mbsl)
1500
2000
2500
3000
3500
4000
4500
Site1184
41–43 Ma
Site 1183
>118 Ma
Site 289
122 Ma
Site 1186
>118 Ma
Site 1185
93–112 Ma
>112 Ma
Site 1187
>115 Ma
Site 803
90 Ma
Site 807
122 Ma
Volcaniclastic rocks
Basalt
122 Ma Basement age (40Ar-39Ar)
>118 Ma Basement age (biostratigraphic)

Figure 37

OPERATIONS SYNOPSIS[1]

Transit to Site 1183

At 2048 hr on 13 September 2000 the *JOIDES Resolution* departed Guam and began the transit to Site 1183. Calm seas, mild weather, and the absence of any significant currents contributed to better-than-expected speed during the voyage. The 2141-km transit was accomplished at an average speed of 11.1 kt. At 0615 hr on 18 September we deployed a beacon on the Global Positioning System (GPS) coordinates for Site 1183.

Hole 1183A

The planned operational scenario for Site 1183 was for two holes. The first hole was to be a pilot hole drilled and cored to bit destruction; the second was to be a double-cased reentry hole. The purpose of the pilot hole was to determine the amount of 16-in and 10.75-in casing to be deployed in the second hole. The bit tagged the seafloor at 1804.7 meters below sea level (mbsl) and was observed with the vibration-isolated television (VIT) system. We began a jet-in test at 1700 hr on 18 September and concluded it by 1900 hr. After completing the jet-in test, we washed ahead through the sediment with a core barrel in place to a depth of 328.0 meters below seafloor (mbsf). After recovering the wash barrel, we dropped another core barrel and initiated coring in Hole 1183A at 0300 hr on 19 September. Coring advanced from 328.0 to 452.7 mbsf with 58.6% average recovery. The material recovered from this interval suggested that ~430 m of 10.75-in casing would be appropriate in the cased reentry hole.

We drilled the interval from 452.7 to 752.0 mbsf without coring using a center bit fitted in the rotary bit. The 299.3-m interval was drilled at an average rate of penetration of 35.4 m/hr with no drilling problems. We then rotary cored Hole 1183A continuously from 752.0 to 1160.6 mbsf. At ~1131 mbsf we contacted basaltic basement. The average recovery in basement from 1136.5 to 1160.8 mbsf was 60% with an average rate of penetration of 1.2 m/hr.

After the bit had accumulated 59.2 rotating hr, we had to decide whether to deepen the pilot hole using a free-fall funnel (FFF) or terminate Hole 1183A and start the reentry site emplacement in Hole 1183B. After considering the risks entailed by using a FFF, the considerable time and resources needed to set a reentry cone and ~430 m of casing, and, particularly, the excellent hole conditions thus far in Hole 1183A, we decided to attempt to achieve the depth objectives with the pilot hole and forego the reentry hole. We deployed a FFF with three floats, and we used the VIT to observe the FFF during extraction of the drill string from the hole. The bit was smoothly withdrawn from the FFF, after which we recovered the VIT and retrieved the drill string. The worn bit, an RBI C-4 coring bit, was replaced with a harder-formation C-7 bit, and we deployed the drill string and positioned it over the FFF. After a 30-min search, we reentered Hole 1183A at 1900 hr on 24 September. The operation was complicated because the FFF had settled into the sediment, and effluent emanating from the hole obscured the funnel and the glass floats marking the position of the hole. Following the recovery

[1] The Operations and Engineering personnel aboard the *JOIDES Resolution* for Leg 192 were ODP Operations Manager Ron Grout and Schlumberger Engineer Steve Kittredge.

of the VIT, we lowered the drill string to 519.7 mbsf, where it encountered a constriction, suggesting that this part of the hole was closing. We picked up the top drive, and we washed and reamed the hole from 442.5 to 577.4 mbsf. After clearing the tight spots in the hole, we set back the top drive and lowered the drill string to bottom. There was ~2 m of soft fill at the bottom of the hole.

We resumed rotary coring in Hole 1183A at 0530 hr on 25 September, and we advanced from 1160.6 to 1211.1 mbsf at an average rate of penetration of 1.2 m/hr. The average recovery for this interval was 54%. To reduce the chances of core jamming in the liner, we used no liners and employed a sleeveless core catcher. After the bit had accumulated 44.1 rotating hours, we decided to make another bit change. After circulating a 50-bbl sepiolite mud flush, we pulled back the drill string to 318 mbsf, where we spotted a 50-bbl solution of 10.5 lb/gal mud. The heavy mud was to serve as a density cap to prevent effluent exiting the FFF and complicating reentry operations.

We recovered the drill string and replaced the worn bit with a new, harder-formation RBI C-9 coring bit. While lowering the drill string, we also launched the VIT and ran it down for the reentry. At 0558 hr on 28 September we reentered Hole 1183A after a 20-min search for the FFF. The FFF was not visible, but we could clearly see the circular sediment pond formed from hole cuttings. The spotting of heavy mud at the top of the hole appeared to have prevented material from the hole from venting to the water column and obscuring the visibility, as happened during the first reentry.

We lowered the drill pipe to 202 mbsf, where unassisted progress was prevented by increasing hole drag. We recovered the VIT and picked up the top drive. After dropping a wash barrel, we washed and reamed the hole in an attempt to work past the tight section. However, the tight hole conditions did not improve. From 0815 hr on 28 September to 0530 hr on 29 September, we advanced the bit to 953 mbsf, where the penetration rate dramatically slowed. We recovered the wash barrel and dropped a center bit to drill ahead through the obstruction. We made no further progress and terminated operations in the hole. We deployed the wireline to recover the center bit, but a failed pin connection on the bottom inner barrel prevented the retrieval of the center bit, inner barrel sub, and landing sub, which remained in the bottom-hole assembly (BHA).

During the washing and reaming of the hole, the relatively rapid rate of advance compared with the rate of coring over the same depth interval strongly suggested that the bit was in the original hole and not drilling a new hole. The drillers commented that it felt as if there was something being pushed ahead of the bit as they tried to advance to 1211 mbsf. We terminated the attempts at getting to the bottom 258 m short of the bottom of the hole. We retrieved the drill string with no noticeable resistance experienced on the way out of the hole. Inspection of the bit showed an unusual amount of wear on the tungsten carbide inserts on the nose of each of the cones. After recovering the beacon and retracting the thrusters and hydrophones, we began the transit to Site 1184 at 1430 hr on 30 September.

During operations at Hole 1183A, we cored 583.8 m of sediment and basement with 260.7 m recovered (44.7% average recovery). An additional 627.3 m of sediment was washed and drilled.

We cored ~80.7 m of basaltic basement and recovered a total of 44.2 m of basalt (54.8%).

Transit to Site 1184

Because we were unable to obtain clearance from the Solomon Islands to drill at the second site planned for Leg 192 (prospectus site OJ-7D), we proceeded to Site 1184. We accomplished the 911-km transit in 47 hr at an average speed of 10.5 kt. The vessel proceeded directly to the GPS coordinates of the site, and at 1346 hr on 1 October we deployed a beacon.

Hole 1184A

We spudded Hole 1184A with the rotary core barrel (RCB) at 2000 hr on 1 October. The bit tagged the seafloor at a depth of 1661.5 mbsl. We drilled ahead without coring to 134.4 mbsf at an average rate of penetration of 67 m/hr. After retrieving the wash barrel, we dropped another core barrel and began rotary coring. Hole 1184A was rotary cored from 134.4 to 326.6 mbsf with an average recovery of 76.3%. We contacted acoustic basement at 201 mbsf; it consisted of volcaniclastic rocks. The average recovery for acoustic basement was 77.1% (96.4 m recovery). The average penetration rate in acoustic basement was 2.5 m/hr.

After coring to 326.6 mbsf, the bit had accumulated 54 rotating hours, and we decided to change the bit. A 50-bbl sepiolite mud flush was circulated in the hole and the bit pulled back to 142 mbsf. Following the successful deployment of the second FFF of the leg, we observed the withdrawal of the bit from the top of the FFF with the VIT. Most of the FFF was covered by sediment, but the three glass floats were clearly visible. The used bit cleared the rotary table at 0800 hr on 5 October. An inspection of the bit found that it was, remarkably, in nearly pristine condition with no visible wear evident except a slight rounding of the chisel inserts on the cones. The crew removed the old bit and mechanical bit release and replaced these with a new RBI C-7 harder-formation bit and a new mechanical bit release.

We successfully reentered Hole 1184A at 1400 hr on 5 October after a 30-min search. The drill string was run in to 238 mbsf, where the driller observed 20,000–30,000 lb of drag. After the top drive was picked up, the drill string became stuck in the formation. Fortunately, circulation was never lost, and the pipe came free after applying 200,000 lb of overpull above the weight of the drill string. Routine hole maintenance was conducted by washing and reaming the hole from 238 to 326 mbsf. We resumed coring operations in Hole 1184A at 1730 hr on 5 October. The interval from 326.2 mbsf to 538.8 mbsf was cored at an average rate of penetration of 4 m/hr and 86% average recovery. We terminated operations in Hole 1184A when the time allocated for this site had expired. After the crew retrieved the drill string, recovered the beacon, and retracted the thrusters and hydrophones, we began the transit to Site 1185 at 0530 hr on 9 October.

The cored interval in Hole 1184A was 404.4 m with 328.8 m recovered (81.3%) and an average penetration rate of 3.8 m/hr. Apart from the momentary sticking of the drill string following the bit change, we encountered no hole problems.

Transit to Site 1185

During operations at Site 1184, we continued to wait for clearance from the Solomon Islands to drill at proposed site OJ-7D. Because we had not received clearance by the time operations were terminated, Site OJ-7D was abandoned from further consideration, and we proceeded to Site 1185. The 591-km transit to Site 1185 was accomplished in 28.8 hr at an average speed of 11.1 kt. The vessel proceeded directly to the GPS coordinates of the site, and at 1036 hr on 10 October we deployed a beacon.

Hole 1185A

The plan at Site 1185 was to drill two holes. The first was to be a pilot hole drilled to basement and the second a reentry hole with a reentry cone and short section of 16-in casing. We spudded Hole 1185A with the RCB at 2100 hr on 10 October and began a jet-in test. The purpose of the jet-in test was to determine the amount of 16-in casing to affix to the reentry cone on the second hole. The crew observed the bit with the VIT system to tag the seafloor at a depth of 3898.9 mbsl. The jet-in test was concluded at 2300 hr after the bit had advanced 38 m. The results of the test indicated that a 30-m string of 16-in casing would be sufficient to anchor a reentry cone. Following the jet-in test, we drilled ahead with a wash barrel in place to a depth of 250.6 mbsf, where we initiated coring. The average rate of penetration through the washed interval was 53 m/hr.

We rotary cored the sediment portion of Hole 1185A from 250.6 to 308.5 mbsf (57.9 m interval) with an average recovery of 23.7%. Headspace gas analysis of the sediment cores yielded <2 ppm of methane and no heavier hydrocarbons. We contacted basement at 308.5 mbsf. Rotary coring continued into basement to a depth of 328.7 mbsf. The average recovery for basement was 56.1% (20.2 m), and average penetration rate was 2.3 m/hr. After determining the depth to basaltic basement, we realized the objective of the pilot hole, and we ceased coring in Hole 1185A. We retrieved the drill string, replaced the bit, and the vessel was offset 20 m west of Hole 1185A in preparation for the next hole.

Hole 1185B

The objective of Site 1185 was to penetrate at least 100 m into basaltic basement. Because of the difficulty of locating FFFs that had sunk into the sediment at previous sites, we decided to set a reentry cone with 28 m of 16-in casing in Hole 1185B to ensure that we would be able to make multiple round trips of the drill string in order to change bits.

A reentry cone that was fabricated for Hole 1183A but unused was positioned in the moonpool and centered under the rotary table. After removing and securing the upper guide horn, the 16-in casing hanger was connected to the Dril-Quip cam-actuated-drill-ahead (CADA) tool and secured in the derrick. Two joints of 16-in casing and a shoe joint were then assembled and affixed to the casing hanger. Once the casing was assembled, a stand of 5.5-in drill pipe with the 16-in CADA tool was connected to the casing hanger. The hanger and casing assembly were then lowered through the rotary table just above the throat of the reentry cone. However, the throat of the reentry cone was too narrow and prevented the assembly from landing properly.

After the welder modified the internal throat clearance, the hanger and casing were successfully latched into the reentry cone. The CADA running tool was then removed.

The crew assembled a jetting-in BHA with a 14.75-in tricone drill bit and a stand of 8.25-in drill collars. This was followed by connecting the CADA tool to a stand of two 8.25-in drill collars and one tapered drill collar. We then lowered the BHA and CADA tool through the rotary table and connected them to the casing hanger. We lowered the complete assembly the seafloor and deployed the VIT during the pipe trip. We spudded Hole 1185B at 0930 hr on 13 October. It required 2 hr to jet in the 16-in casing. After successfully uncoupling the CADA tool from the casing hanger, we recovered the drill string and prepared a RCB BHA with a new C-7 bit.

The crew lowered the BHA to the seafloor and deployed the VIT. We positioned the bit over the reentry cone and reentered Hole 1185B at 0833 hr on 14 October after an 8-min search. We deployed the BHA to 31 mbsf and recovered the VIT. At 1000 hr, we began to drill ahead with a wash barrel in place and advanced to 308.0 mbsf. The wash barrel was retrieved and a fresh core barrel dropped. We began rotary coring at 1900 hr and contacted basaltic basement at 309.5 mbsf.

We continued coring in basement and advanced to a depth of 434.6 mbsf (125.1 m into basement) by the afternoon of 17 October. After we added a new stand of pipe and dropped a fresh core barrel, the bit nozzles clogged and the pump pressure reached a maximum of 3000 psi, indicating that all circulation was lost. The driller was able to work the drill string and partially clear some of the blockage. Because the bit had accumulated 52 rotating hr, we decided to conduct a round trip of the drill string to replace the bit. Average recovery in the cored basement section was 40.1%, at an average penetration rate of 2.7 m/hr.

After the drill string was recovered, inspection of the bit showed that it was evenly worn, had two plugged nozzles, and had a slightly undergage body. The drilling jars could not be mechanically operated and were replaced. The crew affixed a new C-7 RCB bit to a mechanical bit release and deployed it. At 1330 hr on 18 October, we successfully reentered the hole after a brief search and resumed rotary coring at 1700 hr. Pump pressure was initially high (1500 psi at 75 strokes/min), indicating that a few of the bit nozzles were clogged. After advancing the bit several meters, the pressure gradually stabilized to a nominal value of 650 psi at 75 strokes/min. After heavy use of mud flushes to clean out the hole, we resumed rotary coring in basement. Coring advanced from 434.6 to 502.1 mbsf with an average rate of penetration of 1.7 m/hr and average recovery of 58.5%.

When Cores 25R and 26R were retrieved with no recovery, we deployed a bit deplugger twice in an attempt to clear a possible obstruction in the throat of the bit. We then cored a 1-m interval but had no recovery, so the deplugger was deployed a third time. After this, we dropped another core barrel, advanced 1 m, and recovered 0.98 m of basalt and a small segment of a bit seal O-ring. The latter suggested that the blockage of the bit was caused by partial disintegration of the bit seal. We dropped a new core barrel (Core 192-1185B-29R), but, after coring 7.6 m, the top-drive motor stalled at 600 A. The torque was slowly released, and the driller observed a loss of 500 psi standpipe pressure. The crew immediately turned off the active heave compensator, so they could use the Martin Decker weight indicator to determine downhole conditions. The driller

noted a loss of ~40,000 lb of drill-string weight, indicating a failure somewhere in the BHA.

The crew circulated a 50-bbl sepiolite sweep to ensure a clean hole for fishing operations and pumped a 20-bbl slug of heavy mud downhole. They set back the top drive and pulled the drill string out of the hole. After considering the time that would be required to attempt fishing of the BHA vs. the time that would be lost for scientific operations, we decided to abandon the site. Upon recovery of the BHA, we found that the outer body of the drilling jars had broken apart. We inspected the remaining components of the BHA above the jars but found no deficiencies.

During operations at Hole 1185B, we cored 216.6 m of basaltic basement with 42% average recovery. At 0515 hr on 22 October, the vessel began the transit to Site 1186.

Transit to Site 1186

Before departing from Site 1185, we obtained approval for the new site, designated OJ-12A (Site 1186). The 207-km transit to Site 1186 was accomplished in 8 hr at an average speed of 13.8 kt. The vessel proceeded directly to the GPS coordinates for Site 1186, and, at 1340 hr on 22 October, we deployed a beacon on the site.

Hole 1186A

The crew spudded Hole 1186A with the RCB at 2130 hr on 22 October. We drilled ahead with a wash barrel in place to a depth of 697.4 mbsf, where we initiated coring. The formation was unexpectedly soft, and drilling through this interval required only 9.45 hr. The average rate of penetration was 60 m/hr.

We rotary cored the sediment portion of Hole 1186A from 697.4 to 968.6 mbsf (271.2 m interval). The low average recovery of 18% was caused by very soft sediment with abundant chert stringers that left fragments in every core to a depth of 957 mbsf. Below that depth, recovery began to improve. We contacted basaltic basement at 968.6 mbsf. This depth is based on the recovery of 1.4 m of basalt from a cored interval (Core 192-1186A-30R) that ended at 970.0 mbsf. This is slightly deeper than the value of 966.8 mbsf calculated using standard ODP conventions for curated positions of core material. We continued coring in basaltic basement until we reached 1034.0 mbsf. The average recovery in basement was 59% at an average penetration rate of 1.8 m/hr. The only problem we encountered during coring operations was when a fresh core barrel, dropped after retrieval of Core 192-1186A-31R (970.0–976.2 mbsf), failed to land properly in the BHA. This problem was cleared by deploying a bit deplugger. We surmised that some basalt may have slipped out of the previous core barrel during recovery and partially obstructed the landing of the new core barrel.

After reaching 1034.0 mbsf (67.2 m into basement), we decided to end coring operations for several reasons: (1) slow penetration rates, (2) concerns that a bit change and reentry with a FFF would be risky because of ~970 m of open hole in chert-rich sediment, (3) chemical analyses of the basalt indicated that it was closely similar to basalt at Site 1183, and (4) we wanted to leave enough time to drill an additional basement site.

In preparation for logging, we circulated a 50-bbl sepiolite mud flush in the hole from a depth of 1033 mbsf. After filling the borehole with 340 bbl of sepiolite mud, we released the bit

at the bottom of the hole. The crew assembled the Schlumberger logging equipment and placaed the bottom end of the BHA at 123 mbsf. Hole 1186A was logged with a single pass of the triple combination (triple combo) tool string and two passes of the Formation MicroScanner logging tool (FMS)/sonic tool string. During the first logging run, we lowered the triple combo from the bottom of the pipe at 123 mbsf to 1030 mbsf, coming within 4 m of the bottom of the hole without difficulty. We logged upward to 675 mbsf, just above the top of the cored interval. During the second logging run, we lowered the FMS/sonic tool string to 1032 mbsf (within 2 m of bottom) without difficulty, and logging proceeded upward. The first pass was interrupted by a loss of telemetry from the tool string, requiring reinitialization of the instrument. Logging then continued up to 696 mbsf. We then lowered the tool back to the bottom of the hole and made a second pass up to 686 mbsf.

After rigging down the logging equipment, we recovered the drill string and dismantled the BHA in preparation for the transit to Site 1187. The vessel departed for Site 1187 at 2115 hr on 28 October.

Transit to Site 1187

We accomplished the 256-km transit to Site 1187 (new proposed site OJ-14A) in 13.5 hr at an average speed of 10.2 kt. The vessel proceeded directly to the GPS coordinates for Site 1187, and, at 1112 hr on 29 October, we deployed a beacon on site.

Hole 1187A

The depth objective in this hole was to core into basement until time expired or the bit failed as a result of excessive wear. We spudded Hole 1187A with the RCB at 1920 hr on 29 October. The bit tagged the seafloor at 3803.6 mbsl. We drilled ahead with a wash barrel in place to a depth of 365.5 mbsf, where progress became very slow because of a change in formation. From our interpretation of the seismic profile, we expected to encounter basement at ~ 410 mbsf. However, we encountered the sediment/basalt interface in the first RCB core (Core 192-1187A-2R) and inferred it to be at 372.5 mbsf, based upon the change in drilling parameters noted by the driller. We continued rotary coring in basement to a depth of 508.3 mbsf, where the bit expired after 65 rotating hours. The failure was manifested by high, erratic torque, indicating that one or more cones had fallen off the bit. The average recovery in basement was 74.3%, and the average penetration rate was 2.4 m/hr. Total penetration into basaltic basement was 135.8 m.

After retrieving the drill string and BHA, we found that the bit was missing two cones and one cone shank. The two remaining cones had chipped and missing teeth in all rows. After retracting the hydrophones and thrusters and securing the drilling equipment, the crew put the vessel under way to Guam at 0330 hr on 3 November.